

**Organisation of the cytoskeleton
of the *Drosophila* oocyte**

Inaugural-Dissertation
zur
Erlangung des Doktorgrades
der Mathematisch-Naturwissenschaftlichen Fakultät
der Universität zu Köln

vorgelegt von
Ying Wang
aus V. R. China

Köln 2007

Referenten:

Prof. Dr. S. Roth

Prof. Dr. A. A. Noegel

Tag der Prüfung: 15.02.2008

To my parents

献给我的父母

CONTENTS

1. INTRODUCTION.....	1
1.1. Cell polarity	1
1.2. <i>Drosophila</i> oogenesis	1
1.3. MT nucleation and the generation of non-centrosomal MT arrays.....	4
1.4. MT organisation of the oocyte during <i>Drosophila</i> oogenesis.....	5
1.5. The role of actin for the MT organisation of the <i>Drosophila</i> oocyte	8
1.6. The function of Par-1 during <i>Drosophila</i> oogenesis	9
1.7. Screening for targets of Par-1 kinase.....	11
1.8. Tao-1 kinase	11
1.9. Aims.....	12
2. MATERIALS AND METHODS	13
2.1. Genomic sequence, EST and fly stock searches.....	13
2.2. Fly strains and genetics.....	13
2.2.1. <i>Drosophila melanogaster</i> strains	13
2.2.2. Fly maintenance and egg laying collection	14
2.2.3. Expression using the UAS/GAL4 system	14
2.2.4. Generation of HA-Tao-1 transgenic flies.....	15
2.2.5. Generation of P-element imprecise deletions.....	15
2.2.6. Generation of the Exelixis deficiency	15
2.2.7. Induction of germline clones by the FLP/FRT system.....	16
2.3. Preparation of egg shell and larval cuticle.....	17
2.4. Drug treatment.....	17
2.4.1. LatrunculinA treatment	17
2.4.2. Colcemid treatment	18
2.5. Immunohistochemistry and in situ hybridisation	18
2.5.1. Immunohistochemistry, mounting and sectioning	18
2.5.2. Primary antibodies for immunohistochemistry	19
2.5.3. In situ hybridisation.....	19
2.6. Microscopy and image processing	21
2.6.1. Confocal microscopy and image analysis	21
2.6.2. Time lapse microscopy	21
2.7. Genomic PCR and sequencing	22
2.7.1. Oligonucleotides	22
2.7.2. Extraction of genomic DNA	24
2.7.3. Genomic PCR.....	24
2.7.4. Sequencing	25
2.8. Northern blot analysis.....	25
2.9. Western blot analysis	26
3. RESULTS	28
3.1. Cytoskeletal organisation in the wild type oocyte from stage 9/10a to stage 10b	28

3.1.1.	Optimal markers to detect cytoskeletal elements and a combination of multiple angles to analyse the oocyte.....	28
3.1.2.	Organisation of the oocyte cytoskeleton at stage 9/10a	31
3.1.3.	Changes in the oocyte cytoskeleton at stage 10b	37
3.1.4.	Cortical localisation of MT minus-ends is dependent on the actin bundling ..	38
3.2.	The oocyte cytoskeletal organisation in the mutants affecting actin-regulatory proteins	44
3.2.1.	Profilin is required for actin bundle formation.....	44
3.2.2.	Capu and Spire act downstream of actin bundling for MT anchoring at the cortex	45
3.2.3.	Cortical actin bundling is independent on the Capulet, Swallow and Moesin functions	47
3.3.	Different steps in the reorganisation of the oocyte cytoskeleton	49
3.4.	A novel cytoskeletal phenotype exhibited by a mutation in <i>Tao-1</i> gene.....	52
3.4.1.	Characterisation of <i>Tao-1</i> gene	52
3.4.1.1.	<i>Tao-1</i> is a Serine/Threonine protein kinase	52
3.4.1.2.	<i>Tao-1</i> transcripts are expressed during oogenesis	54
3.4.1.3.	<i>Tao-1</i> protein is localised at the oocyte cortex	55
3.4.2.	Anterior-posterior and dorsal-ventral patterning defects manifested in <i>Tao-1</i> ^{No.7} mutants	56
3.4.2.1.	Generation of a <i>Tao-1</i> mutant by imprecise P-element excision.....	56
3.4.2.2.	<i>Tao-1</i> ^{No.7} is a novel allele of <i>Tao-1</i> affecting the anterior-posterior and dorsal-ventral patterning	59
3.4.2.3.	The patterning phenotype of <i>Tao-1</i> ^{No.7} is the result of mislocalisation of transcripts of axis determinants during mid-oogenesis.....	64
3.4.3.	Cytoskeletal organisation is disrupted in <i>Tao-1</i> ^{No.7} oocytes	66
3.4.3.1.	MT organisation is disrupted in <i>Tao-1</i> ^{No.7} oocytes	66
3.4.3.2.	Cortical actin bundles are disrupted in <i>Tao-1</i> ^{No.7} oocytes.....	71
3.5.	Screen for new <i>Tao-1</i> alleles.....	73
3.5.1.	<i>Tao-1</i> ^{ETA} complements <i>Tao-1</i> ^{No.7}	73
3.5.2.	<i>Deficiency 14.1</i> complements <i>Tao-1</i> ^{No.7}	76
4.	DISCUSSION	80
4.1.	Cytoskeletal organisation and reorganisation of the oocyte from stage 9/10a to stage10b	80
4.2.	Cortical anchoring of MT minus-ends of the oocyte.....	81
4.3.	The cortical actin bundling of the oocyte, a novel actin based structure in the egg chamber.....	82
4.4.	The assembly of actin bundles at the oocyte cortex.....	84
4.5.	The role of Capu and Spire in the cytoskeletal organisation of the oocyte	84
4.6.	Alternative splicing of <i>Tao-1</i> transcripts during oogenesis.....	87
4.7.	The molecular and genetic nature of <i>Tao-1</i> ^{No.7}	88
4.8.	The unique patterning defects of <i>Tao-1</i> ^{No.7} mutants	90
4.9.	The novel cytoskeletal organisation phenotype of <i>Tao-1</i> ^{No.7} mutant oocytes....	92
5.	SUMMARY	94

6. ZUSAMMENFASSUNG	95
7. REFERENCES.....	97
8. ABBREVIATIONS.....	110
9. ACKNOWLEDGEMENT.....	111
10. ERKLÄRUNG.....	112
11. LEBENSLAUF.....	113

FIGURE INDEX

Fig. 1 Overview of <i>Drosophila</i> oogenesis and MT organisation in the oocyte.....	3
Fig. 2 Markers to detect cytoskeletal elements and multiple angles to analyse the oocyte.....	29
Fig. 3 Architecture of the oocyte cytoskeleton	34
Fig. 4 Reorganisation of the oocyte cytoskeleton between stage 9/10a and stage 11	36
Fig. 5 Endosome movements in stage 9/10a oocytes.....	39
Fig. 6 Regulation of actin and MT organisation.....	41
Fig. 7 Regulation of the cortical anchoring of MT minus-ends.....	43
Fig. 8 Cortical localisation of GFP-Capu and GFP-SpireD	46
Fig. 9 Actin organisation in <i>cap</i> and <i>swa</i> mutant oocytes	49
Fig. 10 Cytoskeletal organisation in <i>Khc</i> mutant oocytes.....	51
Fig. 11 Schematic drawing of the <i>Tao-1</i> genomic locus, <i>Tao-1</i> translations and the genomic structures of <i>Tao-1</i> associated alleles.....	53
Fig. 12 The expression of <i>Tao-1</i> transcripts and the localisation of <i>Tao-1</i> protein during oogenesis.....	56
Fig. 13 Fertility and patterning defects in <i>No.7</i> mutants.....	58
Fig. 14 Localisation defects of Oskar and Gurken protein in <i>No.7</i> mutant oocytes, rescue experiment by <i>Tao-1</i> transcripts and molecular characterisation of <i>No.7</i> allele	62
Fig. 15 Localisation of <i>bicoid</i> , <i>gurken</i> and <i>oskar</i> mRNAs in <i>Tao-1^{No.7}</i> mutant oocytes.....	65
Fig. 16 MT organisation and colcemid treatment of <i>Tao-1^{No.7}</i> mutant oocytes.....	67
Fig. 17 The distribution of MT polarity markers in <i>Tao-1^{No.7}</i> mutant oocytes	68
Fig. 18 The distribution of MT minus-ends in <i>Tao-1^{No.7}</i> mutant oocytes.....	70
Fig. 19 Actin organisation in <i>Tao-1^{No.7}</i> mutant oocytes	72
Fig. 20 The organisation of MT cytoskeleton and the localisation of Oskar protein in <i>Tao-1^{ETA}</i> and <i>Df.14.1</i> mutant oocytes.....	75
Fig. 21 Schematic drawing of genomic structures for Exelixis P-element insertions and <i>deficiency 14.1</i>	77
Fig. 22 Scheme of the oocyte cytoskeleton.....	86

TABLE INDEX

Table 1 Actin bundle formation in stage 10a oocytes	45
Table 2 <i>Tao-1^{ETA}</i> and <i>Df.14.1</i> complements the localisation defect of Oskar protein in <i>Tao-1^{No.7}</i> mutants.....	78
Table 3 Summary of the oogenesis phenotypes in various mutants of <i>Tao-1</i> alleles.....	78

1. INTRODUCTION

1.1. Cell polarity

Cell polarity is fundamental for many aspects of cell and developmental biology. It is important for differentiation, proliferation and morphogenesis in both the unicellular and multicellular organisms. For instance, establishment and maintenance of cell polarity is the prerequisite for asymmetric cell division, which contributes to cell fate diversification by generating daughter cells with distinct identities. In epithelial cells, the loss of cell polarity is associated with tumor development and metastasis (Bilder et al., 2000; Mueller-Klieser, 2000; Wodarz, 2000).

Usually cell polarity is induced by the localisation of proteins to distinct subcellular regions. In many cases, the localised protein is accomplished by localising the corresponding mRNA. For example, 71% of the expressed genes during early *Drosophila* embryogenesis are found to encode mRNAs exhibiting clear subcellular distribution patterns (Lecuyer et al., 2007). There are a number of mechanisms by which mRNAs are localised. The most and best characterised examples of mRNA localisation are thought to be accomplished by active transports along the cytoskeleton. The studies come from a range of organisms, and the localisation can occur in actin-, or microtubule (MT)-dependent fashion (St Johnston D., 2005). Prominent examples of MT-based transport come from studies of the *Drosophila melanogaster* oocyte.

1.2. *Drosophila* oogenesis

Drosophila ovaries are composed of parallel bundles of developmentally ordered egg chambers, each of which supports the development of a single oocyte. These bundles, called ovarioles, are divided into the anterior germarium and the posterior vitellarium (Fig. 1A). Oogenesis is initiated in the anterior germarium, by a stem cell division that

produces a cystoblast and regenerates a stem cell (Fig. 1B). The cystoblast proceeds through four mitotic divisions to produce a cyst of 16 germline cells. Cytokinesis is incomplete in each of the cystoblast divisions, so that these 16 germline cells are interconnected by cytoplasmic bridges called ring canals (Fig. 1B). This interconnected cluster of germline cells is encapsulated by a layer of somatically derived follicle cells to form the complete egg chamber, which is the functional unit of oogenesis. Soon after this occurs, the egg chamber pinches off from the germarium and enters the vitellarium as a stage 2 egg chamber (Fig. 1B). Ultimately at stage 14 a mature egg chamber is produced (Fig. 1A). During oogenesis, one of the 16 germline cells differentiates to form the single oocyte and the rest become nurse cells. The nurse cells synthesise maternal components that are transported to the oocyte.

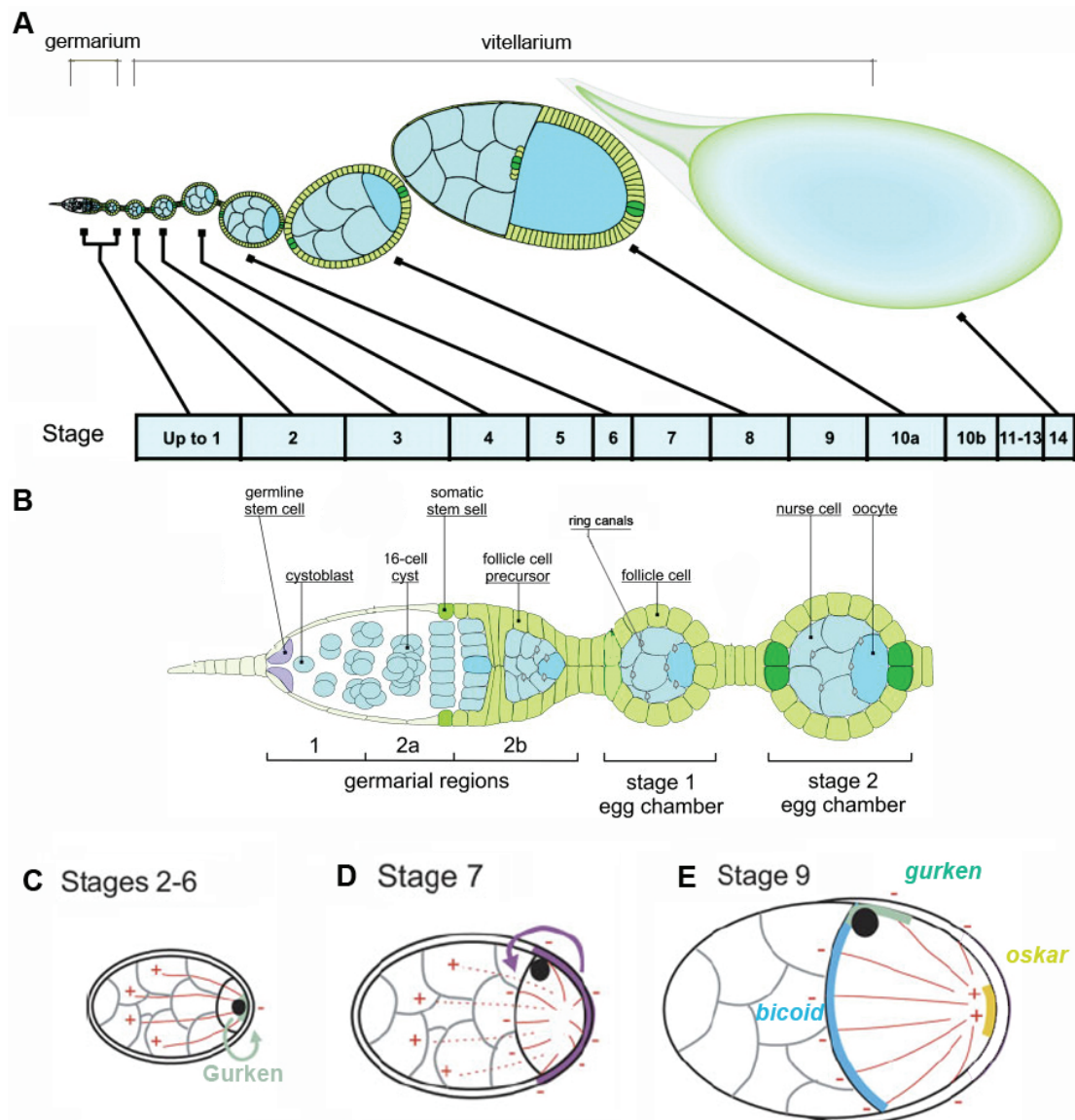


Fig. 1 Overview of *Drosophila* oogenesis and MT organisation in the oocyte (A) Drawing of a wild-type ovariole, with somatic cells in green and germ cells in blue. Oogenic stages are indicated. (B) Drawing of the construction of an egg chamber. The large variety of cell types and the basic structure found within the germarium and early egg chambers are indicated. (C) In stages 2–6, the germline MTs (red) are organized with their minus-ends at the oocyte posterior and their plus-ends extending into the nurse cells. During these stages, the oocyte sends signals to the overlying follicle cells at the posterior with Gurken (green). (D) At about stage 6 to 7, upon receiving the back signaling (purple arrow) from the posterior follicle cells (purple), MTs in the oocyte undergo a rearrangement, and oocyte nucleus migrates to the dorso-anterior corner of the oocyte. The posterior MTOCs established in stage 2 disassemble (red dashed lines). MTs are emanating from the anterior and lateral oocyte cortex (red solid lines). (E) At stage 9, the organised MT network directs the localisation of *bicoid* mRNA (blue) to the anterior corners and *gurken* mRNA (green) to the dorso-anterior corner of the oocyte, probably via MT minus-end directed motor Dynein. The localisation of *oskar* mRNA (yellow) is directed to the posterior pole by MT plus-end directed motor Kinesin. A-B adapted and edited from Bilder (Horne-Badovinac and Bilder, 2005); C-E adapted and edited from Steinhauer and Kalderon (Steinhauer and Kalderon, 2006).

1.3. MT nucleation and the generation of non-centrosomal MT arrays

MTs are the cytoskeletal filaments with the largest diameter. MTs are constructed from α/β -tubulin heterodimers. The head to tail assembly of α/β -tubulin heterodimers into linear protofilaments confers polarity on the MT, with α -tubulin at the slower growing minus-end and β -tubulin at the faster growing plus-end (Desai and Mitchison, 1997). MTs act as directional tracks for the transport of organelles and cargos by molecular motors: Kinesin subfamily drives cargos to the plus-end; while Dynein drives cargos to the minus-end (Kamal and Goldstein, 2002).

In most of the proliferating and migrating animal cells, the centrosome is the main MT organisation centre (MTOC), leading to the formation of radial MTs, with minus-ends at the centrosomes and plus-ends extended to the cell periphery. The centrosome consists of a pair of centrioles and a pericentriolar matrix (PCM). PCM contains the γ -tubulin ring complex (γ TuRC), which is necessary to regulate the MT nucleation (Wiese and Zheng, 2006). By contrast, in some differentiated cells, for example muscle, epithelial and vascular plant cells, MTs are organised in non-centrosomal arrays that are not radial but usually linear. A three step model has been proposed for generating linear, non-centrosomal MT arrays: (1) generation of non-centrosomal MTs; (2) movement of non-centrosomal MTs to assembly sites and (3) assembly of non-centrosomal MTs into linear arrays. Non-centrosomal MTs are the key building blocks for the formation of non-centrosomal MT arrays. They can be generated by three mechanisms: release from centrosomes, nucleation from non-centrosomal sites and breakage distal to the non-centrosome. Once non-centrosomal MTs are generated, they are brought to sites where they can be assembled into linear arrays (Bartolini and Gundersen, 2006).

1.4. MT organisation of the oocyte during *Drosophila* oogenesis

Throughout oogenesis, MTs in the oocyte are highly dynamic and successively required in several steps for the establishment of the oocyte polarity. The following will address the role of MTs in polarity establishment at three different developmental stages: early oogenesis (stage 2-6); mid-oogenesis (stage 7-10a) and late-oogenesis (after stage 10b).

During early oogenesis, MTOCs reside at the posterior of the oocyte, from where MTs extend through ring canals into the nurse cells (Theurkauf et al., 1992; Clark et al., 1997). Along these MTs, a number of mRNAs produced in the nurse cells are transported into the oocyte and accumulate at the posterior (Bashirullah et al., 1998; Pokrywka and Stephenson, 1995). *gurken* mRNA is one of these mRNAs and encodes a TGF- α homologous protein. The locally restricted TGF- α signaling from the oocyte to the underlying follicle cells at the posterior specifies those follicle cells to adopt a posterior fate (Fig. 1C). These posterior cells then send an unidentified signal back to the oocyte, thereby inducing the repolarisation of the MT cytoskeleton and the migration of the oocyte nucleus to the dorso-anterior corner of the oocyte (Fig. 1D) (Neumansilberberg and Schupbach, 1993; Roth et al., 1995).

During mid-oogenesis, upon receiving the back signaling from the posterior follicle cells at about stage 6 to 7, MTs within the oocyte rearrange, and mediate the establishment of the final axial polarity within the oocyte. The reorganised MTs direct the localisation of *bicoid* mRNA to the anterior corners and *gurken* mRNA to the dorso-anterior corner of the oocyte, probably via MT minus-end directed motor Dynein (Duncan and Warrior, 2002; Januschke et al., 2002; Schnorrer et al., 2000). Analogously, MTs direct the localisation of *oskar* mRNA to the posterior pole by MT plus-end directed motor Kinesin (Brendza et al., 2000). Such asymmetric RNA localisation is essential for embryonic patterning: localisation of *bicoid* mRNA to the anterior and *oskar* mRNA to the posterior specifies the anterior-posterior (A/P) axis; localisation of *gurken* mRNA to the dorsal-anterior corner specifies the dorsal-ventral (D/V) axis (Riechmann and Ephrussi, 2001). Thus, axis determination of the fly

occurs during mid-oogenesis.

Given that the MT dependent transport of mRNAs exhibit a clear anterior-posterior polarity, the MTs of the oocyte are thought to be polarised from anterior to posterior. This idea is supported by the studies using MT motor proteins fused to the *E.coli* β -galactosidase protein. Fusion protein KHC:: β -Gal contains the motor domain of Kinesin heavy chain (KHC) and accumulates at the posterior pole of the oocyte, indicating the posterior MT plus-ends accumulation (Clark et al., 1994). Conversely, fusion protein NOD:: β -Gal contains the motor domain of Kinesin-related protein (NOD) and accumulates at the anterior corners of the oocyte. As NOD:: β -Gal is found at the minus-ends of MTs in other cell types, in which the MT polarity is well established, the localisation of NOD:: β -Gal in the oocyte is taken as the area where minus-ends are focused (Clark et al., 1997). However, the use of these markers is not enough to explain the complex MT organisation of the oocyte at this stage. The study of MT organisation in fixed samples at the level of individual MTs does not reveal a clear anterior-posterior polarisation within the MT network of the oocyte (Cha et al., 2001). Live images of stage 9 oocytes with fluorescently labelled MTs from transgenic GFP:: α -tubulin reveal that the MT organisation appears as a random network lacking detectable order; and MTs are more abundant at the anterior than at the posterior of the oocyte (Serbus et al., 2005). In support of the gradient of MT density from the anterior to posterior, the measurement of fluorescent signals of the MT marker along the oocyte cortex depicts a decrease of signals from anterior to posterior (Cha et al., 2002).

Although numerous genes affecting the MT organisation during mid-oogenesis have been identified (Steinhauer and Kalderon, 2006), none of them is shown to be a MT organising factor or to interact directly with MTs. Thus, how the organising of MTs in the oocyte is regulated remains elusive. An early study using the MT inhibitor colcemid to depolymerise MTs of the oocyte suggested that MTs nucleate primarily at the anterior cortex, as short MTs were only found at the anterior cortex after treatment (Theurkauf et al., 1992). Recent studies suggest that MTs are emanating from the anterior and lateral cortex of the oocyte at stage 9-10. This is supported by the fact

that antibodies for components of the γ TuRC are detected at the entire oocyte cortex. Given that the density of MTs is extremely low at the posterior pole of the oocyte, it was proposed that the γ TuRC might be locally inactivated (Cha et al., 2002). Recently, Januschke (Januschke et al., 2006) showed that during stage 7 to 8, MTs nucleate from a centrosome that is associated with the oocyte nucleus at the anterior-dorsal corner. The authors proposed that MTs nucleate from the centrosome and are released and subsequently captured at cortical sites at stage 9. If this is true, it would be analogous to the situation in epithelial cells mentioned above, where MTs nucleate from the centrosome, and subsequently are released and captured at the apical cortex (Bartolini and Gundersen, 2006). Nevertheless, considering the γ TuRC detected at the oocyte cortex, several issues remain to be elucidated: First, whether the γ TuRC is capable for nucleating MTs or solely for anchoring MTs; second, how the γ TuRC localisation to the cortex is mediated; and third, what is the biological significance of cortical localisation of the γ TuRC.

From stage 10b, the content produced in nurse cells is rapidly transferred into the oocyte in a process called dumping. Dumping is accompanied by a fast and unidirectional movement of cytoplasm called fast ooplasmic streaming. Streaming facilitates the dispersal of nurse cell contents within the oocyte. It has been shown that fast ooplasmic streaming is essential for the posterior accumulation of the axis determinant *nanos* mRNA (Forrest and Gavis, 2003). In addition, *oskar* mRNA can be localised by fast ooplasmic streaming (Glotzer et al., 1997).

Concomitantly with fast ooplasmic streaming, MTs in the oocyte are rearranged into parallel arrays in the subcortical region (Serbus et al., 2005; Theurkauf et al., 1992). It has been shown that MTs are required for fast ooplasmic streaming as treating egg chambers with colcemid blocked the streaming (Theurkauf, 1994). Another factor required for the onset of fast streaming is Kinesin, as in *Kinesin heavy chain (Khc)* null mutants fast ooplasmic streaming is completely abolished (Palacios and St Johnston, 2002; Serbus et al., 2005). A model for fast ooplasmic streaming involving MTs and Kinesin has been proposed: Kinesin transports cargos to the MT plus-ends, exerting the force on the surrounding cytoplasm. The concerted movement of multiple

Kinesin transportations along the MTs that are oriented in the same general direction creates the fast streaming (Serbus et al., 2005). In weak *Khc* mutants parallel MT arrays completely disappear at stage 11. As in 27% of weak *Khc* mutants fast streaming is still initiated, it was proposed that the Kinesin dependent fast ooplasmic streaming activity above a certain threshold is required to wash the MTs into arrays in subcortical regions (Serbus et al., 2005). Nevertheless, how the rearrangement of the MT cytoskeleton is accomplished from mid-oogenesis to late-oogenesis (stage 10a to stage 10b) remains to be further elucidated.

1.5. The role of actin for the MT organisation of the *Drosophila* oocyte

Actin is a globular protein that exists in a dynamic equilibrium, cycling between monomeric and filamentous states. Filamentous actin occurs in many different forms, for example, the cortical actin found in all cells; the thin filaments found in muscle sarcomeres. The question rises that what determines the organisation of actin into different structures. In many organisms multiple actin isoforms are expressed. For example, in *Drosophila*, there are six actin proteins. The sequence of different actins does affect their ability to incorporate into different actin structures (Roeper et al., 2005). It has been proposed that different actin isoforms interact with different sets of actin-binding proteins to perform specialised functions (Jacinto and Baum, 2003). Although individual actin-binding proteins can influence the formation of different actin structures, the cell needs to coordinate the activity of distinct sets of actin-binding proteins to build up specific structures as required. The small Rho GTPases have been shown to play important roles for mediating the construction of different actin structures in response to specific intracellular or extracellular cues (Hall, 1998).

For long time it has been proposed that the MT reorganisation in the *Drosophila* oocyte from stage 10a to 10b is regulated by the actin cytoskeleton. The finding, that the thick peripheral network of actin filaments observed in stage 10a oocyte is

decreased in the thickness at stage 10b when MTs reorganise, suggests that MTs can not reorganise until the actin dissipates (Riparbelli and Callaini, 1995). This idea is supported by the fact that the treatment with drugs sequestering actin monomers of stage 9/10a oocytes induces premature fast ooplasmic streaming and the formation of subcortical MT arrays (Manseau et al., 1996). Additionally, mutations in the actin-binding proteins *chickadee* (*chic*), *spire* (*spir*) and *cappuccino* (*capu*) cause similar phenotypes, with the induction of premature streaming and the formation of MT arrays (Emmons et al., 1995; Manseau et al., 1996; Theurkauf, 1994). These evidences support the hypothesis that the actin cytoskeleton is regulating the reorganisation of the MT cytoskeleton in the oocyte. However, how the regulation between actin and MT cytoskeleton is achieved and the functional relationships between these two cytoskeletal elements remain elusive.

1.6. The function of Par-1 during *Drosophila* oogenesis

The *par* (*partitioning defective*) genes have been discovered in a screen for mutants that affect anterior-posterior polarity in the *C.elegans* one cell embryo (Kemphues et al., 1988; Morton et al., 2002; Watts et al., 1996). In *Drosophila* homologues of *par* genes which have been identified to be essential for the polarity establishment in epithelial cells, neuroblasts and the oocyte (Benton et al., 2002; Kuchinke et al., 1998; Petronczki and Knoblich, 2001; Shulman et al., 2000; Tomancak et al., 2000; Wodarz, 2000). The mammalian homologues were implicated in the specification of distinct membrane domains in cultured epithelial cells (Suzuki et al., 2001; Lin et al., 2000; Joberty et al., 2000; Izumi et al., 1998).

One of the *par* genes is *par-1*, which encodes a serine/threonine kinase. In the *Drosophila* female germline, Par-1 is involved in several polarisation events. First, Par-1 is required to maintain the oocyte cell fate. In germline clones of *par-1* null allele, the oocyte fails to polarise during early oogenesis and reverts to nurse cell fate, resulting in the egg chamber with 16 nurse cells (Cox et al., 2001; Huynh et al., 2001). Second, during mid-oogenesis Par-1 is required for proper MT organisation in the

oocyte. In *par-1* mutants MT are nucleating from the entire oocyte cortex including the posterior pole, directing their plus-ends towards the centre of the oocyte. In these mutants, *oskar* mRNA is mislocalised to the centre of the oocyte, which is most likely the consequence of aberrant MT organisation (Tomancak et al., 2000; Shulman et al., 2000). Finally, beginning from stage 9, accumulation of Par-1 at the posterior pole of the oocyte guarantees the maintenance of posterior polarity by phosphorylating, and thus stabilising, Oskar protein (Riechmann et al., 2002).

Multiple isoforms encoded by *par-1* gene (N1, N2, and N3) have been identified. The Par-1 N1 isoform appears to play an important role in polarising the oocyte because Par-1 N1 fully rescues the polarity defects of *par-1* hypomorphs. GFP-tagged Par-1 N1 (GFP- Par-1 N1) is recruited to the posterior cortex of the oocyte at stage 7 in response to the back signaling from the follicle cells. Thus, it has been suggested that the posterior Par-1 N1 polarises the MT cytoskeleton (Doerflinger et al., 2006).

The mammalian Par-1 homologues belong to MAP/MT affinity regulating kinase (MARK) family. MARK proteins phosphorylate MT associated proteins (MAPs) Tau, MAP2 and MAP4, thereby reducing their affinity for MTs and consequently destabilising MTs (Drewes et al., 1995). This suggests the possibility that Par-1 is a direct mediator for MT organisation in the oocyte. However, mutations in *Drosophila* Tau do not disrupt oocyte polarity, implying that Tau may be not an essential target of Par-1 in the oocyte. On the other hand, *Drosophila* Par-1 seems to regulate MTs by a different mechanism from that proposed for MARKs, because Par-1 stabilises MTs in epithelial cells, while the MARKs destabilise MTs (Doerflinger et al., 2003). Thus, downstream effectors of *Drosophila* Par-1 for regulating MTs of the oocyte remain to be identified.

As GFP- Par-1 N1 is recruited to the posterior cortex of the oocyte at stage 7, it has been suggested that GFP- Par-1 N1 is the earliest posterior marker of the oocyte (Doerflinger et al., 2006). One question raised by this result is how the posterior recruitment of Par-1 N1 is accomplished. The treatment with the actin-destabilising drug latrunculinA abolishes the posterior enrichment of GFP Par-1 N1, suggesting that Par-1 N1 is recruited to the posterior in an actin dependent way (Doerflinger et al.,

2006). However, the upstream activators that regulate the actin cytoskeleton organisation for directing the posterior recruitment of Par-1 N1 remain elusive.

1.7. Screening for targets of Par-1 kinase

To identify Par-1 substrates a proteomic screen has been performed (Riechmann and Ephrussi, 2004). The first release of the *Drosophila* collection of Expressed Sequence Tags (EST) produced by the Berkeley *Drosophila* Genome Project (BDGP) was screened. Among the 5849 screened cDNAs, 133 (2.2%) encode proteins that were phosphorylated by Par-1 kinase in vitro. Those were analysed using data provided by the BDGP and FlyBase. Based on the presence of certain protein domains, homologies to proteins from other species and functional data, seven groups of substrates were classified: Cytoskeletal proteins (11), proteins involved in different aspects of signal transduction (35), DNA-associated proteins (34), RNA-associated proteins (11), enzymes (9), novel proteins (25) and others (9).

1.8. Tao-1 kinase

CG14217 gene was identified in the screen for Par-1 phosphorylation substrates and classified into the group of proteins involved in the signal transduction. CG14217 is the *Drosophila* homologue of mammalian Tao-1 (Thousand And One amino acid). *Drosophila* Tao-1 shares 50% identity to Human Tao-1 and 43% to Rat Tao-1. Tao-1 belongs to the Ste20 like kinase family. The Ste20 group kinases are characterised by the presence of a conserved kinase domain and a non-catalytic region of great structural diversity that enables the kinases to interact with various signaling molecules and regulatory proteins of the actin cytoskeleton (Dan et al., 2001).

In vitro studies revealed that mammalian Tao-1 is an upstream kinase of the mammalian Par-1 homologue MARK. Tao-1 activates Par-1 by phosphorylation. In cell culture experiment, the activity of Tao-1 enhances MT instability through the activation of MARK and leads to phosphorylation and detachment of Tau and other MAPs from MTs (Timm et al., 2003).

In the *Drosophila* oocyte, Tau is not an essential target of Par-1 as mentioned above. Nevertheless, overexpression of Tau in *Drosophila* eyes reduces the size of eyes and disrupts the regular arrays of lenses. To investigate the mechanism responsible for Tau function, a screen was conducted to search for genetic modifiers which enhance or suppress the eye phenotype induced by overexpression of Tau. Both Par-1 and Tao-1 were recovered in this screen. Overexpression of Par-1 suppresses, while overexpression of Tao-1 enhances the eye phenotype (Shulman and Feany, 2003).

To summarise, *Drosophila* Tao-1 was identified as a Par-1 phosphorylation target. Studies in the *Drosophila* eye revealed that Par-1 and Tao-1 have opposite roles in regulating the function of Tau. This raises the possibility that *Drosophila* Par-1 negatively regulates Tao-1 by phosphorylation. This suggestion is in contrast to the cell culture studies of mammalian homologues of Par-1 and Tao-1. The mammalian homologue of Tao-1 was shown to activate Par-1 by phosphorylation. These evidences implicate a complex cross regulation between Tao-1 and Par-1. The study of the role of Tao-1 in the oocyte may help to gain insight into Tao-1 function in regulating the cytoskeleton.

1.9. Aims

The first aim of this thesis is to understand the architecture of the *Drosophila* oocyte cytoskeleton. Of particular interest is the reorganisation of the cytoskeleton at the onset of fast ooplasmic streaming and the functional relationship between the actin and MT cytoskeleton. The second aim is the characterisation of different *Tao-1* alleles regarding their oogenesis phenotypes.

2. MATERIALS AND METHODS

2.1. Genomic sequence, EST and fly stock searches

Searches for annotated *Drosophila* genomic sequences, *Drosophila* ESTs and *Drosophila* P-element insertion strains were conducted using Flybase (<http://flybase.bio.indiana.edu/>). EST and cDNA sequences were obtained from the Berkeley *Drosophila* Genome Project (BDGP). (<http://www.fruitfly.org/EST/>).

2.2. Fly strains and genetics

2.2.1. *Drosophila melanogaster* strains

Stock genotype	Reference	Source
w; <i>γTub37C</i> ^l 40A 42B/CyO	(Schnorrer et al., 2002)	In our lab
w;;UASp <i>Dgrip75- GFP</i>	(Schnorrer et al., 2002)	In our lab
w; <i>oskar</i> ⁵⁴ / TM3 Ser	(Kimha et al., 1991)	In our lab
w;; <i>Df(3R)p-XT103</i> / TM3 Sb	(Lehmann and Nusslein-Volhard, 1986)	BL 1962
w; <i>UASp Actin5C-GFP</i> ;	(Verkhusha et al., 1999)	BL 7310
w; <i>maternal α-tubulin: Gal4-VPI6</i> ;TM2/TM3	(Martin and St, 2003)	In our lab
w;Bl/CyO; <i>nanos:Gla4-VPI6 Sb</i> /TM6	(Van et al., 1998)	In our lab
w; <i>chic</i> ¹³²⁰ ;	(Cooley et al., 1992)	BL 4891
w; <i>capu</i> ¹ ;	(Emmons et al., 1995)	In our lab
w; <i>spire</i> ¹ ;	(Wellington et al., 1999)	BL 5113
w; <i>Df Exel 6046</i> /CyO;		BL 7528
w; <i>GFP-Capu</i> ;	(Rosales-Nieves et al., 2006)	S. Parkhurst lab
w; <i>GFP-SpireD</i> ;	(Rosales-Nieves et al., 2006)	S. Parkhurst lab
w; <i>capulet</i> ¹⁰ FRT40A /CyO	(Baum et al., 2000)	B.Baum lab
w; <i>ovo</i> ^{D1} FRT 40A / Ms(2)M ¹ / CyO	(Chou et al., 1993)	In our lab
w <i>moesin</i> ^{G0415} /FM7;;	(Jankovics et al., 2002)	BL 12015
w <i>moesin EP</i> ¹⁶⁵²	(Jankovics et al., 2002)	BL 11272
w; <i>swallow</i> ¹ ;;	(Meng and Stephenson, 2002)	In our lab
w; FRT 42B <i>Khc</i> ²⁷ /CyO;	(Brendza et al., 2000)	In our lab
w; FRT 42B <i>ovo</i> ^{D1} / Ms(2)M ¹ / CyO	(Chou et al., 1993)	In our lab
w <i>hs Flp</i> ;Sp5/ SM6-TM6	(Chou and Perrimon, 1992)	In our lab
w <i>P{EP}Tao-1</i> ^{EP1455} ;;	(Spradling et al., 1999)	BL 11458

w; <i>transposase Δ2-3</i> , Sb/TM6	(Robertson et al., 1988)	In our lab
w;Grk/CyO; <i>Kin LacZ</i>	(Clark et al., 1994)	In our lab
w; <i>Nod LacZ143.2</i> /TM3 Sb	(Clark et al., 1997)	In our lab
w <i>PBac{RB}e01713</i> ;;	(Thibault et al., 2004)	Exelixis collection
w <i>P{XP}d02300</i> ;;	(Thibault et al., 2004)	Exelixis collection
w;; <i>hs Flp MKRS</i> /TM6	(Chou and Perrimon, 1992)	In our lab
w <i>GFP FRT 19A</i> / FM6;;	(Xu and Rubin, 1993)	In our lab

2.2.2. Fly maintenance and egg laying collection

The flies were maintained under standard conditions (Ashburner, 1989). Without specification, the flies were grown up at 25°C. Three- to four-day old females were well fed with yeast paste before dissection.

For the egg laying and embryo collection, females were kept in a cage and the eggs were collected on an apple juice agar plate. The plate was changed once a day and the hatching rate was counted at least two days later.

2.2.3. Expression using the UAS/GAL4 system

In *Drosophila*, the GAL4/UAS system is widely used to express genes of interest in a temporally and spatially regulated manner (Brand and Perrimon, 1993). This system uses two transgenes, a GAL4 driver and a GAL4-responsive UAS (upstream activation sequence) expression vector. The driver directs tissue or time point specific expression of the yeast transcription activator, GAL4, a sequence specific transactivator. The UAS vector contains its target sequence, UAS, and designed to drive the expression of the inserted cDNA sequence downstream of the UAS sequence when GAL4 is present. Combining appropriate GAL4 driver and UAS transgene allows conditional expression of cloned genes temporally and spatially. The original GAL4/UAS (Brand and Perrimon, 1993) system does not work in the germline. A modified UAS vector UASp overcomes this problem and allows the expression in the germline during oogenesis (Rorth, 1998).

2.2.4. Generation of HA-Tao-1 transgenic flies

4-kb *Tao-1* cDNA was cloned into pUASp2 vector (Rorth, 1998). To generate transgenic flies, DNA was injected into blastoderm stage embryos, according to Spradling and Rubin (Rubin and Spradling, 1982; Spradling and Rubin, 1982). The injected embryos were allowed to develop into flies, which were crossed to flies carrying balancers of the second and third chromosomes. The progeny with colored eyes were selected and stocks were established.

2.2.5. Generation of P-element imprecise deletions

In the Bloomington fly stocks, one P-element *Tao-1*^{EP(X) 1455} was identified to be inserted into the 5'UTR of *Tao-1* about 2kb upstream of the start codon. Homozygous females carrying this P-element *Tao-1*^{EP(X)1455} were crossed to males carrying the $\Delta 2-3$ transposase transgene (Robertson et al., 1988). The progeny males carrying both the P-element and the transgene were crossed to females carrying the X chromosome balancer. Individual progeny females with white eyes were selected to cross with males carrying the X chromosome balancer to establish stocks. The lethality and the fertility of these flies were subsequently analysed.

2.2.6. Generation of the Exelixis deficiency

In the Exelixis collection of piggyBac and P-element insertions (Parks et al., 2004; Thibault et al., 2004), one piggyBac insertion *PBac{RB}e01713* was found to be inserted at the position about 300bp upstream of the *Tao-1* open reading frame. Downstream of the *Tao-1* locus, P-element insertion *P{XP}d02300* was found to be in the first intron of CG32532, the third gene downstream of *Tao-1*. Females carrying *PBac{RB}e01713* were crossed to males carrying the transgene of the heat shocked induced Flipase (FLP) recombinase. Progeny males carrying both the insertion and the transgene were crossed to females carrying *P{XP}d02300*. After two days the progeny were heat shocked for one hour at 37°C per day. This procedure was repeated

for four days. The progeny were then raised to adulthood, and virgin females were crossed to males carrying the balancer of the X chromosome, FM6. The progeny females with white eyes were selected to cross with FM6 males to establish the stocks. The loss of colored eyes is the result of the trans-recombination between the FLP-recombination target (FRT) sites of *PBac{RB}e01713* and *P{XP}d02300*. Finally genomic PCR was conducted to verify the occurrence of the recombinant event.

2.2.7. Induction of germline clones by the FLP/FRT system

capulet¹, *Khc²⁷*, *Tao-1^{ETA}* and *Df 14.1* are lethal. To examine the oogenesis phenotype of these mutants, the FLP/FRT system of mitotic recombination was used to generate the homozygous clones of these lethal alleles (Xu and Rubin, 1993). The clones are marked either by the loss of GFP (Xu and Rubin, 1993) or by the loss of the dominant female sterile insertion *ovo^{D1}* (Chou et al., 1993).

[*w hs Flp;Sp5/ SM6-TM6*] females were crossed to [*w; ovo^{D1} FRT 40A / Ms(2)M¹ / CyO*] and [*w; FRT 42B ovo^{D1} / Ms(2)M¹ / CyO*] to harvest the males of [*w hs Flp/Y; ovo^{D1} FRT 40A/SM6-TM6*] and [*w hs Flp/Y; FRT 42B ovo^{D1} /SM6-TM6*] in the next generation respectively. These males were subsequently crossed to [*w; capulet¹⁰ FRT40A /CyO*] and [*w; FRT 42B Khc²⁷ /CyO;*] respectively. 24 hour pulses of progeny from these crosses were allowed to develop for another 24 hours, and then heat shocked for four days at 37°C for one hour per day in a water bath. In the non-*CyO* female individuals, heat shock induced expression of the FLP recombinase led to the mitotic recombination between the two FRT sites on the second chromosome homologs. A fraction of the germline cells thus became homozygous for *capulet¹⁰* or for *Khc²⁷*, while the others remaining *ovo^{D1}* would not develop further than stage 6.

For the lethal alleles of the X chromosome, *Tao-1^{ETA}* and *Df 14.1* were recombined to FRT 19A sites. [*w;;hs Flp MKRS/TM6*] females were crossed to [*w GFP FRT 19A/ FM6;*] to harvest [*w GFP FRT 19A/Y;; hs Flp MKRS/+*] males, which were subsequently crossed to [*w Tao-1^{ETA} FRT 19A/ FM6;*] or [*w Df 14.1 FRT 19A/ FM6;*]

females. The progeny were heat shocked as described above. A fraction of the germline cells thus became homozygous for *Tao-1^{ETA}* or for *Df 14.1* monitored by the loss of the copy of GFP.

2.3. Preparation of egg shell and larval cuticle

To visualise the egg shell under the microscope, eggs were washed with tap water and mounted in Hoyer's medium. For larval cuticle preparation, collected embryos were dechorionated using 50% bleach and washed in water with 0.1% Triton X-100 and followed in tap water. Embryos without chorions were fixed in 4% Formaldehyde (Polyscience) in PBS: heptane 1:1 solution at room temperature for 20 minutes, followed with vigorous shaking and removing the lower (aqueous) phase afterwards. Devitellinisation was done by adding methanol: heptane 1:1 solution and vortexing for half a minute, followed by removing all the supernatant and washing with methanol for several times. The devitellinised embryos were then transferred to a slide and mounted in a mixture of Hoyer's medium and lactic acid 2:1 after the methanol was evaporated. The mounted samples were incubated at 60°C for at least 24 hours before they were analysed by Zeiss Axiovert.

2.4. Drug treatment

2.4.1. LatrunculinA treatment

LatrunculinA (Molecular Probes) was initially dissolved in DMSO in a concentration of 1mM and stored in -20°C. Before use it was further diluted to the Graces insect medium (Sigma) to working concentrations described following. Controls were performed by adding identical volume of DMSO to the Graces medium. For immunohistochemistry, ovaries were dissected in the Graces medium and subsequently incubated for 45 minutes in Graces medium containing 2.8 µM latrunculin A at room temperature. Treated ovaries were fixed and immunolabelled. For time lapse microscopy, Graces medium containing 100µM latrunculinA and 0.4%

Trypan Blue (Sigma) was injected into the female abdomen. Live imaging was taken after two hour incubation.

2.4.2. Colcemid treatment

Colcemid (Sigma) was initially dissolved in water in a concentration of 1mg/ml and stored in 4°C. It was further diluted before use to 200µg/ml in water and mixed with some dry yeast. 2- to 3-day old female flies were fed with yeast paste containing the drug for 16 hours after five hours starvation. Afterwards ovaries were dissected and fixed as described below.

2.5. Immunohistochemistry and in situ hybridisation

2.5.1. Immunohistochemistry, mounting and sectioning

Ovaries were dissected in the Graces medium and then fixed for 10 minutes at room temperature in 8% methanol free formaldehyde (Polyscience) diluted in PBS. After 2 short washes in 0.1% PBT ovaries were blocked for one hour in 1%PBT containing 0.5% BSA. Incubation with the primary antibody was performed overnight at room temperature in 0.3% PBT with 0.5%BSA. After two short washes with 0.1% PBT, and one hour wash with 0.1 PBT containing 10% NGS, ovaries were incubated for two hours with a secondary antibody coupled to Alexa flouorochromes (Molecular Probes), and for Actin staining with rhodamine coupled phalloidin (Molecular Probes), followed by a final wash with 0.1% PBT.

For whole mounts, ovaries were mounted in vectashield (Vector Laboratories). For sections, stained ovaries were separated on a coverslip on a droplet of 0.1%PBT under a Stereomicroscope. Individual egg chambers were sorted and stage was determined according to the size, the ratio of nurse cells versus the oocyte and the epithelium morphology. Selected egg chambers were transferred from PBT to a droplet of Aquapolymount (Polysciences) on the same coverslip, and PBT was removed with a tissue. Egg chambers were cut manually into two slices of approximately 60µm with a

0.40*20mm injection needle (Sterican, Braun). Aquapolymount was polymerised overnight at room temperature. On the following day the coverslip was flipped upside down and mounted on a slide with Aquapolymount. After four hour incubation Aquapolymount was polymerised.

2.5.2. Primary antibodies for immunohistochemistry

The following primary antibodies were used:

antigen	source	working concentration	distributer
α -Tubulin FITC	mouse	1:10	Sigma
α -tyrosinated -Tubulin	rat	1:3000	Sero Tec
γ -Tubulin	mouse	1:100	Sigma
Green Fluorescent Protein (GFP)	mouse	1:100	Roche
Green Fluorescent Protein (GFP)	rabbit	1:2000	Molecular Probes
Oskar	rabbit	1:3000	In our lab
Gurken	mouse	1.50	Developmental Studies Hybridoma Bank, Iowa city, US
β -Galactosidase (Gal)	rabbit	1:100	Molecular Probes
Hemagglutinin (HA)	rat	1:100	Roche

2.5.3. In situ hybridisation

Digoxigenin (DIG)-labelled RNA probes corresponding to full-length *Tao-1*, *oskar*, *bicoid* and *gurken* mRNA were generated using Ambion Megascript kit and DIG RNA labelling mix (Roche). RNA *in situ* hybridisation was performed according to Tautz and Pfeifle (Tautz and Pfeifle, 1989). Ovaries were dissected in the Graces medium and fixed for 10 minutes at room temperature in 8% methanol free formaldehyde diluted in PBS. For alkaline-phosphatase detection, after a wash in 0.1%PBT, ovaries were incubated for five minutes with proteinase K (50 μ g/ml). After one wash with 2mg/ml glycine for two minutes to stop the digestion, ovaries were post-fixed in 4% formaldehyde in PBS for 10 minutes. The treatment of proteinase K and subsequent

post fixation was skipped for the fluorescence detection. After fixation or post-fixation, ovaries were washed with 1:1 hybridisation solution (Hyb1)/PBS for ten minutes and for next ten minutes with Hyb1. Pre-hybridisation required at least one hour of ovaries incubated in Hybridisation solution with 100 μ g/mg salmon sperm DNA (Sigma) (Hyb2) at 55°C. 1-2 μ l of the probe was added to 50 μ l Hyb2 and allowed to hybridise over night at 55°C. On the next day, the probe was removed and the ovaries were rinsed with the prewarmed Hyb1 and washed four times 30 minutes at 55°C in Hyb 1 and in a series of Hyb1/ PBST mixture in proportions of 4:1, 3:2, 2:3 and 1:4 for 10 minutes at 55°C except the last wash, which was done at room temperature (RT).

For the fluorescence detection, ovaries were incubated with POD-conjugated anti-DIG antibody in 0.1%PBT (1:100, Roche) for at least one hour at RT. After three ten minute washes with 0.1%PBT, Cy3-conjugated HRP (anti-horse radish peroxidase) (1:75) antibody was added to the amplification solution and allowed to incubate for 30 minutes. After 2 washes in 0.1%PBT ovaries were mounted in vectashield medium. For the alkaline-phosphatase detection, ovaries were incubated with alkaline-phosphatase conjugated anti-DIG antibody in 0.1%PBT (1:500, Dianova) for at least one hour. After several washes in 0.1%PBT over 45 minutes, ovaries were transferred into alkaline-phosphatase staining buffer (100mM NaCl, 50mM MgCl₂, 100mM Tris-Cl, pH 9.5, 0.2% Tween) and incubated for five minutes. The antibody bound to the epitope was visualised by a blue alkaline-phosphatase reaction. The reaction was initiated by adding NBT and X-phosphate to the staining buffer (for 1ml staining buffer: 4.4 ml of 75mg/ml NBT and 3.5ml of X-phosphate). The reaction was monitored and stopped with several washes of 0.1% PBT. Ovaries were mounted in 100% glycerol.

2.6. Microscopy and image processing

2.6.1. Confocal microscopy and image analysis

All pictures were taken with a Leica SP2 confocal microscope. Fluorescence intensities in the region of interest from the oocyte cortex to the interior were measured by ImageJ v1.35 (National Institutes of Health, Bethesda, Maryland, USA, <http://rsb.info.nih.gov/ij/>). The measurement results were imported as ascii format to the graphing and analysis program Origin Pro v6 (OriginLab cooperation, www.originlab.com). The intensities of the fluorescence signals were normalized by the maximum value. Pixels at the exterior border of cortex were set as zero in the pixel sequences. The graphs in Fig. 7, 10 and 18 were plotted using pixel sequence (from the cortex to the center as the X axes) and the normalized intensities of fluorescence signals (as Y axes). The full width at half maximum (FWHM), used to describe the width of the distribution curve, was defined by the distance between points on the curve at which normalized intensity value is 0.5.

2.6.2. Time lapse microscopy

For live imaging, 0.4% Trypan Blue dye (Sigma) in the Graces medium was injected into the female abdomen. For latrunculinA treatment, Graces medium containing 100 μ M latrunculinA and 0.4% Trypan Blue was injected. After two hour incubation, the ovaries were dissected under halocarbon oil and covered with a YSI Do membrane (Yellow Springs Instrument, Ohio) for live imaging. Time-lapse movies were recorded with a Leica SP2 confocal microscope by taking images every 30 second. All movies were compressed to 232 x real time using QuickTime. Thus, 3.8 seconds of movie represents 15 minutes of real time. As an alternative way to visualise the endosome movements of the oocyte, the Kalman stacks function provided by ImageJ v1.35 was applied. Although Kalman averaging is normally used to reduce noise in images of stationary objects, moving particles become increasingly blurred as the

number of scans is increased, and the direction of blurring indicates the orientation of their motion. Using this technology, ten images representing 10 consecutive time points was projected into a single layer.

2.7. Genomic PCR and sequencing

2.7.1. Oligonucleotides

Oligonucleotides were designed by Vector NTI 9.0.0 and purchased from Sigma. The pellet was resuspended in water at a concentration of 100 μ M and stored at -20° C. Aliquots of 10-20 μ M were made and 1 μ l was used in 25 μ l PCR reactions.

Oligo Name	Purpose	Sequence
UP1	EP excision mapping& sequencing	ATACACACACGTACACGAGC
Low9	EP excision mapping& sequencing	CGGTATTTGACTTAGCGAACTGA
Invert seq in EP	EP excision mapping& sequencing	TCGACGGGACCACCTTATGTTATTCATCATG
For1	<i>Tao-1</i> locus sequencing	TGCGTTAAAGCGTGCAAAGC
Rev1	<i>Tao-1</i> locus sequencing	TTCAGGCGCACATCGATTGC
SeqA403	<i>Tao-1</i> locus sequencing	ACCAAGGACACGGTAGCGA
SeqA801	<i>Tao-1</i> locus sequencing	CAGTACCACATCCTGTTC
SeqA1201	<i>Tao-1</i> locus sequencing	CCACACAACCTCACCTACG
SeqA1603	<i>Tao-1</i> locus sequencing	ACGAACAGGTGAACGCGGT
SeqA2001	<i>Tao-1</i> locus sequencing	TTTAGGATGTTGCTACAT
SeqA2401	<i>Tao-1</i> locus sequencing	CACGAAGGTGGTCAACAA
SeqA2810	<i>Tao-1</i> locus sequencing	TGCAAATCCCATTATTC
SeqA3205	<i>Tao-1</i> locus sequencing	TGTAATTAGTGATAGAGC
SeqA3602	<i>Tao-1</i> locus sequencing	TAGATACTCGACTAAAAC
SeqA4005	<i>Tao-1</i> locus sequencing	ATGAACAATTTTATAAAC
SeqA4401	<i>Tao-1</i> locus sequencing	GGCGTGGAGTTTGTGTG
SeqA4802	<i>Tao-1</i> locus sequencing	TTGAATCAAATCGAATCG
For2	<i>Tao-1</i> locus sequencing	CGATTCCCTCGGAATGTTGG
Rev2	<i>Tao-1</i> locus sequencing	CATAGATAATCCACCTCCATGGGC
SeqB415	<i>Tao-1</i> locus sequencing	CTTTTATTTGAATCAAATCG
SeqB801	<i>Tao-1</i> locus sequencing	TTTGTTGATCTTTGCTTG
SeqB1201	<i>Tao-1</i> locus sequencing	TAGCGGCGATTTCTGTTG
SeqB1611	<i>Tao-1</i> locus sequencing	GCGCGTTCCTGGTTGAAT
SeqB2008	<i>Tao-1</i> locus sequencing	TGTTACCGAGCAGCGTCA

Oligo Name	Purpose	Sequence
SeqB2401	<i>Tao-1</i> locus sequencing	GTGCATTATGGCTGGGCA
SeqB2801	<i>Tao-1</i> locus sequencing	CGTCGACTCATCCATGGA
SeqB3201	<i>Tao-1</i> locus sequencing	TCTGTTCGTGCATCTCCT
SeqB3601	<i>Tao-1</i> locus sequencing	ACCTTGGTCCTTTTCGGGA
SeqB4003	<i>Tao-1</i> locus sequencing	AGTGTTTAAACTATTGAG
SeqB4412	<i>Tao-1</i> locus sequencing	GGGGGTAACGAGTACAGT
SeqB4805	<i>Tao-1</i> locus sequencing	TGGATGGCGGAAGCGTAGC
For3	<i>Tao-1</i> locus sequencing	CTCCGCTCTGGCTAGGAAATTACACAGG
Rev3	<i>Tao-1</i> locus sequencing	TCGGTGCTTGGCACTCGAGATG
SeqC2	<i>Tao-1</i> locus sequencing	TCCGCTCTGGCTAGGAAA
SeqC401	<i>Tao-1</i> locus sequencing	GATCCCTTATAGTGCCCA
SeqC812	<i>Tao-1</i> locus sequencing	ATGCGGCAGCACGGAAAT
SeqC1201	<i>Tao-1</i> locus sequencing	AAGGACAGCTCATGCTCA
SeqC1618	<i>Tao-1</i> locus sequencing	CATTCAAATTGCACTTAC
SeqC2008	<i>Tao-1</i> locus sequencing	GTATTGGCCCTCGTCCAT
SeqC2401	<i>Tao-1</i> locus sequencing	GATTAGAAGTCACTCGGG
SeqC2801	<i>Tao-1</i> locus sequencing	AAAGGCGATTCCGGTTAG
SeqC3201	<i>Tao-1</i> locus sequencing	CAGCTGCTTTTTGGCCAG
SeqC3613	<i>Tao-1</i> locus sequencing	AGCTCCGGCTTTCGCCTAT
SeqC4001	<i>Tao-1</i> locus sequencing	GCCGAAAAAGAACGCACG
SeqC4401	<i>Tao-1</i> locus sequencing	CCAAAACGCAAACGCGAA
SeqC4803	<i>Tao-1</i> locus sequencing	ACGAATCCGCACTGGCTA
For4	<i>Tao-1</i> locus sequencing	ATTCTGGGGGATCGTTACGTCG
Rev4	<i>Tao-1</i> locus sequencing	CTCGCCGCTAAGCATTATGC
SeqD1902	<i>Tao-1</i> locus sequencing	AGGTGGCGCGAGAAAAGC
SeqD1519	<i>Tao-1</i> locus sequencing	GACTATGACTATGATGCG
SeqD1106	<i>Tao-1</i> locus sequencing	CACCAAGTGCTTCGCGAT
SeqD718	<i>Tao-1</i> locus sequencing	TGCATAGTTGTAAATAAC
SeqD304	<i>Tao-1</i> locus sequencing	AACTAATTGAATTGAGCG
RB+NR1(genomic)	Exelixis deficiency sequencing	ATGTGGACTACGCTGATCCTCCGG
XP+(genomic)	Exelixis deficiency sequencing	GGACATCCCGACCATTCTGGCC
RB+	Exelixis deficiency sequencing	ACCACGGACATCACCACCCG
RB3'+	Exelixis deficiency sequencing	TGCATTTGCCTTTTCGCCTTAT
XP5'+	Exelixis deficiency sequencing	AATGATTCGCAGTGGGAAGGCT

2.7.2. Extraction of genomic DNA

8-15 freshly hatched flies were collected and frozen at -80°C . After a minimum of five minutes, the flies were added with 200 ml of Buffer A (100mM Tris-HCl, pH 7.5; 100mM EDTA; 100mM NaCl; 0.5% SDS) and smashed by a 200 μl tip. After the mixture got homogeneous, another 200 ml of Buffer A was added. After 30 minute incubation at 65°C , 800ml of 1:2.5 [5M] KOAc: [6M] LiCl mixture was added, followed by ten minutes precipitation on ice. After centrifuging at 14000 rpm for 15 minutes, the supernatant was transferred to new tubes. Approximately 7/10 volume ethanol was added before centrifuging at 14000 rpm for another 15 minutes. The supernatant was removed and the pellet was washed with 1ml of cold ethanol, before centrifuging at 14000 rpm for five minutes. The supernatant was removed and the pellet was suspended in 100ml of TE. Equal volume of phenol was added to the sample and mixed vigorously. After centrifuging, the top (aqueous) phase was transferred to new tubes. The same procedure was applied with phenol: chloroform: isoamyl alcohol (25:24:1) and chloroform: isoamyl alcohol (24:1) subsequently. The volume of the recovered sample was noted. 1/10 volume of NaOAc (3M, pH 5.2) and 2X volume of ethanol were added and followed by a centrifuging at 14000 rpm for 15 minutes. The ethanol was removed and 1ml of cold 70% ethanol was added, followed by centrifuging at 14000 rpm for five minutes. Finally, after the ethanol was removed, the pellet was dried completely and resuspended in 50 μl of water, which can be used as the template for PCR reactions.

2.7.3. Genomic PCR

1 μl of genomic DNA (approximately 10ng) and 1 μl of each primer were used in 25 μl PCR reaction. The other components of the PCR reaction were 1 μl of 10mM dNTP, 0.5 μl of High Fidelity Taq Polymerase and 2.5 μl 10X (Mg^{2+} containing) Buffer 3 (Expand Long Template PCR System, Roche). The reaction was carried out in Mastercycler gradient (Eppendorf). The PCR program included a denaturation step of

two minutes at 94°C followed by 30 cycles: 15 seconds at 94°C, 15 seconds at 50°C, the annealing temperature and a few minutes at 68°C, the extension temperature, dependent on the length of the amplified fragment. The amplification speed was calculated as approximately 1kb per minute. The program ended with a final extension of 10 minutes at 72°C. If the amplified fragment is longer than 5kb, after ten cycles the extension time was prolonged with 20 seconds per cycle in last 20 cycles. PCR products were analysed in a 1% agarose gel. For sequencing analysis, PCR products at expected size were purified by DNA and Gel band Purification Kit (GE Healthcare)

2.7.4. Sequencing

For sequencing, the DNA template of approximately 200ng and 1µl of primer were added to the buffer and the Big Dye provided by the Big Dye Terminator v3.1 Cycle Sequencing Kit. The reaction program included one minute in 94°C and 90 cycles as following: 30 seconds at 94°C, 15 seconds at 50°C and four minutes at 60°C. The sequencing analysis was done by the Sequencing Facility Centre, University of Cologne. Sequencing results were aligned by Basic Local Alignment Search Tool (BLAST) provided by The National Centre for Biotechnology Information (NCBI) (<http://www.ncbi.nlm.nih.gov/BLAST>)

2.8. Northern blot analysis

Ovaries from 15 females were dissected in Graces medium and immediately frozen in liquid nitrogen. Total RNA was extracted by RNeasy Mini Kit (QIAGEN). 2 to 5µl of RNA about 10µg was mixed with 2.5 µl 10X MOPS [0.2 M MOPS (Sigma), 50mM Sodium Acetate (Roth), 10mM EDTA, pH 7.0], 4µl of 37% Formaldehyde (Roth), 10µl of Formamid (Roth), 1µl of Ethidium Bromide (Sigma). The mixture was incubated at 65°C for ten minutes and kept on ice with the addition of 2.5µl RNA loading buffer. The RNA is separated in 1.5% Agarose gel containing 1X MOPS and 6.66% Formaldehyde. The electrophoresis was done in 1X MOPS buffer at 40 to 50 V

for three to four hours. The gel was photographed together with a ruler. After one time wash of DEPC water, 20 minutes in 0.05N NaOH and 20X SSC buffer, the gel was ready for transfer. The nylon membrane was rinsed with DEPC water and washed for five minutes in 10X SSC. RNA in the gel was transferred to the membrane in 20X SSC over night. On the next day the membrane was rinsed in 6X SSC for five minutes and subject to UV-crosslinking for six minutes. Pre-hybridisation required at least three hours of the membrane incubated in the hybridisation solution at 48°C. The ³²P-labeled probe for the hybridisation prepared from the fragment of *Tao-1* full cDNA digested by BamH1-EcoR1 was added to the hybridisation solution and allowed to hybridise over night at 48°C. On the next day, the probe was removed and the blot was washed three times 20 minutes at 68°C in a series of mixtures of 2XSSC/ 0.1%SDS, 1XSSC/ 0.1%SDS and 0.5XSSC/ 0.1%SDS. The blot membrane was covered with Saran Wrap and exposed to films.

2.9. Western blot analysis

Ovaries from 3-8 females were dissected in Graces medium and immediately frozen in liquid nitrogen. The ovaries were homogenised in 95°C preheated 1x SDS buffer (60mM tris-Cl pH 6.8, 6.4% glycerol, 2% SDS, 100mM DTT, Bromophenol blue) calculated by approximately 15ml per female followed by two times of the following procedures: three minutes in sonification bath, vortexing, three minute incubation at 95°C. The ovary extracts were then centrifuged at 14000 rpm for one minute. The aliquots of the supernatant were stored in -20°C and ready for the electrophoresis.

The ovary extracts were loaded into the 15% Anderson gel (For the separation gel: 15ml of 30% Acrylamide; 2.58ml of 1% bis-Acrylamide; 7.5ml of 1.5M Tris pH 8.8; 4.74ml of water; 150µl of 10% Ammonium Persulphate and 15µl of TEMED. For the stacking gel: 2.5ml of 30% Acrylamide; 2.0ml of 1% bis-Acrylamide; 1.875ml of 1.5M Tris pH 6.8; 8.625ml of water; 150µl of 10% Ammonium Persulphate and 15µl of TEMED). A gradient of loading amounts were made for each ovary extract. The electrophoresis was done at 100 Volt and 250 Volt for the stacking and separation gel

respectively. Proteins were transferred to Immobilon P transfer Membrane (Millipore) at about 7 V/cm over night in cold transfer buffer (10% methanol in 10mM CAPS-NaOH pH 11). Prestained Standards protein ladder (Invitrogen) was used as molecular weight marker. The blot was blocked using 5% dry milk in 0.1% PBST, and incubated with anti-Oskar antibody diluted 1:1000 in the mixture of 5% dry milk in 0.1% PBST. The membrane was washed with 0.1% PBST and incubated with HRP coupled goat anti-rabbit secondary antibody diluted 1:2000 in a mixture of 5% dry milk in 0.1% PBST. Signals were detected by ECL chemiluminescent detection kit (GE health care). The same blot was incubated in the stripping buffer (62.5mM tris-Cl pH 6.8; 100mM mercaptoethanol; 2% SDS) at 65°C for half an hour. Anti-actin (Sigma) antibody diluted 1: 2000 for incubation was added. The incubation and detection were done as described above.

3. RESULTS

3.1. Cytoskeletal organisation in the wild type oocyte from stage 9/10a to stage 10b

3.1.1. Optimal markers to detect cytoskeletal elements and a combination of multiple angles to analyse the oocyte

To analyse the cytoskeleton of the oocyte, several markers were tested. To examine microtubule (MT) organisation, two types of antibodies were compared. One widely used antibody, which recognises all forms of α -tubulin, gave a strong signal in the follicle cells and in the oocyte (Fig. 2A). In contrast, another antibody that recognises specifically the tyrosinated form of α -tubulin (Wehland et al., 1983) revealed a strong signal only in the oocyte, while the signal intensity in the surrounding follicular epithelium was very low (Fig. 2B). As dynamic MTs are thought to be tyrosinated, while stable MTs are detyrosinated (Idriss, 2000), this result suggests that the majority of the MTs in the oocyte are more dynamic and less stable than the majority of the MTs in the follicular epithelium. It had to be noted that some of the MTs stained by the anti- α -tubulin antibody in the anterior centre of the oocyte were not detectable by the anti-tyrosinated α -tubulin antibody (Fig. 2C, arrows). This absence of staining raises the question of whether it reflects the inability of the anti- α -tubulin antibody to penetrate into the centre of the oocyte, or whether the central MTs are not tyrosinated. The answer to this question is not yet clear. Nevertheless, as the anti-tyrosinated α -tubulin antibody allowed a high resolution for visualising the MTs in the oocyte due to the absence of interfering signal from the epithelial cells, this antibody was subsequently used to label MTs in the oocyte in the following studies.

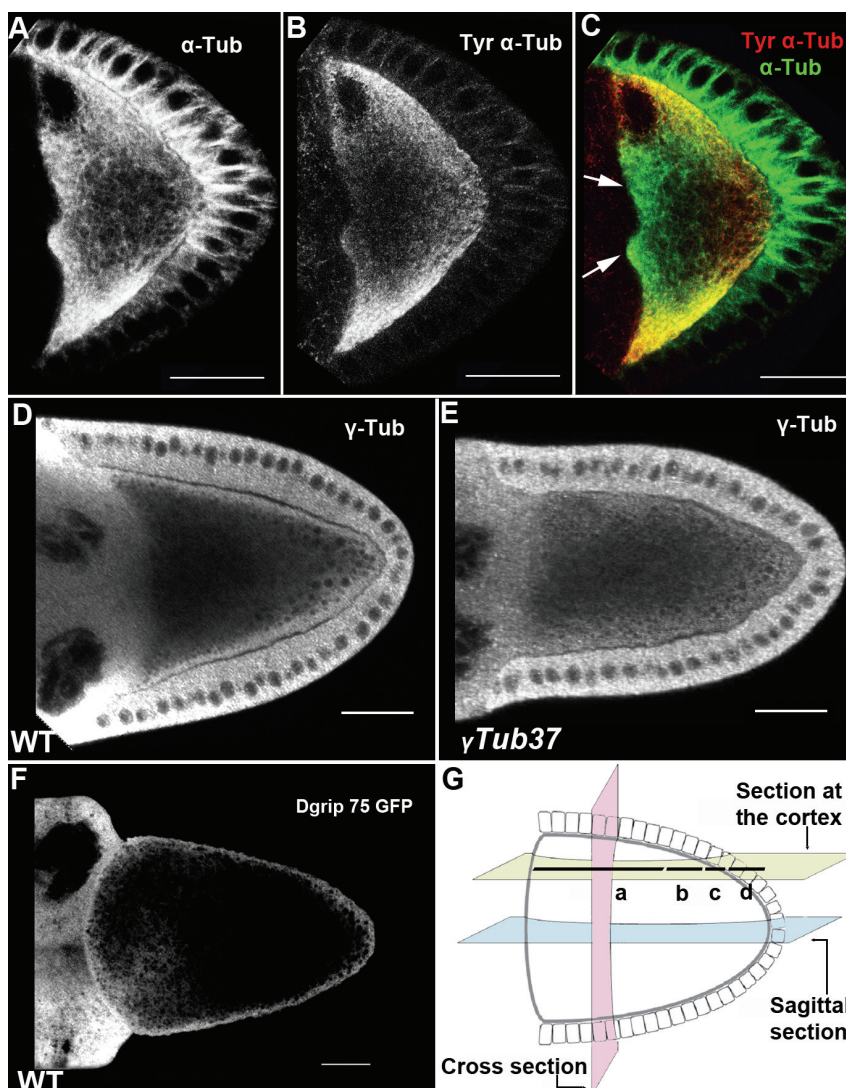


Fig. 2 Markers to detect cytoskeletal elements and multiple angles to analyse the oocyte (A-C) Sagittal section of a wild type stage 9 oocyte stained with an antibody recognising all forms of α -tubulin together with an antibody that recognises only the tyrosinated form of α -tubulin. (A, B) Single channels for the staining as indicated. (C) Overlay of two channels. Some of the MTs stained by the anti- α -tubulin antibody (green) in the anterior centre of the oocyte are not detectable (arrows) by the anti-tyrosinated α -tubulin antibody (red). (D, E) Sagittal sections of stage 10a oocytes stained for γ -tubulin. (D) In wild type, γ -tubulin is enriched at the entire oocyte cortex. (E) In $\gamma Tub37C^l$ null mutant, the signal in the oocyte cortex is greatly reduced. (F) Sagittal section of a stage 10a oocyte expressing *Dgrip75 GFP* fusion protein by *maternal- α -tubulin:Gal4* stained with an antibody recognising GFP. The fusion protein is enriched at the entire oocyte cortex. (G) Scheme depicts the multiple angles for analysing a stage 10a oocyte and the surrounding follicular epithelium. The blue plane represents the optical sagittal section; the pink plane represents the manual cross section; the yellow plane represents the optical section at the oocyte cortex. The dark lines represent the four structures observed from the optical section at the oocyte cortex in a direction from anterior to posterior: (a) the inside of the oocyte, (b) subcortical and (c) cortical layers of the oocyte and (d) the follicle cells. In the following studies, for sagittal sections and cortical sections egg chambers are oriented that anterior is left and posterior is right. Scale bar: 25 μ m

The γ -tubulin ring complex (γ TuRC), which consists of γ -tubulin, several Grips (γ -tubulin ring proteins) and GCPs (γ -tubulin complex proteins), has been shown to localise to the MT minus-ends and to mediate MT nucleation (Wiese and Zheng, 2006). An antibody recognising γ -tubulin was used to investigate the localisation of MT minus-ends. Fig. 2D shows that γ -tubulin accumulates along the entire oocyte cortex (Cha et al., 2002). To verify the specificity of the γ -tubulin detection, the null mutant of γ -tubulin37C, γ Tub37C^l, was analysed (Schnorrer et al., 2002). In *Drosophila* two γ -tubulins are known, γ -tubulin23C and 37C. In the absence of γ -tubulin37C, γ -tubulin23C provides the necessary γ -tubulin function required for mid-oogenesis (Schnorrer et al., 2002; Tavosanis and Gonzalez, 2003). In γ Tub37C^l mutant oocyte, the signal of γ -tubulin at the cortex was greatly reduced, indicating that the detection by the anti- γ -tubulin antibody is specific (Fig. 2E). In addition to γ -tubulin, another component of γ TuRC, Dgrip 75, was also examined. Dgrip 75 is a *Drosophila* γ -tubulin ring complex protein of 75 kDa (Schnorrer et al., 2002). To investigate the localisation of Dgrip 75, GAL4/UAS system was used, which is widely used to drive tissue-specific expression of genes in *Drosophila* (Brand and Perrimon, 1993; Rorth, 1998). When the Dgrip 75 GFP fusion protein was expressed in the germline by *maternal- α -tubulin:Gal4-VP16* line, the protein, like γ -tubulin, showed a cortical enrichment in the oocyte (Fig. 2F). This result confirms the existence of the γ TuRC at the oocyte cortex.

Phalloidin is a group of toxins from poisonous mushrooms, known as phallotoxins. It binds to actin filaments (F-actin) and prevents the filament depolymerisation. This property allows the fluorescent derivatives of phalloidin to be used to detect actin filaments in fixed cells (Cooper, 1987). Below F-actin in the oocytes was visualised by rhodamine conjugated phalloidin.

The analysis of the cytoskeletal organisation of the oocyte was optimised not only by the selection of markers, but also by using different observation angles. Conventionally, optical sagittal sections made by the confocal microscope are used to analyse oocytes (Fig. 2G). To better understand the spatial organisation of the oocyte cytoskeleton, we decided to examine the oocyte from different angles. We first made

manual cross sections of individual egg chambers stained with markers for the actin and the MT cytoskeletons. To this end, a method developed to section *Drosophila* embryos was adopted. In these sections, the oocyte was cut perpendicular to the anterior-posterior (A-P) axis; and the cutting line was located in the central part of the oocyte along the A-P axis (Fig. 2G). Furthermore, we made optical sections at the level of the oocyte cortex by the confocal microscope. These sections cut successively four structures in a direction from anterior to posterior: (a) the inside of the oocyte, (b) subcortical and (c) cortical layers of the oocyte, and (d) the follicle cells (Fig. 2G). Finally, 50 sections, ranging from the centre to the cortex of the oocyte, were projected into a single layer.

To summarise, in this study we have selected optimal markers to detect the cytoskeletal elements and combined multiple angles to examine the oocyte. These improvements allowed a careful re-examination of the cytoskeletal organisation of the oocytes.

3.1.2. Organisation of the oocyte cytoskeleton at stage 9/10a

We first examined cross sections of stage 9/10a oocytes triple stained for γ -tubulin, F-actin and tyrosinated α -tubulin. A continuous layer of γ -tubulin was detected at the cortex (Fig. 3A and C), which was consistent with previous descriptions, confirming the cortical localisation of the MT minus-ends. A dense MT network, with a gradient from high to low density was detected from the cortex to the interior (Fig. 3A and D). To better describe the spatial distribution of the different cytoskeletal elements, the intensity of the fluorescent signal from the cortex to the interior was measured. To reach a statistically meaningful quantification, six samples have been analysed. Further, measurements starting from various cortical locations in one sample were compared, which gave similar results. A representative example of a stage 10a cross section is shown in Fig. 3A and A'. This analysis showed that the main part of the MTs was interior to the γ -tubulin layer, with only a narrow overlap between these two signals at the cortex (Fig. 3A and A'). Notably, the cortical region stained for

γ -tubulin overlapped with the region stained for F-actin, indicating that MT minus-ends were in proximity to actin (Fig. 3A and A'). The confocal picture of cross sections revealed that within this cortical layer, these two elements displayed differences in their structures: γ -tubulin formed a continuous homogenous layer; while F-actin was more filamentous and had several gaps (Fig. 3B, arrow heads).

Next, we analysed the stained oocytes by optical confocal sections at the cortex level. In these sections, the γ -tubulin signal appeared homogeneous without a defined structure (Fig. 3F and F'). MT formed a network, within which individual MTs were interweaving in random orientation (Fig. 3F and F'). Interestingly, the actin cytoskeleton revealed a well defined arrangement. F-actin was organised in long structures that were aligned in parallel (Fig. 3F, F' and Fig. 4D, D'). These long structures have not been analysed at an ultrastructural level, and it is unknown how the actin filaments are crosslinked. As their organisation was reminiscent of bundles, we called these structures "actin bundles". These bundles were thin at the cortex, and became thicker towards the oocyte interior (Fig. 4D), suggesting that they tend to fuse or twist.

Fig. 3

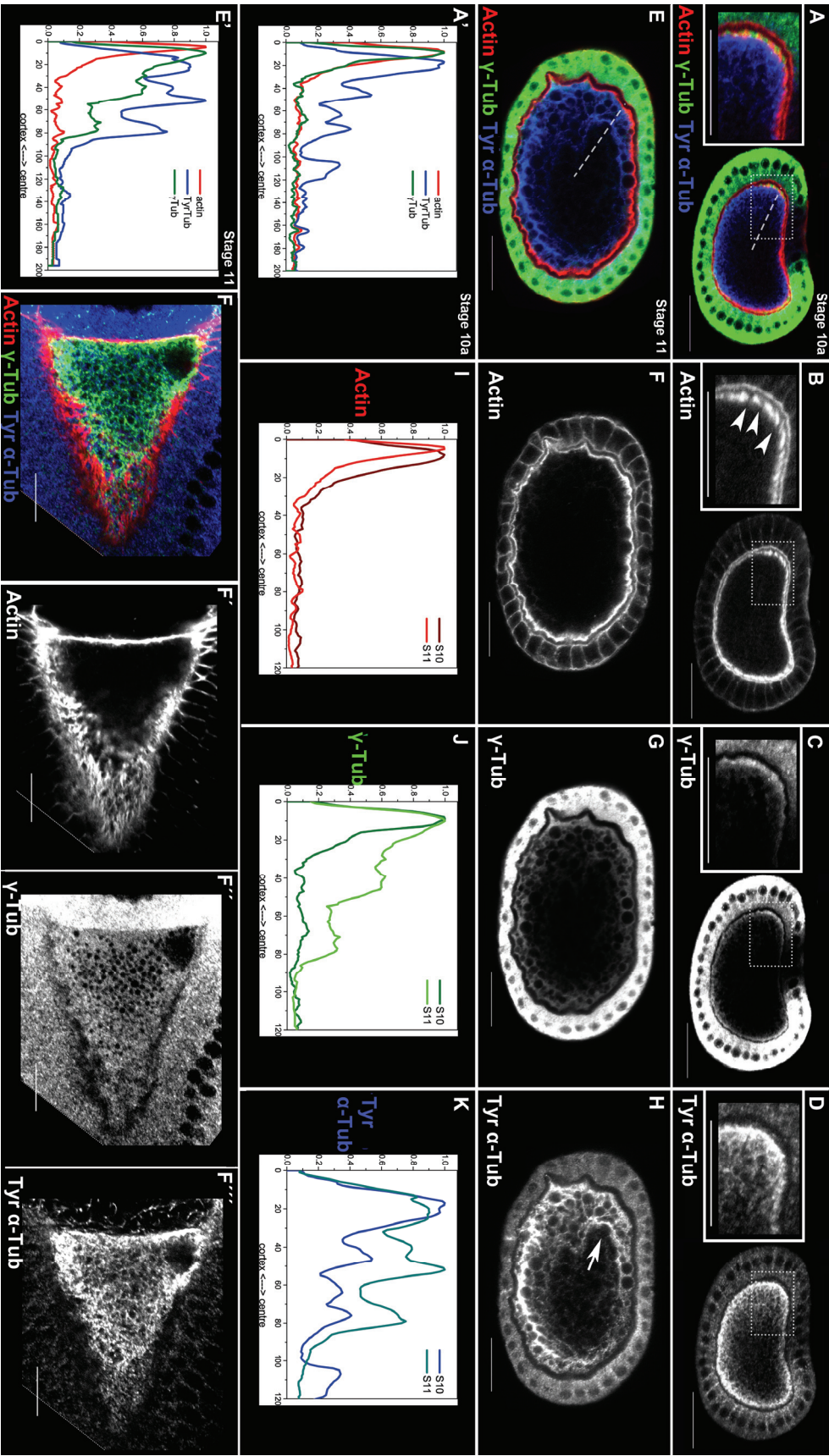


Fig. 3 Architecture of the oocyte cytoskeleton (A-H) Cross sections of oocytes triple stained for actin, γ -tubulin and tyrosinated α -tubulin. (A) Stage 10a oocyte stained for actin (red), γ -tubulin (green) and tyrosinated α -tubulin (blue). Inset shows the marked region in higher magnification. (A') Graph shows fluorescence signal intensities along the dash line from the oocyte cortex to the interior. Analysis of five other stage 10a egg chambers revealed the same distribution of signal intensities from the cortex to the centre of the oocyte. (B, C, D) Single channels for the staining as indicated. (B) Cortical actin is filamentous and discontinuous. Arrowheads point to the gaps in the actin layer. (C) γ -tubulin is restricted at the cortex as a continuous layer. Cutting occasionally affects the staining in the region of the follicular epithelium, where the needle penetrates the egg chamber explaining the absence of γ -tubulin staining in the uppermost follicle cells. (D) MTs form a continuous network with density decreasing from the cortex to the interior. (A, A') γ -tubulin layer overlaps with the cortical actin layer and locates exterior to the MT network, having a narrow overlapping. (E-H) Stage 10b oocyte stained as indicated. (E') Measurements of fluorescence signal intensities along the dash line from the oocyte cortex to the interior. The shown graph is representative for seven analysed samples. (I-K) Comparisons of indicated fluorescence signal intensities between stage 10a and stage 11 (F, I) Cortical actin at stage 11 oocyte becomes thinner. (H, J) MTs are organised into parallel arrays in subcortical regions (Arrow heads in H). (G, K) γ -tubulin displays a broader and more diffuse distribution in subcortical regions. (F) Optical section at the cortex of a stage 10a oocyte stained as indicated. (F') Actin is organised into long bundles. (F'') γ -tubulin appears homogeneous. (F''') MTs are interweaving in random orientation. Scale bar: 25 μ m

Furthermore, the projection of 50 sections was analysed. The projection of the stained actin revealed that these actin bundles were predominantly oriented in an anterior-posterior direction (Fig. 4B). Surprisingly, the density of the actin bundles at the posterior pole was very low (Fig. 4B). Hence, the actin bundling exhibits features of an anterior-posterior polarity. During mid-oogenesis, *oskar* mRNA is localised to the posterior, where the translation starts (Riechmann and Ephrussi, 2001). Oskar has been proposed to be involved in polarising the MT cytoskeleton in the oocyte (Zimyanin et al., 2007). This raises the question of whether Oskar is also involved in polarising the oocyte actin cytoskeleton. To address this question, it was examined whether the posterior domain of lower density of actin bundles overlapped the Oskar protein localisation domain. Egg chambers were double stained for actin and Oskar, and projections from these two channels were overlaid. This revealed that the area of low actin bundle density at the posterior indeed overlaps with the domain of Oskar localisation (Fig. 4B'). Further, it was tested whether Oskar is responsible for the different actin organisation at the posterior. Therefore, the actin cytoskeleton organisation was examined in females transheterozygous for an *oskar* null allele, *oskar*⁵⁴ and a deficiency deleting the *oskar* locus, which produced no detectable Oskar translation (Kimha et al., 1991). The projection of stained actin in this mutant was indistinguishable from that of the wild type (Fig. 4E). This result shows that the organisation of the actin cytoskeleton at the posterior pole does not require Oskar.

In addition, the organisation of the MT network was analysed by projection of confocal sections in the wild type. The projection of the stained MTs revealed that the bulk MTs do not adopt a clear orientation (Fig. 4A). Optical sagittal sections, however, revealed a gradient of MT density from anterior to posterior (Fig. 4C), which was already described previously (Serbus et al., 2005).

Taken together, our data suggest that at stage 9/10a the actin cytoskeleton at the oocyte cortex is assembled into long bundles and the MT minus-ends reside among these bundles. Originating from the cortical minus-ends, MTs are spreading into the interior of the oocyte.

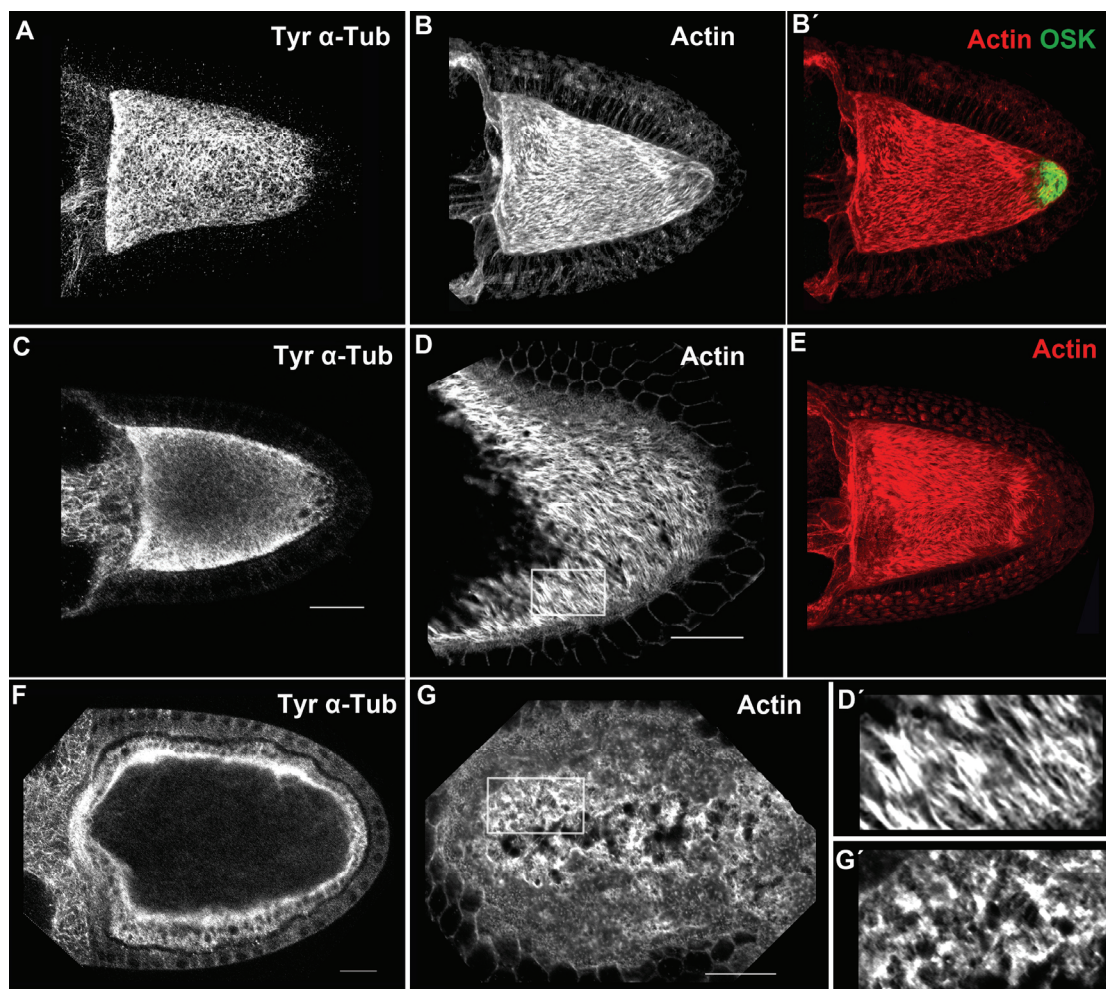


Fig. 4 Reorganisation of the oocyte cytoskeleton between stage 9/10a and stage 11 (A-E) Stage 10a oocytes. (A, B, E) Projection of 50 sections from the centre to the cortex of oocytes stained as indicated. (A) The projection reveals a MT network with no clear polarity. (B) The projection of stained actin reveals that the actin bundles are predominantly oriented in an anterior-posterior direction. The density of the actin bundles at the posterior pole is very low. (B') The same oocyte showing Oskar protein localisation (green) together with actin (red) reveals that the region of low density of actin bundles coincides with Oskar localisation domain. (E) The projection of the *oskar* mutant oocyte that produces no detectable Oskar protein reveals normal formation of actin bundles at the cortex. (C) Sagittal section of a stage 10a wild type oocyte stained for tyrosinated α -tubulin. The highest concentration of MTs occurs at the anterior and lateral cortex and lowest concentration is present at the posterior pole. The bulk MTs spread from the cortex to the interior of the oocyte. (D) Optical section at a stage 10a oocyte cortex stained for actin. (D') depicts marked region in higher magnification. Cortical actin is organised into bundles. These bundles are thin at the cortex, and become thicker towards the oocyte interior. (F, G) A stage 10b oocyte double stained for tyrosinated α -tubulin and actin. (F) Sagittal section of the tyrosinated α -tubulin staining shows a reorganisation of MTs into parallel arrays at the subcortical region. (G) Cortical section of the actin staining and (G') the marked region in higher magnification. Actin bundles disappear and actin is organised into patches and small filaments. Scale bar: 25 μ m

3.1.3. Changes in the oocyte cytoskeleton at stage 10b

The above described organisation of the MT cytoskeleton changes dramatically at stage 10b. MTs form loose and parallel arrays at this stage (Fig. 3H, arrows and Fig. 4F), indicating the onset of fast ooplasmic streaming (Gutzeit and Koppa, 1982). However, it is not clear where the MT minus-ends are located during the fast streaming. To address this question, cross sections of stage 10b egg chambers stained for the actin and MT cytoskeleton were examined. In total seven samples have been analysed. Within each sample the measurements starting from various cortical positions have been compared, which gave similar results. A representative example is shown in Fig. 3E and E'. At stage 10b, the thin and dense cortical γ -tubulin layer was no longer present. Instead, a broader and more diffuse subcortical layer developed (Fig. 3E, G and J). Thus, concomitantly with the onset of fast ooplasmic streaming and the formation of MT arrays, the MT minus-ends redistribute from the cortex to subcortical regions. The finding, that the MT minus-ends are embedded within the cortical actin bundles before stage 10b, raised the question of whether the change in γ -tubulin localisation was accompanied by structural changes in the actin cytoskeleton. To test this, F-actin of the stage 10b oocyte was investigated by cross sections and optical cortical sections. Strikingly, at stage 10b the cortical actin became thinner (Fig. 3F and I) and the actin bundles disappeared from the cortex (Fig. 4G). Instead, actin patches and thin filaments with random orientation were present (Fig. 4G and G').

Thus, corresponding with the onset of fast ooplasmic streaming at stage 10b, the actin structure at the cortex rearranges and γ -tubulin redistributes. This result raises the possibility that the cortical actin organisation is responsible for the change in the localisation of the MT minus-ends.

3.1.4. Cortical localisation of MT minus-ends is dependent on the actin bundling

To test the hypothesis that the cortical actin organisation is responsible for the change in the localisation of the MT minus-ends, we first examined the role of actin bundles for the localisation of the MT minus-ends at the cortex during stage 9/10a. To this end, we interfered with the bundle formation by treating egg chambers with latrunculinA, which inhibits the actin polymerisation by binding to and sequestering actin monomers. It has been shown that the treatment of the stage 9/10a oocyte with cytochalasin D, which inhibits the actin polymerisation in a similar way as latrunculinA, induced fast ooplasmic streaming before stage 10b (Manseau et al., 1996). However, the underlying mechanism has not been elucidated.

First it was tested whether treating egg chambers with latrunculinA also resulted in premature fast ooplasmic streaming. To this end, latrunculinA in a concentration of 100 μ M was injected into the abdomen of wild type females. To visualise the streaming in the oocytes, the yolk granules within the ooplasm were traced. To make yolk granules visible, Trypan blue dye was injected into the abdomen, which was subsequently endocytosed with yolk by the oocyte and marked the yolk granules with fluorescence. Then time lapse fluorescence microscopy was performed to analyse the endosomes (Gutzeit and Arendt, 1994). In stage 9/10a wild type oocytes, the endosomes showed slow movements at multiple locations, which were primarily restricted in the anterior half of the oocyte. These movements were orientated to different directions (Serbus et al., 2005). After drug injection a strong increase in the speed of the endosome movement (6 out of 6) was observed. Moreover, the movement appears unidirectional (Fig. 5B and B'). Thus, latrunculinA treatment induces premature fast ooplasmic streaming in the stage 9/10a oocyte.

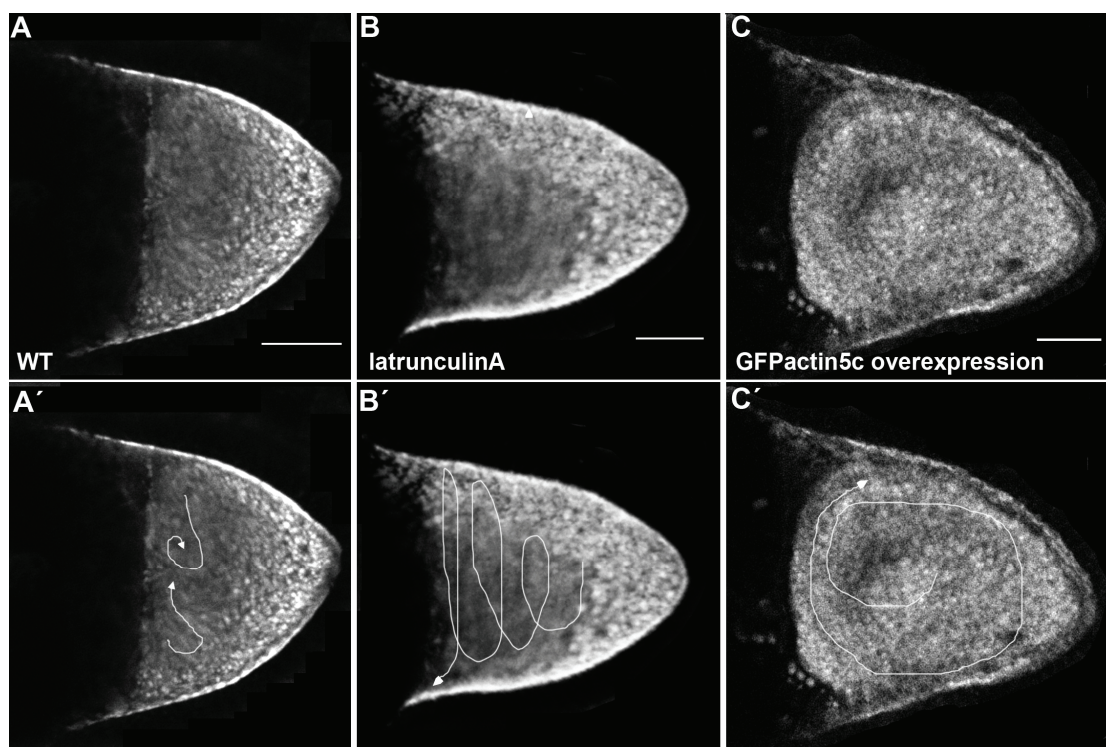


Fig. 5 Endosome movements in stage 9/10a oocytes (A-C) Fluorescent yolk endosomes were imaged in stage 9/10a egg chambers. Each panel is a projection of ten images from one focal plane acquired at 15-second intervals (see Materials and Methods). Moving endosomes appear as elongated streaks, while the non-moving endosomes appear as spots. (A'-C') The streaks are outlined by lines and the direction is indicated by arrows. (A, A') In the wild type stage 9 oocyte, endosomes show slow movements at multiple locations in the anterior half of the oocyte. These movements are oriented to different directions. (B, B') In a stage 10a oocyte after latrunculinA injection, endosomes show a fast and unidirectional movement. Note the spiral pattern formed by the endosomes movement is orientated in parallel to the dorsal-ventral axis. This movement spans the entire oocyte from the posterior to the anterior. (C, C') In a stage 10a oocyte overexpressing *GFPactin5C*, a fast and unidirectional endosome movement is formed. The moving orientation is in perpendicular to the dorsal-ventral axis. Scale bar: 25 μ m

The next step was to test whether the organisation of the cortical actin cytoskeleton is affected after the latrunculinA treatment. To assess this, dissected ovaries from the wild type were incubated in medium containing a lower concentration of latrunculinA (2.8 μ M), and then fixed and stained for the cytoskeleton markers. This treatment did not induce a fully penetrant phenotype regarding the formation of MT arrays indicative of the fast streaming, probably due to the lower concentration and shorter incubation time of the drug than that in the injection treatment. Statistical analysis revealed that in 45% (n=33) of the treated stage 10a egg chambers the subcortical MT arrays were formed (Fig. 6C); while in 40% the MT cytoskeleton appeared unaffected

(Fig. 6A). Importantly, analysis of the actin cortex revealed that the actin bundling was not affected in those oocytes with normal MT organisation (Fig. 6B). In contrast, in those oocytes displaying the formation of MT arrays at the subcortical region, the actin bundles disappeared from the cortex (Fig. 6D). The actin cortex was not completely vanished; instead, it appeared like short filaments or patches, which resembled the actin cortex in stage 10b wild type oocytes (compare Fig. 6D and Fig. 4G). Thus, the presence or absence of the actin bundles correlates perfectly with the absence or presence of fast ooplasmic streaming, strongly suggesting that the actin bundles are required to prevent fast ooplasmic streaming at stage 9/10a.

To test whether the destruction of actin bundles led to a premature redistribution of MT minus-ends from the cortex to subcortical regions, cross sections of the egg chambers treated with latrunculinA were analysed. To better characterise the γ -tubulin distribution pattern, a quantitative analysis has been applied: Multiple cross sections stained for γ -tubulin were included. Within each sample, γ -tubulin signals starting from different cortical positions to the interior were measured. The plotted results revealed maximal signal intensities restricted within a certain area of the cross section. The width of the area with the maximal signal intensities was calculated. For each sample, the average value of five different measurements was also calculated. In addition, the average value for all analysed samples was calculated. This procedure was applied in the following studies to analyse the γ -tubulin distribution in cross sections. After latrunculinA treatment (2.8 μ M), eight samples exhibiting the formation of MT arrays, were analysed. These revealed that when the MT arrays indicative of fast ooplasmic streaming were formed, γ -tubulin was distributed in a region approximately three times broader than the narrow region observed in the untreated wild type (Fig. 7C and D). This indicates that γ -tubulin relocates from the cortex to the subcortical regions when MT arrays are formed. Thus, when the cortical actin bundles are disrupted due to latrunculinA treatment, γ -tubulin redistributes to subcortical regions prematurely at stage 9/10a. This suggests that the actin bundles are required to anchor the MT minus-ends at the cortex.

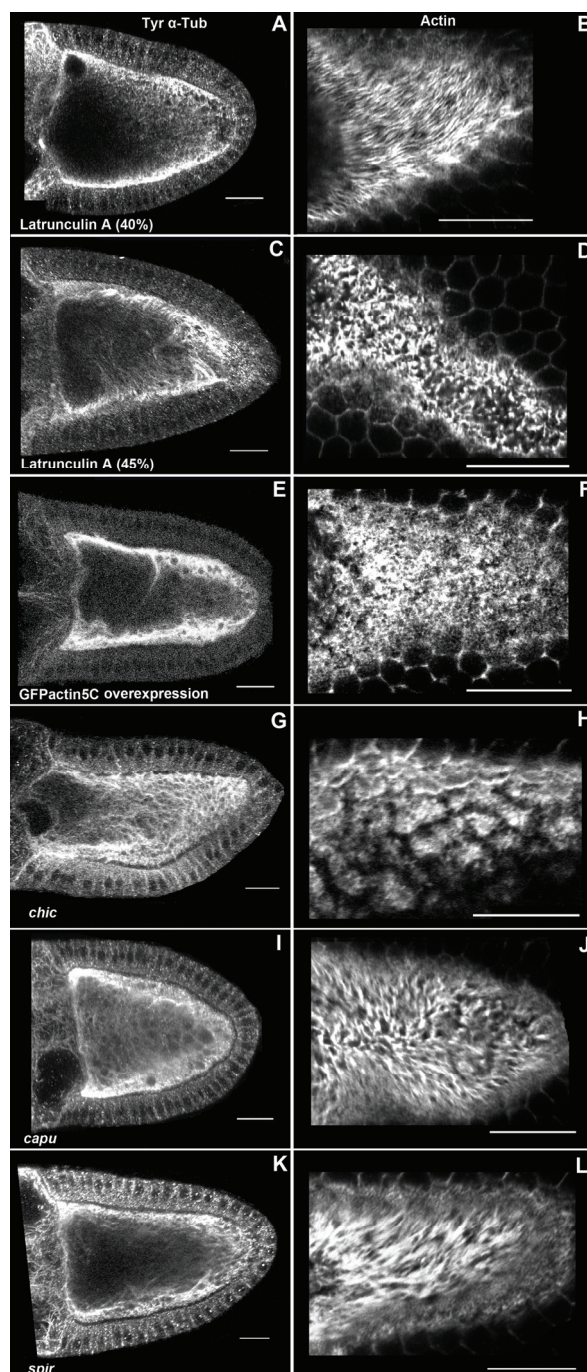


Fig. 6 Regulation of actin and MT organisation Stage 10a egg chambers double stained for tyrosinated α -tubulin and actin. Each row depicts the same oocyte showing MTs in a sagittal section (A, C, E, G, I, K) and actin in a cortical section (B, D, F, H, J, L). (A-D) Egg chambers treated with latrunculinA. (A, B) In 40% of the drug treated oocytes MT organisation and actin bundling is not altered. (C, D) In 45% of the drug treated oocytes MTs are organised in subcortical arrays, and actin bundles are destroyed. (E, F) In an egg chamber expressing *GFP-actin5c* under control of *maternal- α -tubulin:Gal4*, MTs form subcortical arrays, and actin bundle formation is disrupted. (G, H) In *chic* mutant oocyte, MT arrays form prematurely, and actin bundles are absent. (I, J) *capu* and (K, L) *spire* mutants show premature formation of MT arrays, but actin bundles are not affected. Scale bar: 25 μ m

To confirm the role of actin bundles for the localisation of MT minus-ends independently of drug treatment, the actin organisation was altered by overexpression of *actin5C* that was tagged to *GFP*. When the transgene was expressed by *nanos:Gal4-VP16* that gives a high level expression in the female germline starting from early stages, mitotic divisions in the germline were perturbed. This suggests that overexpression of *GFPactin5C* interferes with the formation of the contractile ring during germ cell cytokinesis (Roepert et al., 2005). To test whether *GFPactin5C* expression also interferes with the formation of cortical actin bundles, the early defects in the germline have to be circumvented, so that the oogenesis can proceed and the oocyte can develop. Therefore, another promoter, *maternal- α -tubulin:Gal4-VP16* was tested, which is also expressed in the germline, but at a lower level in the early stages than that of *nanos:Gal4*. The expression driven by *maternal- α -tubulin:Gal4-VP16* did not affect germline cell divisions and allowed the development of oocytes with a normal size. When the expression was induced at 25°C, all examined stage 10a oocytes (n=25) formed subcortical MT arrays indicating the onset of premature fast ooplasmic streaming (Fig. 6E). The fast streaming was confirmed by the time lapse microscopy of endosomes (Fig. 5C and C'). Consistent with this, the analysis of cross sections revealed that when the premature MT arrays formed, γ -tubulin distributed in a broader region, indicating the relocation from the cortex into subcortical regions (Fig. 7E and F). It was next asked whether the relocation of γ -tubulin was correlated with a change in actin organisation at the cortex. When *GFPactin5C* expression was induced in the oocyte, the formation of cortical actin bundles was disrupted, and the actin cortex resembled that of the wild type stage 10b oocyte (Fig. 6F). Thus, overexpression of *GFPactin5C* in the oocyte interferes with the actin bundle formation at the cortex, which is correlated with the γ -tubulin relocation from the cortex. The result supports the hypothesis that actin bundles are required to anchor the MT minus-ends at the cortex.

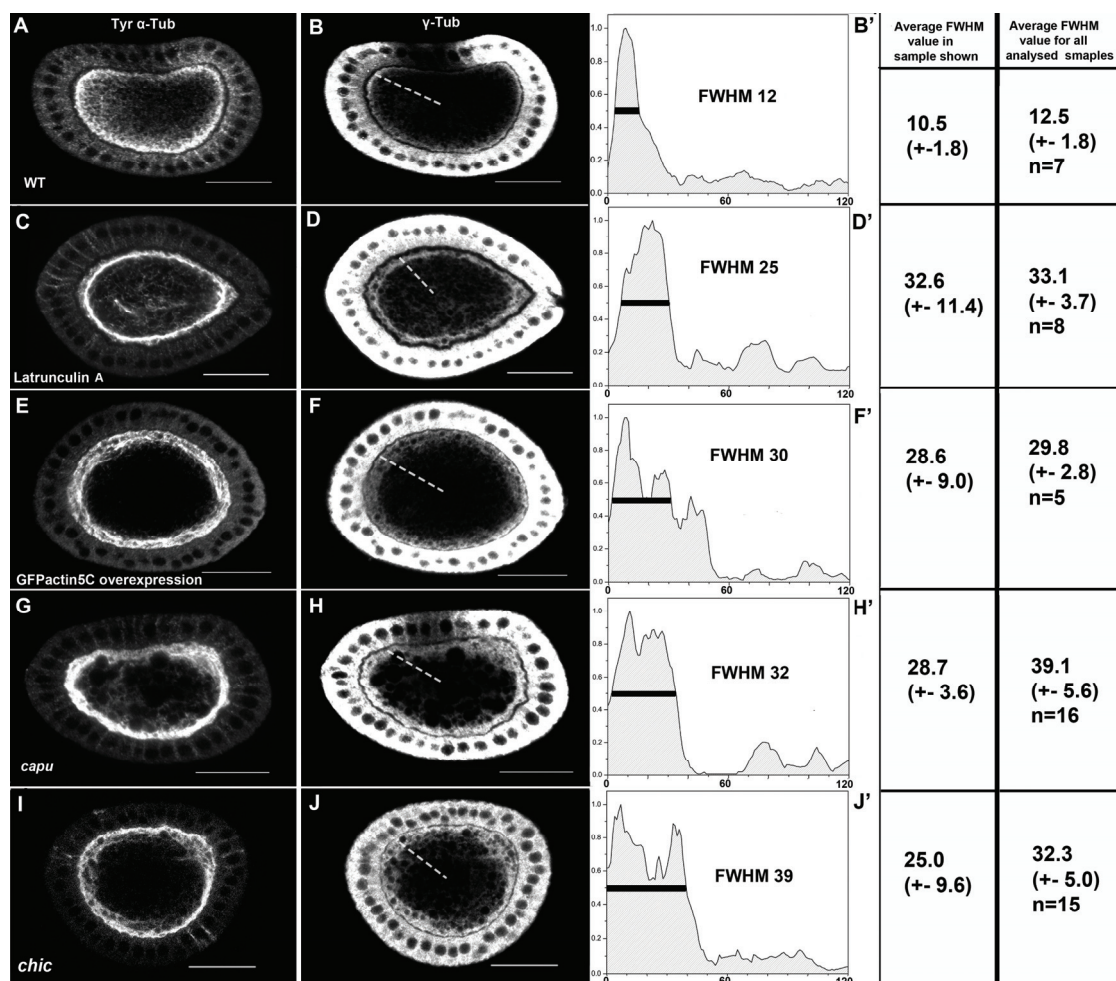


Fig. 7 Regulation of the cortical anchoring of MT minus-ends Cross sections of stage 10a egg chambers double stained for tyrosinated α -tubulin (A, C, E, G, and H) and γ -tubulin (B, D, F, H and J). (B', D', F', H' and J') Plots of the γ -tubulin signal intensities along the dotted line (11 o'clock) from the exterior to the interior of the oocyte shown in corresponding cross sections. The full width at half maximum (FWHM) describes the width of the distribution curve (see Materials and Methods), and the black bar indicates where the value is achieved. The left chart next to the diagram shows the average FWHM value of five measurements achieved along lines at four other locations (3, 6, 9, 12 o'clock) of the shown cross section. The average FWHM value of all analysed samples from corresponding genotypes or treatment is shown in the right chart. (A, B) In wild type MT forms a dense network at the cortex (A) and γ -tubulin is restricted as a continuous layer at the cortex (B, B'). In egg chambers treated with latrunculinA (C, D), overexpressing *GFPactin5C* (E, F), of *capu* mutants (G, H) and *chic* mutants (I, J), the same phenotype is observed: The MTs are reorganised into subcortical arrays and γ -tubulin relocates from the cortex to a broad subcortical region. Scale bar: 25 μ m

In summary, interfering with the actin bundle formation either by overexpression of *GFP-actin* or by actin inhibitory drug treatment leads to a premature redistribution of γ -tubulin from the cortex to subcortical regions and the onset of premature fast ooplasmic streaming. These findings indicate that actin bundling at the cortex of the stage 9/10a oocyte is essential for anchoring the MT minus-ends and for the repression of fast ooplasmic streaming.

3.2. The oocyte cytoskeletal organisation in the mutants affecting actin-regulatory proteins

It was the next step to determine the genes required for regulating actin bundle formation. A number of mutations in actin-regulatory proteins have been shown to induce cytoskeleton defects in the oocyte. Taking them as candidates, cross sections and optical cortical sections were made to examine the MT and the actin organisation, respectively, in these mutants.

3.2.1. Profilin is required for actin bundle formation

The *chickadee* (*chic*) gene of *Drosophila* encodes Profilin, a protein that binds actin monomers (Cooley et al., 1992). A series of *chic* mutants have been shown to display premature fast ooplasmic streaming, with the frequency dependent on the strength of the allele. The *chic*¹³²⁰ allele has dramatically reduced expression of Profilin in the germline (Verheyen and Cooley, 1994) and showed a highly penetrant premature streaming phenotype (Manseau et al., 1996). Our analysis of this allele confirmed the presence of MT arrays at stage 10a indicative of premature fast ooplasmic streaming (Fig. 6G). Additionally, cross sections show that γ -tubulin redistributed to a broader subcortical region at stage 10a, when the MT arrays were prematurely formed (Fig. 7I and J). Importantly, in all *chic* mutant oocytes, in which the formation of MT arrays was unambiguously detected, the cortical actin bundles were disrupted (Table1). The actin cortex of the stage 9/10a *chic* oocyte resembled that of the wild type stage 10b

oocyte when the fast streaming is started (Fig. 6H). This indicates that Profilin is required for actin bundle formation at the cortex of stage 9/10a oocytes.

3.2.2. Capu and Spire act downstream of actin bundling for MT anchoring at the cortex

The cytoskeleton was also examined in *cappuccino (capu)* and *spire (spir)* mutant oocytes, in which the premature fast streaming phenotype was observed in high penetrance (Emmons et al., 1995; Manseau et al., 1996; Theurkauf, 1994). Capu contains Formin homology (FH) domains (Emmons et al., 1995), which is involved in organising the actin cytoskeleton (Evangelista et al., 1997). Spire contains a WASP homology 2 (WH2) domain, which is implicated in actin binding (Machesky and Insall, 1998; Miki and Takenawa, 1998; Wellington et al., 1999). Recently, it has been shown that Spire is able to nucleate actin filaments in vitro (Quinlan et al., 2005). These findings suggest that Capu and Spire may be involved in the formation of cortical actin bundles in the oocyte. On the other hand, the FH domain is known to bind MTs in vitro and in vivo (Wallar and Alberts, 2003). Consistent with this, Capu has been shown to crosslink actin filaments and MTs in vitro, and this crosslinking activity is modulated by binding to Spire (Quinlan et al., 2007; Rosales-Nieves et al., 2006). Therefore, an alternative hypothesis is that Capu and Spire crosslink MTs to actin bundles at the oocyte cortex. To distinguish between these two possibilities, the oocyte cytoskeleton was examined in these two mutants.

	wild type	<i>chic</i>	<i>capu</i>	<i>spire</i>
Actin bundles detected	89%	0%	90%	86%
No actin bundles detected	11%	100%	10%	14%
The number of analysed samples	45	24	50	51

Table 1 Actin bundle formation in stage 10a oocytes Egg chambers were double stained for Actin and tyrosinated α -Tubulin. For *capu*, *chic* and *spire* mutants only those egg chambers were counted, in which the formation of MT arrays indicative of fast ooplasmic streaming was unambiguously detected.

In stage 9/10a *capu* and *spire* mutant oocytes, subcortical MT arrays were detected as expected, indicating the onset of fast streaming (Fig. 6I, K and Fig. 7G). Furthermore, γ -tubulin was detected in a broader subcortical region (Fig. 7H), indicating the redistribution of γ -tubulin from the cortex. The above described data have demonstrated a good correlation between the cortical actin bundles and cortical γ -tubulin anchoring: when the γ -tubulin is relocated from the oocyte cortex, the actin bundles are disrupted. To test whether this is also the case in *capu* and *spire* mutants, the actin cortex was analysed in mutant oocytes in which the presence of MT arrays was clearly determined. Strikingly, in most of mutant oocytes that displayed the MT phenotype unambiguously, actin bundling appeared as normal as in stage 9/10a wild type oocyte (Fig. 6J, L and Table1). Thus, *Capu* and *Spire* are not involved in actin bundling. This result suggests that the premature γ -tubulin redistribution phenotype observed in *capu* and *spire* mutants is downstream of the actin bundle formation.

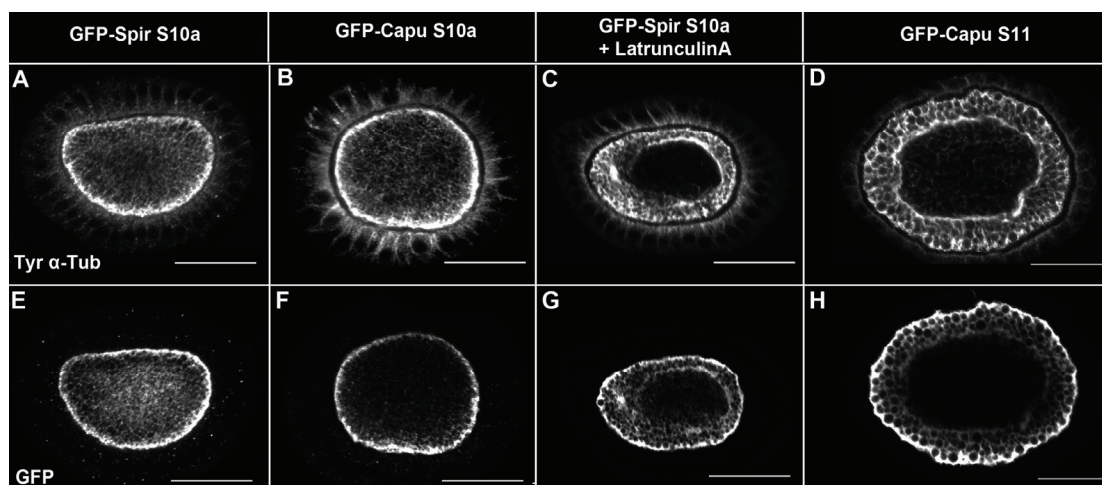


Fig. 8 Cortical localisation of GFP-Capu and GFP-SpireD Cross sections of egg chambers double stained for tyrosinated α -tubulin (A-D) and GFP (E-H) of indicated stages. GFP-Capu and GFP-SpireD are expressed in the germline by *maternal- α -tubulin:Gal4*, and the localisation of the fusion protein is detected with an antibody recognising GFP. (A, B) MT staining reveals normal MT organisation at stage 10a. (C) At stage 10a after latrunculinA treatment and (D) at stage 10b, subcortical MT arrays are formed. (E, F) At stage 10a localisation of GFP-SpireD (E) and GFP-Capu (F) is enriched at the cortex. (G, H) After the onset of the fast ooplasmic streaming at stage 10a with latrunculinA treatment or at stage 10b, the cortical enrichment of GFP-Capu and GFP-SpireD does not change. Scale bar: 25 μ m

This observation favors the possibility that Capu and Spire crosslink MTs to actin bundles at the oocyte cortex. The premature γ -tubulin redistribution and the onset of fast streaming observed in the mutants may be the consequence of impaired MT anchoring within the cortical actin bundles. In support of this view, Spire and Capu have been shown to be enriched at the stage 9/10a oocyte cortex (Quinlan et al., 2007; Rosales-Nieves et al., 2006). This finding raised the possibility that the anchoring of MT minus-ends at the cortex and the inhibition of fast ooplasmic streaming was controlled at the level of the cortical localisation of Capu and Spire. The displacement of these two proteins from the cortex at stage 10b might result in the loss of MT minus-end anchoring, and thereby induce fast streaming. To test this, GFP-Capu and GFP-Spire localisation in the oocyte was examined by cross sections of oocytes. Consistent to previous studies, at stage 10a GFP-Capu and GFP-Spire was restricted at the oocyte cortex (Fig. 8E and F). At stage 10b when MTs reorganised into subcortical arrays, GFP-Capu was still found to be restricted at the cortex (Fig. 8D and H). It was next asked whether there is a displacement of Capu and Spire after the induction of premature fast streaming. Stage 10a oocytes were treated with latrunculinA. In the treated oocyte with the formation of MT arrays, GFP-Spire was still restricted to the oocyte cortex (Fig. 8C and G). Thus, there is no difference in the Capu and Spire localisation before and after the onset of fast ooplasmic streaming. This suggests that the regulation of Capu and Spire localisation is not accounting for the γ -tubulin relocation. Other mechanisms, for example, the regulation of Capu and Spire activities, may thus be considered to modulate the MT anchoring within the cortical actin bundles.

3.2.3. Cortical actin bundling is independent on the Capulet, Swallow and

Moesin functions

The cytoskeleton in *capulet* (*cap*), *Drosophila moesin* (*Dmoe*) and *swallow* (*swa*) mutants was also investigated. Cap encodes the *Drosophila* homologue of cyclase-associated protein (CAP) (Baum et al., 2000). CAPs have been shown to

inhibit the actin polymerization by sequestering actin monomers (Freeman et al., 1995; Gieselmann and Mann, 1992; Gottwald et al., 1996). Dmoe is an ezrin - radixin - moesin (ERM) protein (McCartney and Fehon, 1996), which acts as a cross-linker between plasma membranes and the actin cytoskeleton (Tsukita et al., 1997). Swa is a unique protein only found in *Drosophila* (Huang et al., 2000) and has been shown to associate with *Drosophila* homolog of Dynein light chain (Schnorrer et al., 2000). In *cap*, *Dmoe* and *swa* mutants, ectopic actin clumps accumulate in the oocyte, indicating their roles in regulating the actin organisation of the oocyte (Baum et al., 2000; Jankovics et al., 2002; Meng and Stephenson, 2002; Polesello et al., 2002).

In germline clones of the null allele of *capulet*, *cap*^{l0}, ectopic actin clumps in the stage 10a oocytes were observed (Fig. 9A), confirming the previous finding (Baum et al., 2000). Nevertheless, the actin bundles at the oocyte cortex appeared indistinguishable from that in the wild type (Fig. 9B). Similarly, the actin bundles were not affected in *Dmoe* and *swa* mutant oocyte either, in which ectopic actin clumps were present (Fig. 9C and D and data not shown). Thus, the cortical actin bundling is independent of the Capulet, Swallow and Moesin function. This result suggests that the cortical anchoring of the MT minus-ends is not affected in these mutants. Consistent with this finding, the premature fast streaming phenotype has not been reported in these mutants (Baum et al., 2000; Jankovics et al., 2002; Meng and Stephenson, 2002; Polesello et al., 2002). In conclusion, our data show that Profilin is required for the actin bundle formation in the stage 9/10a oocyte cortex. Capu and Spire act downstream of the bundle formation for regulating the anchoring of MT minus-ends at the cortex, probably by their crosslinking activities between actin and MTs. The crosslinking activity prevents the premature onset of fast ooplasmic streaming. Capulet, Swallow and Moesin are neither involved in the bundle formation nor in inhibition of premature fast ooplasmic streaming.

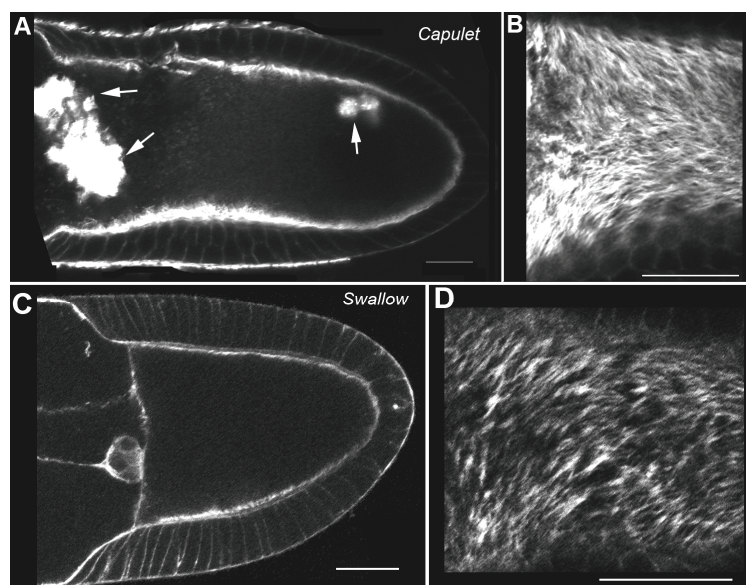


Fig. 9 Actin organisation in *cap* and *swa* mutant oocytes (A, C) Sagittal sections and (B, D) cortical sections of stage 10a oocytes stained for actin with genotypes indicated. (A, B) *cap* mutant. (A) Ectopic actin clumps (arrows) are observed in the oocyte. (B) Cortical actin bundles are not affected. (C, D) *swa* mutant. In our experiment ectopic actin clumps are only detected after stage 10b. (D) Cortical actin bundles are normally formed. Scale bar: 25 μ m

3.3. Different steps in the reorganisation of the oocyte cytoskeleton

Our data show that the relocation of MT minus-ends from the cortex to subcortical regions correlates with the onset of fast ooplasmic streaming. However, it is not clear how the cytoskeletal reorganisation is ordered. This raised the question of whether fast ooplasmic streaming was the prerequisite or the consequence of MT minus-end relocalisation from the cortex to subcortical region. This question could be addressed by analysing the null allele of *Kinesin heavy chain*, *Khc*²⁷, given that in germline clones of *Khc*²⁷ ooplasmic streaming is completely abolished (Serbus et al., 2005; Palacios and St Johnston, 2002).

The first step was to analyse the actin cortex and the γ -tubulin localisation in *Khc* mutants. The formation of cortical actin bundles appeared unaffected in *Khc* mutants at stage 10a (Fig. 10A). In addition, the MT organisation was indistinguishable from that in wild type (Fig. 10B and F). Cross sections also revealed that γ -tubulin was restricted at the cortex of the stage 10a oocyte as a narrow layer (Fig. 10G), demonstrating that MT minus-ends were correctly anchored at the oocyte cortex. Thus,

at stage 10a *Khc* mutants neither display defects in the organisation of the MT cytoskeleton nor for the cortical actin bundling. The next step was to analyse the cytoskeleton organisation in stage 10b *Khc* mutant oocytes. Consistent with previous results, we found that MT arrays were not formed in *Khc* mutants at stage 10b (Fig. 10E and H), indicating the absence of fast streaming (Serbus et al., 2005). However, the MT organisation appeared different from that in stage 10a oocyte. The highest concentration of MTs was no longer restricted to the cortex, but expanded to a broader subcortical region (compare Fig. 10B, E and F, H). This change in the MT organisation strongly suggested a redistribution of MT minus-ends. To test this, cross sections of stage 10b mutant oocytes stained for γ -tubulin were analysed. This revealed that γ -tubulin was present in a broader subcortical region than in stage 10a (Fig. 10I). This result indicates that MT minus-ends are relocated from the cortex into subcortical regions at stage 10b mutant oocytes. Thus, our data show that MT minus-ends redistribute normally in the absence of fast ooplasmic streaming. We therefore conclude that the redistribution of MT minus-ends from the cortex into subcortical regions does not require fast ooplasmic streaming.

As a corollary of the conclusion drawn above, one would expect to find a premature redistribution of γ -tubulin in *Khc* oocyte at stage 9/10a if the actin bundling is disrupted. To assess this, dissected ovaries from *Khc* mutants were incubated in medium containing latrunculinA (2.8 μ M). After drug treatment, actin bundles were disrupted in 7 out of 10 oocytes (Fig. 10C). In these oocytes MTs did not form the parallel arrays. The highest concentration of MTs was not restricted to the cortex, but present in a broader region adjacent to the cortex (Fig. 10D). Cross sections of egg chamber displaying an evident disruption of the cortical actin were examined. As expected, γ -tubulin was present in a broader subcortical region in correlation with the redistribution of MTs (Fig. 10J and K), indicating the relocation of MT minus-ends from the cortex to subcortical regions. This result supports the conclusion that the redistribution of MT minus-ends from the cortex into subcortical regions does not require fast ooplasmic streaming. Thus, it provides further evidence that the redistribution of MT minus-ends is the upstream event of fast ooplasmic streaming.

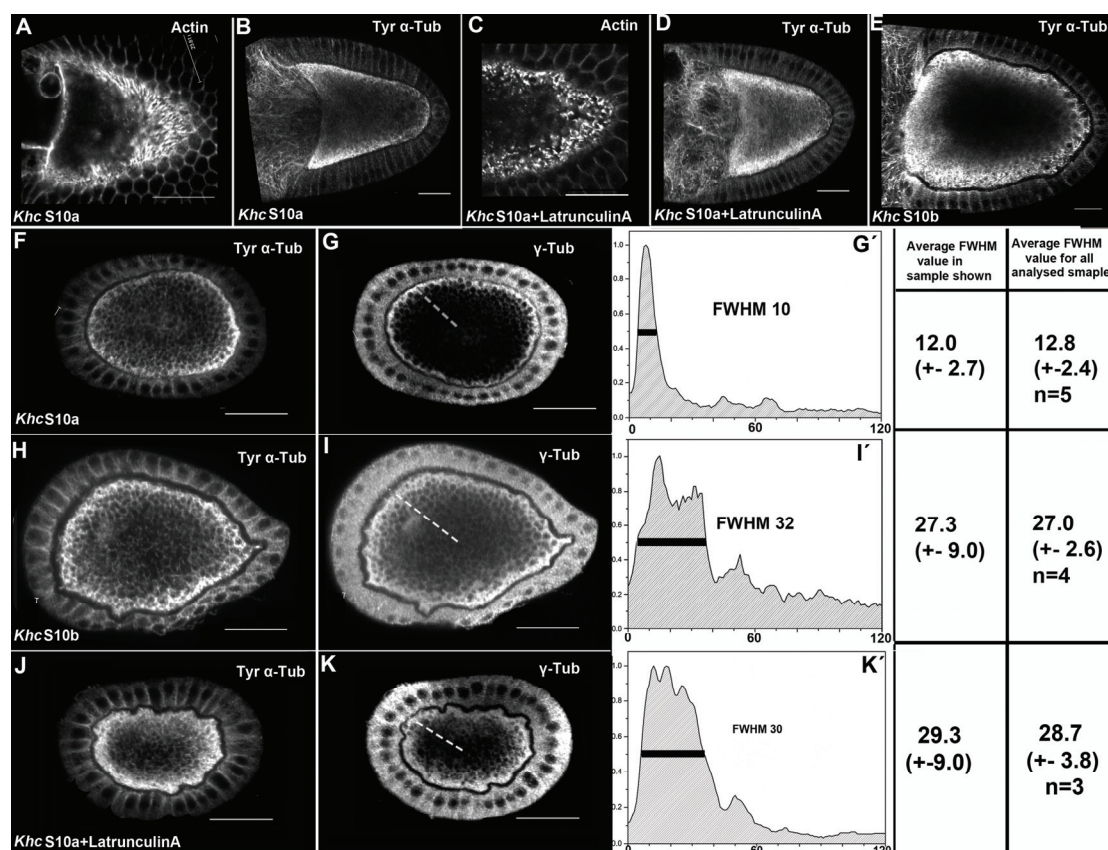


Fig. 10 Cytoskeletal organisation in *Khc* mutant oocytes (A, C) Cortical sections. (A) A stage 10a oocyte reveals the normal formation of actin bundles at the cortex. (C) After latrunculinA treatment, in 70% of the analysed oocytes actin bundling is disrupted. (B, D, E) Sagittal sections of egg chambers stained for tyrosinated α -tubulin. (B) MT staining reveals the normal MT organisation at stage 10a. (D) At stage 10a after latrunculinA treatment and (E) at stage 10b, cortical MTs are reduced, accompanied by an increase of MTs distributed in subcortical regions. (F-K) Cross sections of egg chambers double stained for tyrosinated α -tubulin (F, H, J) and γ -tubulin (G, I, K). (G', I', K') Plots of the γ -tubulin signal intensities along the dotted line (11 o'clock) from the exterior to the interior of the oocyte shown in corresponding cross sections. The black bar indicates where the FWHM value is achieved. The left chart next to the diagram shows the average FWHM value of five measurements achieved along lines at four other locations (3, 6, 9, 12 o'clock) of the shown cross section. The average FWHM value of all analysed samples from corresponding stage or treatment is shown in the right chart. (F, G) At a stage 10a *Khc* mutant oocyte, MT forms a dense network at the cortex (F), and γ -tubulin is restricted as a continuous layer at the cortex (G, G'). In egg chambers at stage 10b (H, I) and at stage 10a after latrunculinA treatment (J, K), similar phenotype is observed: MTs redistribute into a broader region subcortically but do not form arrays; γ -tubulin relocates from the cortex to a broad subcortical region. Scale bar: 25 μ m

3.4. A novel cytoskeletal phenotype exhibited by a mutation in *Tao-1* gene

To examine upstream mechanisms that regulate the organisation of the oocyte cytoskeleton, we investigated the function of *Drosophila* Tao-1. In mammals, Tao-1 is a regulator of the polarity-inducing kinase Par-1 (Timm et al., 2003). Tao-1 belongs to the Ste20 like kinase family, which interacts with various signalling molecules and regulatory proteins of the actin cytoskeleton (Dan et al., 2001). Thus, Tao-1 is a good candidate for an upstream regulator of the cytoskeletal organisation of the oocyte.

3.4.1. Characterisation of *Tao-1* gene

3.4.1.1. Tao-1 is a Serine/Threonine protein kinase

The highly conserved serine/threonine kinase Par-1 has been shown to be required for polarising the MT network in the oocyte during oogenesis (Shulman et al., 2000; Tomancak et al., 2000). To identify the Par-1 phosphorylation substrates, 5849 cDNAs, which contain Expressed Sequence Tags (EST) produced by the Berkeley *Drosophila* Genome Project (BDGP), were screened in a biochemical in vitro assay. Among the 5849 screened cDNAs, 133 encode proteins that were phosphorylated by Par-1 kinase in vitro. These proteins were classified into seven groups: Cytoskeletal proteins (11), proteins involved in different aspects of signal transduction (35), DNA-associated proteins (34), RNA-associated proteins (34), enzymes (9), novel proteins (25) and others (9) (Riechmann and Ephrussi 2004). The gene CG14217 was identified from this screen as a Par-1 phosphorylation substrate and classified into the group of proteins involved in the signal transduction. CG14217 is the *Drosophila* orthologue of mammalian *Tao-1*, which belongs to the Ste20 like kinase family. *Drosophila* Tao-1 shares 50% identity to Human Tao-1 and 43% to Rat Tao-1. Interestingly, in vitro studies revealed that the rat Tao-1 homologue is able to phosphorylate, and thereby activate the rat Par-1 homologue (Timm et al., 2003).

These data suggest a cross regulation between Tao-1 and Par-1. For this reason, *Drosophila* Tao-1 was among the most interesting Par-1 substrates identified in the screen.

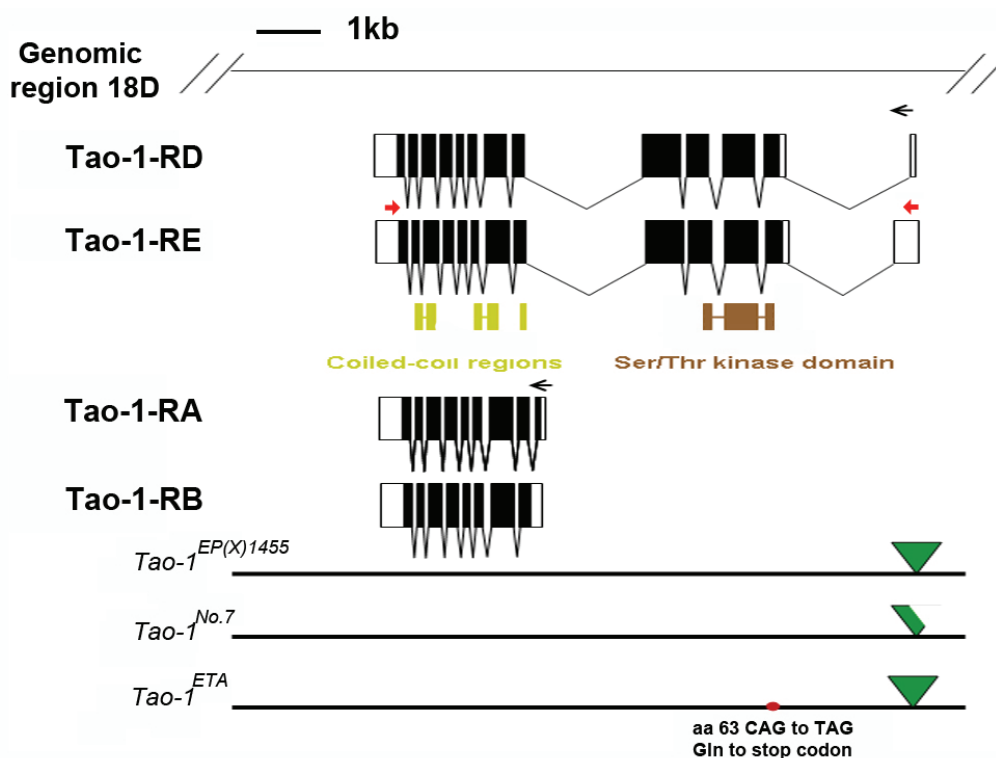


Fig. 11 Schematic drawing of the *Tao-1* genomic locus, *Tao-1* translations and the genomic structures of *Tao-1* associated alleles. The top line shows a representation of genomic region 18D2 to D3 where *Tao-1* is located. Black arrows indicate the direction of transcription. Open boxes indicate the untranslated regions (UTR) and black boxes indicate the coding sequences. The lines connecting boxes indicate the introns. Four transcripts are annotated by the database. Red arrows indicate the primer pair used in RT-PCR. The predicted protein domains contained in the translations were indicated in color boxes below the corresponding coding sequences. The coding sequence for the Ser/Thr domain covers a part of exon2, entire exon3 and a part of exon4. The coding sequence for coiled-coil domain covers eight exons at the C-terminus. EP(X) 1455, represented by the green triangle, is inserted into the 5' UTR of *Tao-1* about 2kb upstream from the start codon. In *Tao-1*^{No.7} mutants, a fragment of about 5 kb from the EP element was left at the original insertion site. In *Tao-1*^{ETA} mutants, the single nucleotide transition indicated by the red point is located 38 base pairs upstream from the 3' prime of exon2. The induced stop codon truncates the translation to approximately 6% of the predicted full length protein and 14% of the catalytic domain. The start codon for short transcripts might not be affected in *Tao-1*^{ETA}.

The *Tao-1* locus is located between 18D2 to 18D3 at the X-chromosome. Four transcripts, *Tao-1*-RA, -RB, -RD, -RE (GenBank accession numbers: NM_134475,

NM_167667, NM_167665, NM_167666) were annotated according to EST clones. The gene structure of each transcript was also annotated (Fig. 11). Tao-1-RD and -RE are about 4 kb long and comprise 13 exons, with mild difference in the length of 5' untranslated region (UTR). Tao-1-RA and -RB are approximately equivalent to the C-terminal part of Tao-1-RD and -RE starting with exon 6, the length of which is about 2.3 kb. Simple Modular Architecture Research Tool (SMART) (Schultz et al., 1998) reveals that the protein product encoded by the long transcripts, Tao-1-RD and -RE contains a serine/threonine protein kinase domain at the N-terminus, with the encoding region extending from exon 2 to 4. The kinase domain is followed by coiled-coil regions at the C-terminus, which are encoded by the common sequence shared by all of the transcripts (Fig. 11).

Here, it has to be noted that the Tao-1 isoform identified to be phosphorylated by Par-1 kinase was encoded by the 2.3-kb transcripts. Whether the other Tao-1 isoform encoded by the 4-kb transcripts, which contains the kinase domain, is also phosphorylated by Par-1 kinase has not yet been tested. This was due to the fact that the *Tao-1* cDNA clones available in the public database only contain the 2.3-kb transcripts; while the clones containing the 4-kb *Tao-1* transcripts were lacking.

3.4.1.2. *Tao-1* transcripts are expressed during oogenesis

To obtain the full length *Tao-1* cDNA expressed during oogenesis, RT-PCR of total mRNAs of ovaries was performed. The primer pair was designed on the basis of the 4-kb transcripts annotated by the database. One primer was located in the 5' UTR and other one was located in the 3' UTR of the 4-kb transcripts (Fig. 11 red arrows). Using this primer pair, a DNA fragment of about 4 kb, which was in agreement the length of predicted full length *Tao-1* transcripts, was specifically amplified by RT-PCR. Therefore, this cDNA fragment was regarded as the *Tao-1* full length cDNA and cloned into vectors for various uses in the following studies.

To confirm the result of RT-PCR, Northern blot analysis of ovarian RNAs was performed using the 4-kb *Tao-1* cDNA obtained from RT-PCR as the probe. If the

annotation of *Tao-1* transcripts was accurate and complete, we would expect to detect one transcript of 4 kb and another one of 2.3 kb by the Northern blot. Surprisingly, the Northern blot analysis revealed one transcript of about 3 kb and another transcript of about 6 kb, neither of which corresponded to the length of the predicted transcripts (Fig. 14F, lanes indicated). Thus, the annotation provided by the database did not completely describe the complexity of *Tao-1* transcripts expressed during oogenesis. The expression of the 4-kb transcripts annotated by EST clones was verified by RT-PCR. The failure to detect these 4-kb transcripts by the Northern blot analysis indicated low expression levels of these transcripts. Given the lower sensitivity of Northern blot analysis, it was not clear whether the predicted 2.3-kb transcripts were present during oogenesis. Nevertheless, even if the 2.3-kb transcripts were expressed, the expression must be in a low level. Instead, the 6-kb and 3-kb transcript of *Tao-1* were predominantly expressed during oogenesis.

To further examine the expression pattern of *Tao-1* during oogenesis, RNA in situ hybridization in ovaries was performed using a probe corresponding to the 4-kb *Tao-1* cDNA. In the germline, signals were detected from stage 2 (Fig. 12A). The expression was consistently high in the nurse cells. At stage 10a the expression level was even increased. In the follicle cells, *Tao-1* expression was also detected, but at a low level (Fig. 12A inset). The expression was first evident at stage 6 and continued through stage 9.

3.4.1.3. Tao-1 protein is localised at the oocyte cortex

To determine the subcellular localisation of Tao-1 protein, the GAL4/UAS system was applied, due to the lack of antibodies recognising *Drosophila* Tao-1 protein. Transgenic flies were generated, which carried the construct of 4-kb *Tao-1* cDNA fused with an N-terminal hemagglutinin (HA) tag epitope sequence. When the HA-Tao-1 fusion protein was expressed in the germline by the *nanos:Gal4-VP16* driver line, notably, the protein was enriched at the oocyte cortex and co-localised with F-actin (Fig. 12B', B'' and B).

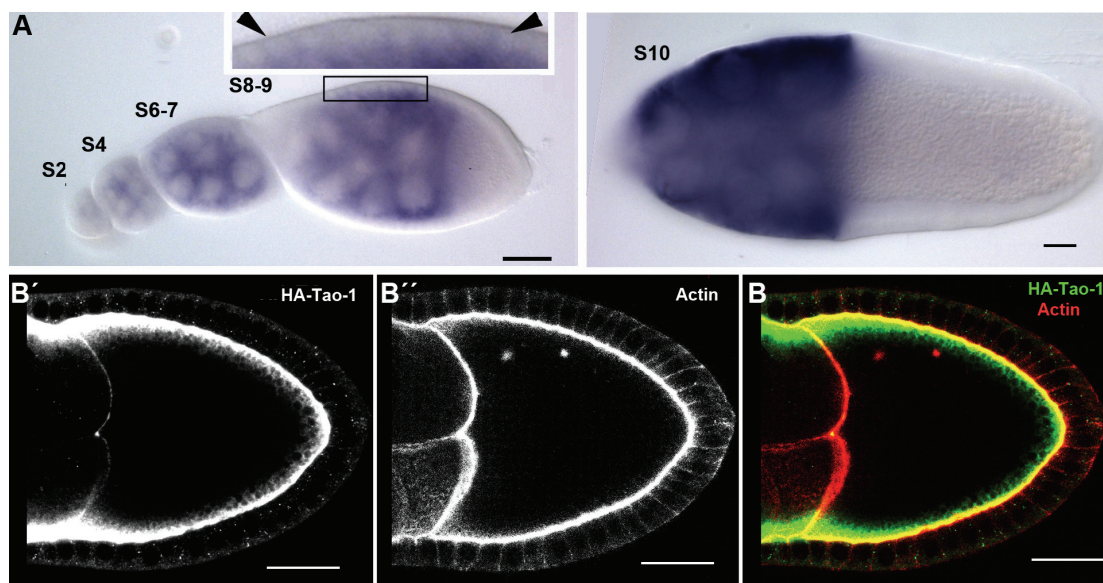


Fig. 12 The expression of *Tao-1* transcripts and the localisation of Tao-1 protein during oogenesis (A) RNA in situ hybridization of *Tao-1* in ovaries. Inset shows the marked region in higher magnification. Signals are detected in the germline from stage 2 on. The expression level is high in the nurse cells. At stage 10a the expression level is even increased. Expression in the follicle cells is in a low level (inset, between arrow heads). The expression is first evident at stage 6 and continuing through stage 9. (B) Sagittal section of a stage 10a oocyte expressing HA-Tao-1 fusion protein by *maternal- α -tubulin:Gal4* double stained with an antibody recognising HA (B') and phalloidin for actin (B''). The HA-Tao-1 fusion protein (green) is enriched at the entire oocyte cortex, overlapping with cortical actin (red). Scale bar: 25 μ m

3.4.2. Anterior-posterior and dorsal-ventral patterning defects manifested in *Tao-1*^{No.7} mutants

3.4.2.1. Generation of a *Tao-1* mutant by imprecise P-element excision

The cortical localisation of Tao-1 protein places Tao-1 in a good location to regulate actin and MT organisation. To investigate the function of Tao-1, mutants in *Tao-1* gene were required. One P-element insertion line, Tao-1 EP(X) 1455, is inserted in the 5' UTR of *Tao-1*, approximately 2kb upstream of the start codon (Fig. 11). Tao-1 EP(X) 1455 flies did not manifest defects regarding the viability and the fertility. By mobilising this P-element using the Δ 2-3 transposase (Robertson et al., 1988), a collection of progeny with excision of the P-element was generated. The excision lines were screened for lethal or sterile mutation, which might be caused by imprecise

excision events that altered the expression of Tao-1 protein. After screening 80 excised lines, one line (*No.7*), was identified because of its lower fertility.

No.7 mutant males were viable and fertile. *No.7* homozygous females also survived to adults. However, they produced fewer eggs than wild type females when they were raised at room temperature (Fig. 13B). As the mutant females were mated with wild type males, the phenotype was maternal effect. To determine whether the severity of the impaired fertility was temperature dependent, the egg production and the hatching rate of mutant females kept at different temperatures were compared. At 29°C, *No.7* flies laid as many eggs as the wild type (Fig. 13 C); a large proportion of these eggs hatched (Fig. 13D). At 18°C, the mutant flies produced significantly fewer eggs than the wild type (Fig. 13A); while most of the eggs did not hatch (Fig. 13D). In following studies, the phenotype was mostly characterised in the flies kept in 18°C, the temperature at which *No.7* flies produced defects with the highest penetrance.

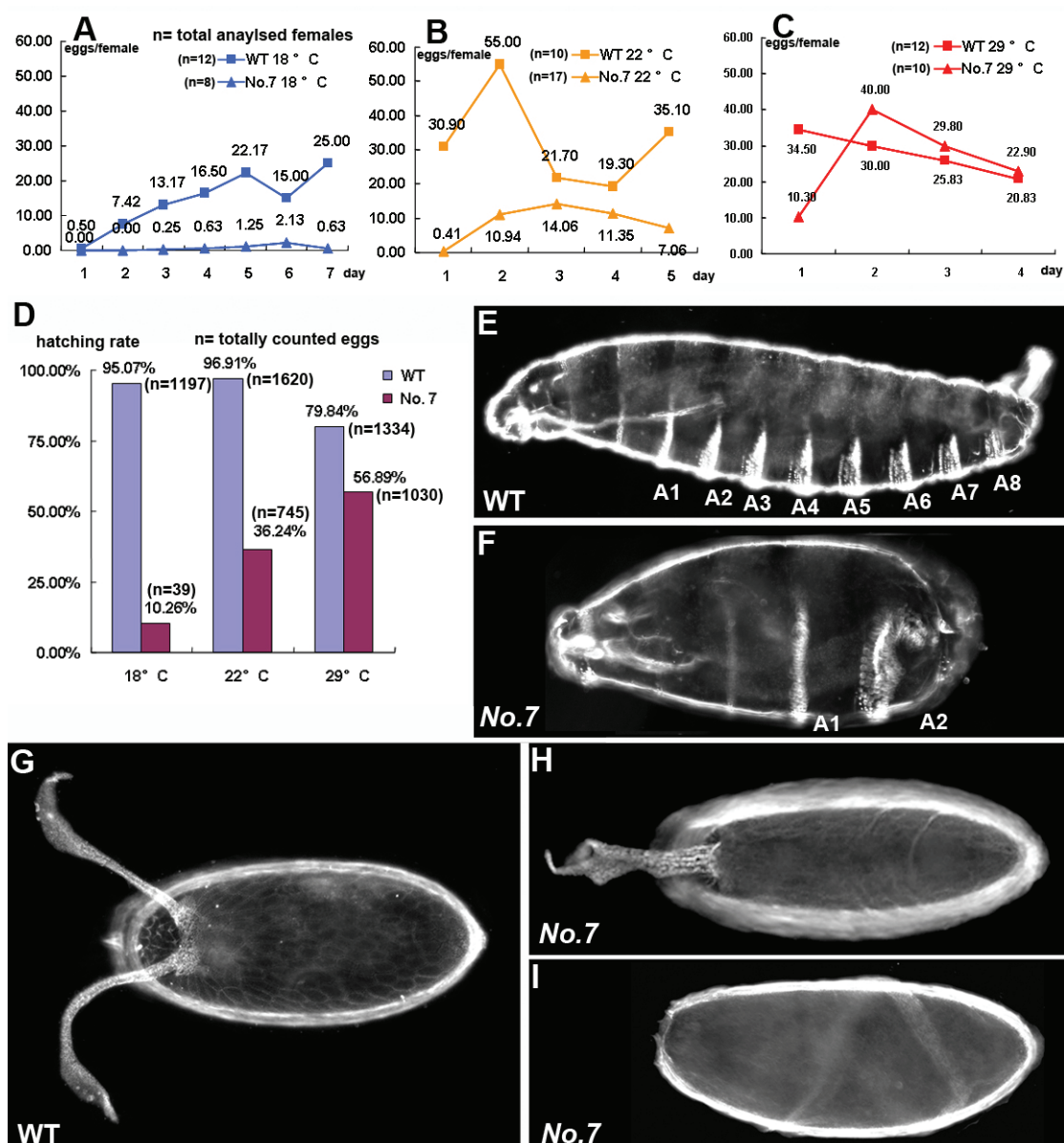


Fig. 13 Fertility and patterning defects in *No.7* mutants (A-C) The comparison of capabilities for egg laying between wild type and *No.7* females, which are raised at different temperatures as indicated. The Y-axis depicts the average number of eggs laid by a female. The X-axis depicts the consecutive days. n represents the number of analysed females. (D) The comparison of hatching rates of the eggs laid by wild type and by *No.7* females, which are raised at different temperatures as indicated. The Y-axis depicts the percentage of hatched eggs. The X-axis depicts different temperatures. n represents the number of eggs totally analysed. (E, F) Larval cuticle preparations. (E) The denticle belts in wild type mark eight abdominal segments (A1-A8). (F) The “posterior group” phenotype manifested in embryos produced by *No.7* mutants. The structures at the posterior including some abdominal segments (A3-A8) are missing. (G, H, I) Eggshells. (G) Wild type with a pair of dorsal appendages at the dorso-anterior position. (H, I) Ventralised eggshells produced by *No.7* mutants with fused appendage (H) or lacking dorsal appendages altogether (I).

3.4.2.2. *Tao-1^{No.7}* is a novel allele of *Tao-1* affecting the anterior-posterior and dorsal-ventral patterning

As the majority of eggs laid by *No.7* homozygous females did not hatch, larval cuticle preparation was examined. This analysis revealed that 19% (n=404) of the eggs displayed a “posterior group” phenotype, characterised by a lack of the posterior structures (Fig. 13F). This phenotype is primarily found in the mutations affecting the genes essential for pole plasm formation at the posterior pole (St Johnston and Nussleinvolhard, 1992). In addition to the “posterior group” defects, the morphology of eggs produced by mutant females appeared abnormal. In the wild type eggshell, there was a clear dorsal-ventral (D-V) polarity, marked by a pair of dorsal appendages at the dorsal-anterior position. A fraction of eggs (16%, n=113) produced by the mutants had a single fused dorsal appendage, among those most eggs (59%) even lacked dorsal appendages altogether (Fig. 13H and I). This eggshell phenotype has been described in the mutants affecting the Gurken/Torpedo pathway, which determines dorsal follicle cell fates (Schupbach, 1987). Thus, *No.7* mutants interfere with both the posterior and the dorsal-ventral patterning.

The finding that the posterior patterning is affected in *No.7* mutants suggests that pole plasm formation is affected. Oskar protein has been shown to be essential to recruit pole plasm components to the posterior pole (Breitwieser et al., 1996; Ephrussi and Lehmann, 1992). Therefore, the localisation of Oskar protein in the oocyte was examined by antibody staining. In this analysis only egg chambers at stage 10a were included, the stage at which Oskar protein is unambiguously localised at the posterior pole of the wild type oocyte (Fig. 14A). In 83% of the mutant oocytes (79 out of 96), Oskar protein was not detectable at the posterior (Fig. 14B). Given that the severity of the impaired fertility manifested by *No.7* mutants is temperature dependent, we asked whether this was also the case for the localisation defect of Oskar protein. To assess this, the localisation of Oskar protein was analysed in the oocyte of mutant flies raised at higher temperatures. When the flies were kept at 29°C, only in 4% of stage 10a

oocytes (n=111), Oskar protein was absent at the posterior of the oocyte. Thus, at lower temperature a higher penetrance of Oskar protein localisation defects was observed, which is consistent with the temperature dependency of the fertility defect. We therefore propose that the temperature dependency is a general feature of the *No.7* phenotype.

In the majority of mutant egg chambers, Oskar protein was not detectable at the posterior pole of the oocyte. To confirm this result by using a different detection method, western blot analysis was performed. Western blot analysis of ovary extracts showed that the expression of Oskar protein was greatly reduced in the mutant ovaries (Fig. 14G, lanes indicated). Taken together, Oskar protein translation is severely affected in *No.7* mutants.

As the dorsal-ventral patterning was also affected, the localisation of Gurken (Grk) protein was examined in stage 10a oocyte by antibody staining. In wild type oocyte, Gurken protein was restricted at the dorsal-anterior corner adjacent to the oocyte nucleus (Fig. 14C). In 88% (60 out of 68) of the mutant oocytes, the expression of Gurken protein was not detectable (Fig. 14D). This result indicates that the translation of Gurken protein, like Oskar protein, is also disrupted in the mutant oocyte.

Fig. 14

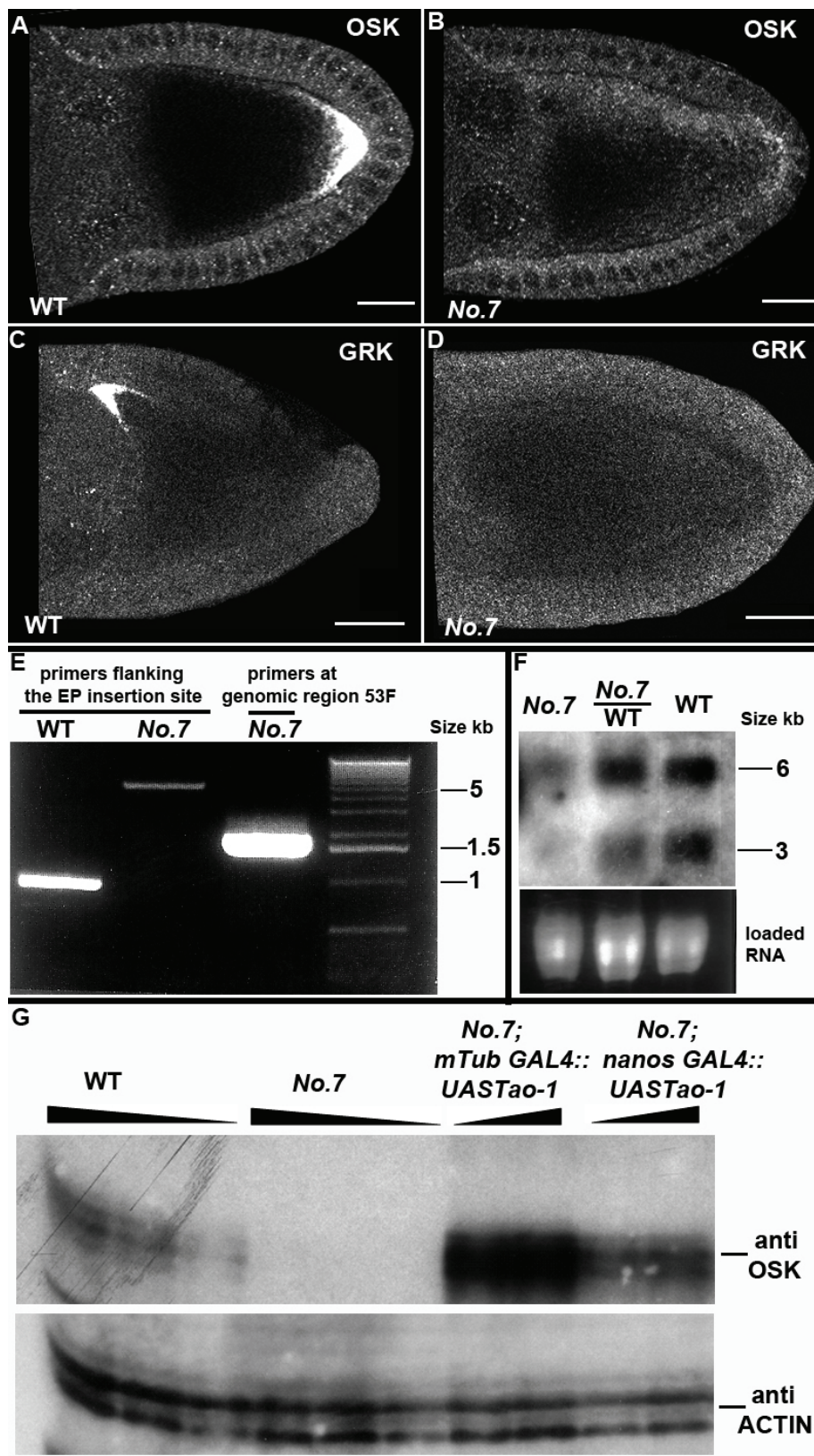


Fig. 14 Localisation defects of Oskar and Gurken protein in *No.7* mutant oocytes, rescue experiment by *Tao-1* transcripts and molecular characterisation of *No.7* allele (A-D) Sagittal sections of stage 10a egg chambers stained for Oskar protein (A, B) and for Gurken protein (C, D). (A) In wild type, Oskar protein is localised at the posterior pole of the oocyte. (B) In 83% of *No.7* mutant oocytes, Oskar protein is not detectable at the posterior. (C) In wild type, Gurken protein is restricted at the dorsal-anterior corner adjacent to the oocyte nucleus. (D) In 88% of the mutant oocytes, Gurken protein is not detectable. (E) Genomic PCR analysis. Using a primer pair flanking the EP(X) 1455 insertion site, an approximately 1 kb fragment is amplified from wild type genomic DNA. A fragment of 5 kb is amplified from *No.7* genomic DNA. To control the specificity of the PCR reaction performed with *No.7* genomic DNA, a primer pair in other genomic region is used, which produces the fragment at the expected size. (F) Northern blot analysis of ovarian RNAs using 4-kb *Tao-1* cDNA as the probe. The amounts of loaded RNAs are identical in different lanes. In wild type one transcript of approximately 3 kb and the other one of about 6 kb are detected. In *No.7* mutants, the transcription level of *Tao-1* is reduced, particularly with regard to the short transcript. (G) Western blot analysis of ovarian protein extracts probed with anti-Oskar antibody. Genotypes are indicated. The loading amounts for different lanes are compared by the blot probed with anti-Actin antibody and the gradient is indicated by the black triangles. In *No.7* mutants, the expression of Oskar protein is greatly reduced. The expression of Oskar protein is restored to wild type level when *Tao-1* transcripts are expressed in the germline. Scale bar: 25 μ m

To progress further, it was necessary to determine whether the phenotype was the result of the disrupted function of *Tao-1*. It was first asked whether the *Tao-1* locus was affected after P-element excision in *No.7* mutants. To this end, PCR was performed using the genomic DNA as the template, and using a primer pair that flanks the EP(X) 1455 insertion site. In the wild type, the PCR amplified a DNA fragment of about 1 kb. In *No.7* mutants, the PCR amplified a DNA fragment of 5 kb (Fig. 14E, lanes indicated). Subsequent sequencing analysis of this 5-kb fragment revealed that this DNA fragment contained sequences of the P-element. Thus, in *No.7* mutants the original P-element was imprecisely excised, and a fragment of about 4 kb from the EP element was left at the original insertion site in the 5' UTR. Sequencing analysis also showed that the rest of the genomic sequence in the *Tao-1* locus was not affected.

To further determine whether this insertion interferes with the transcription of *Tao-1*, Northern blot analysis was performed. The analysis showed that the transcription level of *Tao-1* was greatly reduced in mutant ovaries, particularly with regard to the short transcript (Fig. 14F, lanes indicated). This raised the question whether the reduced transcription level of *Tao-1* resulted in the phenotype described above. This question could be addressed by asking whether this phenotype can be rescued when *Tao-1* transcripts are supplied in the mutant background. For this purpose, the GAL4/UAS system was applied. Both the *nanos:Gal4-VP16* and *maternal- α -tubulin:Gal4-VP16* drivers were used to express *Tao-1* long cDNA in the germline of the mutant females. Western blot analysis with the ovary extracts was examined. Importantly, with the expression of *Tao-1* cDNA in the germline, the expression of Oskar protein in the mutant oocyte was recovered to a level identical to that in wild type (Fig. 14G, lanes indicated). Furthermore, in every stage 10a egg chamber stained with anti-Oskar antibody (n=63), Oskar protein was found to be correctly localised at the posterior pole of the oocyte. In addition, the defect of Gurken translation was completely rescued, with Gurken protein correctly localised at the dorsal-anterior corner adjacent to the oocyte nucleus in every egg chamber (n=47). Thus, these data verify that the phenotypes observed in *No.7* mutants are the result of the reduced *Tao-1* transcription.

In summary, we have identified *Tao-1^{No.7}* as a novel mutant allele of *Tao-1* gene, which reduces *Tao-1* transcription. This mutant affects the translation of Oskar and Gurken protein in the oocyte. The absence of Oskar protein at the posterior pole of the mutant oocyte prevents pole plasm formation and results in embryos lacking posterior structures; while the absence of Gurken protein at the dorso-anterior corner of the mutant oocyte prevents the specification of dorsal follicle cells and causes the ventralisation of the eggshell.

3.4.2.3. The patterning phenotype of *Tao-1^{No.7}* is the result of mislocalisation of transcripts of axis determinants during mid-oogenesis

It has been shown that Oskar protein translation at the posterior of the oocyte requires *oskar* mRNA localisation to the posterior pole of the oocyte. *oskar* mRNA is translationally repressed until it reaches to the posterior of the oocyte, which ensures that the protein activity is restricted at the correct subcellular location (Kimha et al., 1995; Markussen et al., 1995; Rongo et al., 1995). The finding that the translation of Oskar protein is affected in *Tao-1^{No.7}* oocytes raised the possibility that *oskar* mRNA localisation was affected. Therefore, fluorescent in situ hybridisation was performed to examine the localisation of *oskar* mRNA in *Tao-1^{No.7}* oocytes. In wild type oocytes at stage 9/10a, *oskar* mRNA is localised at the posterior pole and remains there until egg deposition (Fig. 15C; Ephrussi, 1991; Kim-Ha, 1991 (Ephrussi et al., 1991; Kimha et al., 1991)). In *Tao-1^{No.7}* oocytes, *oskar* mRNA was not accumulated at the posterior pole, but dispersed ubiquitously within the ooplasm as diffuse particles (Fig. 15F).

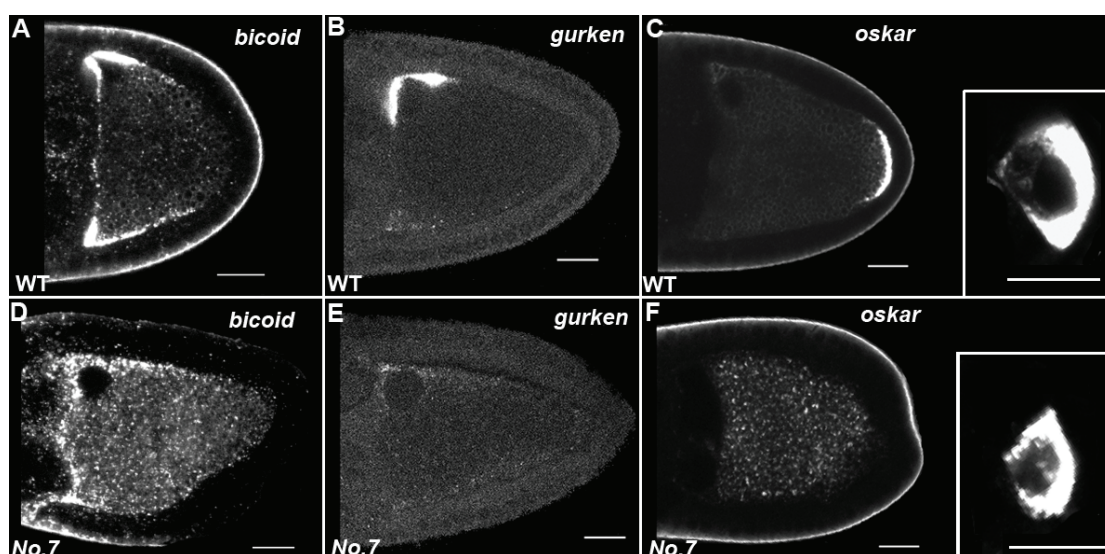


Fig. 15 Localisation of *bicoid*, *gurken* and *oskar* mRNAs in *Tao-1^{No.7}* mutant oocytes
 Fluorescent RNA in situ hybridisations of *bicoid* (A, D), *gurken* (B, E) and *oskar* (C, F) in stage 10a wild type (A, B, C) and *Tao-1^{No.7}* mutant oocytes (D, E, F). (A-C) In wild type, *bicoid* mRNA is restricted at the anterior corners and accumulates as a cortical ring at the oocytes. *gurken* mRNA accumulates as a cap above the nucleus at the dorsal-anterior corner. *oskar* mRNA is localised at the posterior. (D-F) In *Tao-1^{No.7}* mutants, *bicoid* mRNA is not restricted tightly at the anterior. *gurken* mRNA is not accumulated at the dorsal-anterior corner associated with the nucleus. *oskar* mRNA does not accumulate at the posterior. Instead, they are all released into the entire ooplasm and disperse ubiquitously within the ooplasm as diffuse particles. Scale bar in A-F: 25 μ m; Scale bar in C and F insets: 10 μ m

As the translation of Gurken protein was also disrupted in the mutant oocyte, the localisation of *gurken* mRNA was examined. In wild type stage 9/10a oocytes, *gurken* mRNA accumulates as a cap above the nucleus at the dorsal-anterior corner of the oocyte (Neumansilberberg and Schupbach, 1993). In mutant oocytes, *gurken* mRNA was not accumulated at the dorsal-anterior corner associated with the nucleus, but distributed randomly in particles through the ooplasm (Fig. 15E).

In wild type stage 9/10a oocytes, another transcript displaying highly polarised localisation is *bicoid* mRNA, which is required for establishing the head and thoracic patterning of the embryo (Berleth et al., 1988; St Johnston and Nussleinvolhard, 1992). Therefore, the analysis was extended to the *bicoid* mRNA localisation. In wild type oocytes, *bicoid* mRNA was restricted at the anterior corners and accumulates as a cortical ring at the oocytes (Berleth et al., 1988). In mutant oocytes, *bicoid* mRNA

was not restricted tightly at the anterior, but released into the entire ooplasm (Fig. 15D).

Taken together, *oskar*, *gurken* and *bicoid* mRNAs, which are important for the embryo patterning, were all mislocalised in *Tao-1^{No.7}* oocytes at stage 9/10a. A question raised by this result was that during oogenesis when the mRNA localisation defect begins: Does it start at mid-oogenesis or at early-oogenesis? To assess this, we examined the localisation of *oskar*, *gurken* and *bicoid* mRNAs in *Tao-1^{No.7}* oocyte at stage 5, when mRNAs normally accumulate at the extreme posterior of the wild type oocyte (Fig. 15C inset). In all cases of *Tao-1^{No.7}* mutants, *oskar*, *gurken* and *bicoid* mRNAs are correctly accumulated at the posterior of the oocyte (Fig. 15D inset). Thus, the mRNA localisation defect in *Tao-1^{No.7}* mutant is restricted to mid-oogenesis.

3.4.3. Cytoskeletal organisation is disrupted in *Tao-1^{No.7}* oocytes

3.4.3.1. MT organisation is disrupted in *Tao-1^{No.7}* oocytes

The localisation of *oskar*, *gurken* and *bicoid* mRNAs to correct positions within the oocyte depends on MTs and MT motors (Brendza et al., 2000; Clark et al., 1994; Duncan and Warrior, 2002; Januschke et al., 2002; Pokrywka and Stephenson, 1991; Schnorrer et al., 2000). Therefore, the organisation of MT cytoskeleton in *Tao-1^{No.7}* oocyte was investigated.

The MT organisation analysed by optical sagittal sections revealed the following pattern: Unlike in the stage 10a wild type oocyte, where the bulk MTs spread from the cortex to the interior of the oocyte (Fig. 16A), in the mutant oocyte, the amount of MTs emanating from the cortex was greatly reduced. This reduction was accompanied by a strong increase of interlacing MTs that were spreading within the interior of the ooplasm (Fig. 16B). Additionally, it appeared that the level of MTs distributed in the ooplasm was equal from anterior to posterior (Fig. 16B). Thus, this gradient was not correctly formed in the mutant oocyte. Moreover, MTs present in *Tao-1^{No.7}* oocyte appeared thicker than that in wild type (Fig. 16B). As the movement of the oocyte

nucleus at stage 6, from the posterior to the anterior-dorsal corner of the oocyte, depends on MTs (Riechmann and Ephrussi, 2001), we also examined the localisation of the oocyte nucleus in mutant stage 10a oocytes. In the majority of mutant oocytes (53 out of 54), the nucleus was correctly positioned.

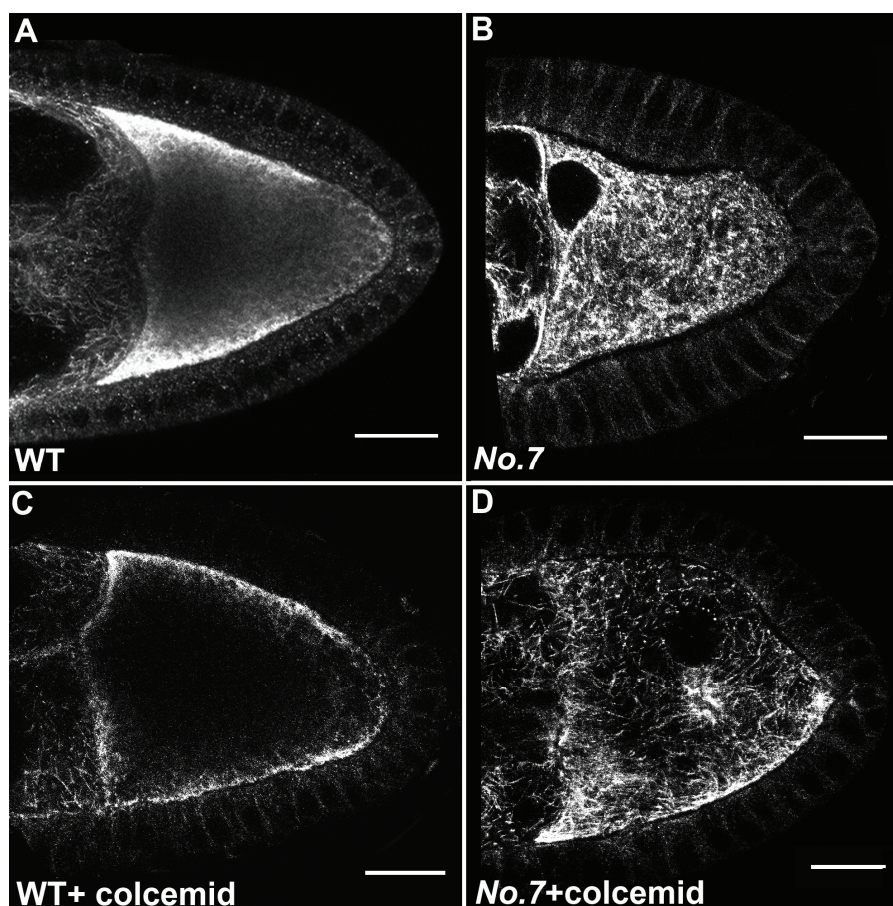


Fig. 16 MT organisation and colcemid treatment of *Tao-1^{No.7}* mutant oocytes Sagittal sections of stage 10a egg chambers stained for tyrosinated α -tubulin with genotypes and the treatment indicated. (A) In wild type, the bulk MTs spread from the cortex to the interior of the oocyte. The highest concentration of MTs occurs at the anterior and later cortex and lowest concentration is present at the posterior pole. (B) In *Tao-1^{No.7}* mutants, cortical MTs are reduced. Instead, the density of MTs present in the ooplasm is increased. These MTs are interlacing in the interior of the ooplasm. Additionally, the MTs appear thicker than that in wild type (compare A and B). (C, D) After colcemid treatment, in the wild type short MTs are associated with the anterior and lateral cortex (C); in *Tao-1^{No.7}* mutants, short MTs are dispersed within the ooplasm (D). Scale bar: 25 μ m

The MT organisation was further examined by using the MT plus-end reporter Khc::lacZ. This fusion protein consists of the motor domain of MT plus-end directed motor Kinesin heavy chain (KHC) and the enzyme, β -galactosidase (β -Gal) (Clark, 1994). Although the direct visualisation of the MTs in wild type oocytes did not

exhibit a clear anterior-posterior orientation, KHC- β -Gal accumulated at the posterior pole of the oocyte (Fig. 17C). This indicates the accumulation of MT plus-ends at the posterior pole. In *Tao-1^{No.7}* mutant oocytes, KHC- β -Gal was not restricted at the posterior pole, but released into the entire ooplasm, indicating that the MT plus-ends are ubiquitously distributed within the ooplasm (Fig. 17D).

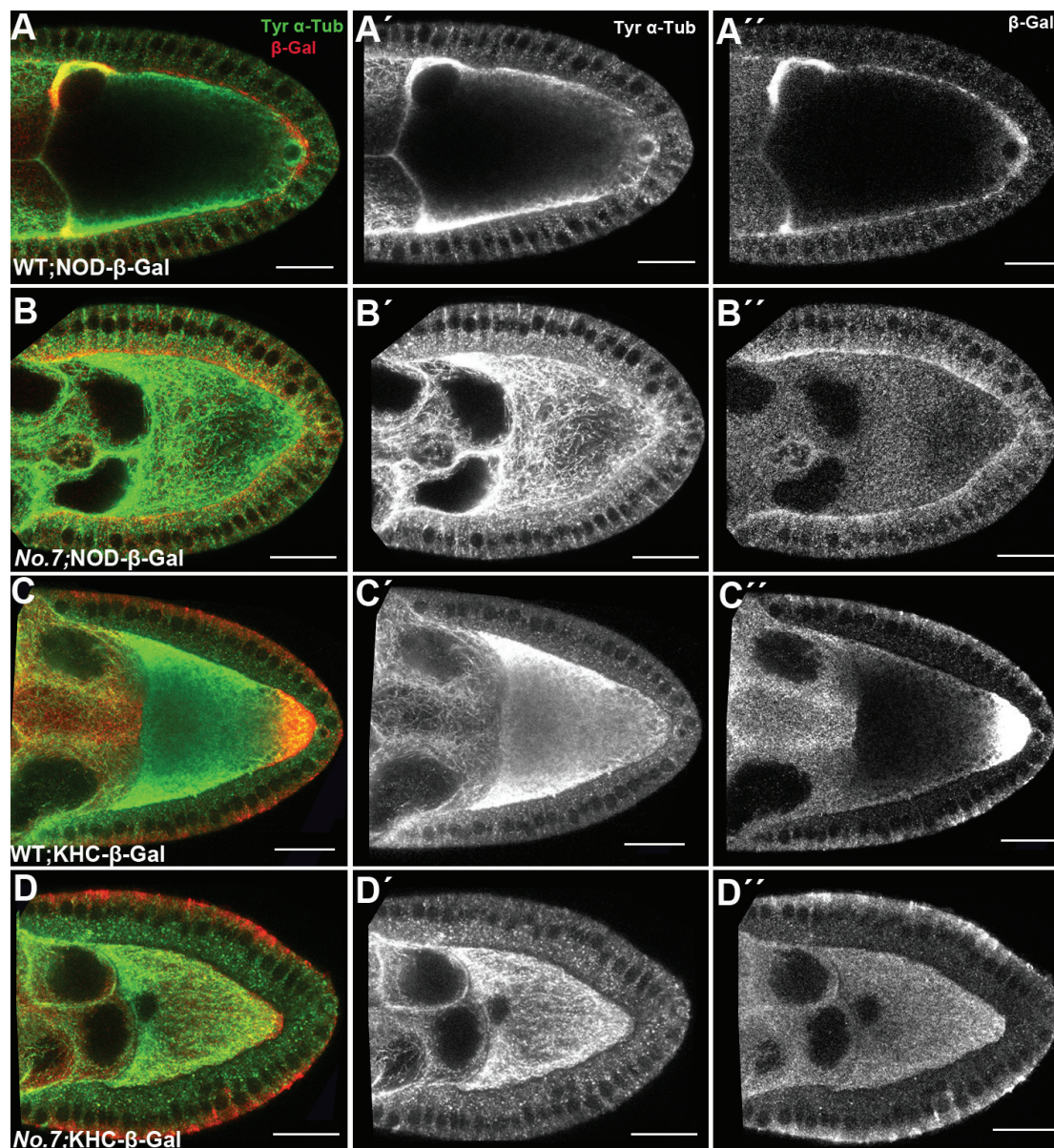


Fig. 17 The distribution of MT polarity markers in *Tao-1^{No.7}* mutant oocytes (A-D) Sagittal sections of stage 10a egg chambers double stained for tyrosinated α -tubulin (A'-D') and β -Gal (A''-D'') with genotypes indicated. (A, C) In wild type, the MT staining reveals normal MT organisation (A', C'). NOD- β -Gal is concentrated at the anterior corners (A'') and KHC- β -Gal accumulates at the posterior pole of the oocyte (C''). (B, D) In *Tao-1^{No.7}* mutants, MTs show the similar phenotype described in Fig. 15B (B', D'). In the corresponding oocyte, KHC- β -Gal is not restricted at the posterior pole (B'') and NOD- β -Gal is not concentrated at the anterior corners (D''). They both are ubiquitously distributed within the oocytes (B'', D''). Scale bar: 25 μ m

The MT minus-end reporter Nod:: lacZ, whose protein product contains the motor domain of Kinesin-related protein (NOD) and β -Gal (Clark et al., 1997) was also investigated. In wild type oocytes, NOD- β -Gal was concentrated at the anterior corners of the oocyte (Fig. 17A). In mutant oocytes, NOD- β -Gal was dispersed within the ooplasm, indicating that the MT minus-ends are also ubiquitously distributed within the oocyte (Fig. 17B). Interestingly, the mislocalisation defect of the minus-end marker NOD- β -Gal (95%, n=128) was more severe than that of the plus-end marker KHC- β -Gal, indicating that the minus-ends are more fragile than the plus-ends (70%, n=35). One speculation is that in mutant oocytes MTs are primarily affected in the minus-ends; subsequently, MT plus-ends are redistributed.

To test the hypothesis, MT minus-ends were examined in *Tao-1^{No.7}* mutant oocytes. Unlike in wild type oocytes, where γ -tubulin and Dgrip75 were present at the anterior and lateral oocyte cortex (Fig. 18A and C), γ -tubulin and Dgrip75 were uniformly distributed in the entire ooplasm in *Tao-1^{No.7}* mutants (Fig. 18B and D). Cross sections of mutant oocytes were further investigated, and the fluorescent signal of the γ -tubulin staining was measured. Consistent with observations acquired by optical sagittal sections, cross sections of mutant oocytes revealed that MTs were not restricted at the cortex, and the gradient from high to low density was not detected from the cortex to the interior. Instead, a high density of evenly dispersed MTs was observed within the entire ooplasm (Fig. 18F). Concomitantly, the thin and dense network of γ -tubulin restricted at the cortex was no longer present (Fig. 18H). Instead, γ -tubulin was homogeneously distributed from the cortex to the interior of the oocyte (Fig. 18H and H'), indicating the relocation of MT minus-ends from the cortex to the entire ooplasm.

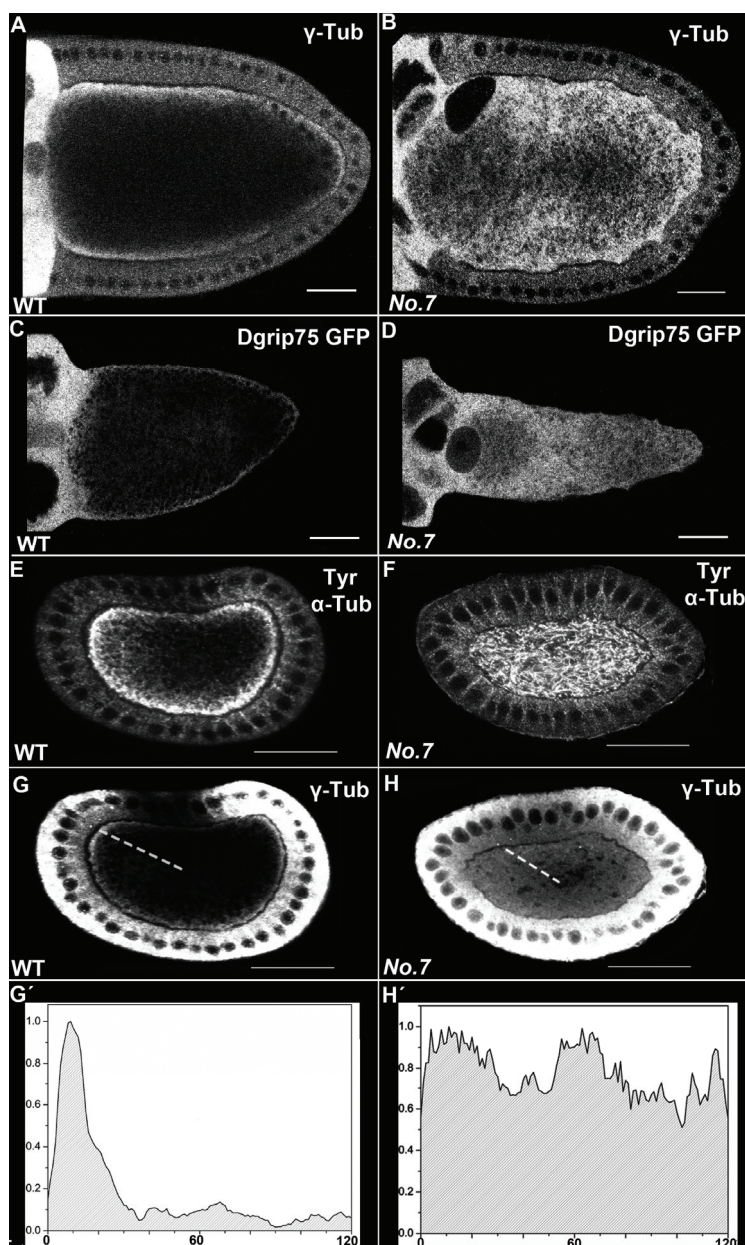


Fig. 18 The distribution of MT minus-ends in *Tao-1*^{No.7} mutant oocytes (A-B) Sagittal sections of stage 10a oocytes stained for γ -tubulin. In wild type, γ -tubulin is enriched at the entire oocyte cortex (A). In *Tao-1*^{No.7} mutants, γ -tubulin is distributed in the entire ooplasm (B). (C, D) Sagittal section of stage 10a oocytes expressing Dgrip75 GFP fusion protein by *maternal- α -tubulin:Gal4* stained with an antibody recognising GFP. (C) In wild type, the fusion protein is enriched at the entire oocyte cortex. (D) In *Tao-1*^{No.7} mutants, the fusion protein is uniformly distributed in the entire ooplasm. (E-H) Cross sections of stage 10a egg chambers double stained for tyrosinated α -tubulin (E, F) and γ -tubulin (G, H). (G', H') Plots of the γ -tubulin signal intensities along the dotted line (11 o'clock) from the exterior to the interior of the oocyte shown in corresponding cross sections. (E, G) In wild type, MTs form a dense network at the cortex (E), and γ -tubulin is restricted as a continuous layer at the cortex (G, G'). (F, H) In *Tao-1*^{No.7} mutant, MTs are not restricted to the oocyte cortex, but spread evenly within the ooplasm (F); γ -tubulin is homogeneously distributed from the cortex to the interior of the oocyte (H). Scale bar: 25 μ m

As an alternative way to visualise the MT minus-ends, a method independent of the MT minus-end markers was applied. MTs normally nucleate at the minus-ends; while polymerisation and depolymerisation preferentially occur from the plus-ends. Therefore, treating MTs with drugs to inhibit the MT polymerisation can leave short MTs at the minus-ends. Previous studies with the MT inhibitor colcemid indicated that MTs nucleate primarily at the anterior cortex (Theurkauf et al., 1992). Our colcemid treatment of wild type females revealed that MTs nucleate not only from the anterior but also from the lateral cortex (Fig. 16C). This result is consistent with the distribution of the MT minus-end marker γ -tubulin to the anterior and lateral cortex. In *Tao-1^{No.7}* mutant oocytes, colcemid treatment resulted in short MTs, which were dispersed within the ooplasm (Fig. 16D). This result supports the idea that MT minus-ends are released from the anterior and lateral cortex into the ooplasm in *Tao-1^{No.7}* mutants. Thus, our data indicate that the anchoring of MT minus-ends at the cortex is affected in *Tao-1^{No.7}* oocytes.

In summary, our data show that in *Tao-1^{No.7}* oocytes, the MT minus-ends are not anchored at the cortex, but relocate to the entire ooplasm. As a result, the MTs are spreading through the ooplasm, with minus-ends and plus-ends randomly distributed. The gradient of MT from anterior to posterior is not properly formed, and the MT network is not correctly organised. These results imply that the motor dependent transport of cargos along the MTs to the plus-ends or minus-ends can not be directed properly in *Tao-1^{No.7}* oocyte. Thus, the transcripts for the axis determinants are not transported to the correct subcellular locations.

3.4.3.2. Cortical actin bundles are disrupted in *Tao-1^{No.7}* oocytes

Tao-1 protein is present at the oocyte cortex (Fig. 12B). This raises the possibility that Tao-1 regulates the actin and MT organisation. The above described observation indicated that MT minus-end anchoring at the cortex of *Tao-1^{No.7}* mutant oocytes is affected. Therefore, it is possible that the actin bundling is affected in *Tao-1^{No.7}* mutant oocytes. To test this, the actin organisation in *Tao-1^{No.7}* mutant oocyte was

examined. The analysis of optical sagittal sections showed that the actin cortex in *Tao-1^{No.7}* oocyte was wavy (Fig. 19C), which was different from the smooth actin cortex observed in wild type oocyte (Fig. 19A). Optical cortical sections at the cortex of the stage 10a mutant oocyte revealed that actin bundles were not formed the cortex (Fig. 19D). Instead of the bundles, actin patches and thin filaments were observed, which was reminiscent of the cortex of wild type stage 10b oocytes, when the fast streaming has started. In addition to the actin bundling defect, ectopic actin clumps were observed in the mutant oocyte (Fig. 19C, arrows), indicating that actin aggregates irregularly. Our studies of *cap*, *Dmoe* and *swa* mutants showed that ectopic actin clumps in the ooplasm are not necessary coupled to actin bundling defects. In *Tao-1^{No.7}* oocyte, the simultaneous occurrence of ectopic actin clumps and the disruption of cortical actin bundling suggest that *Tao-1^{No.7}* may affect more than one pathway that regulates the actin cytoskeleton of the oocyte.

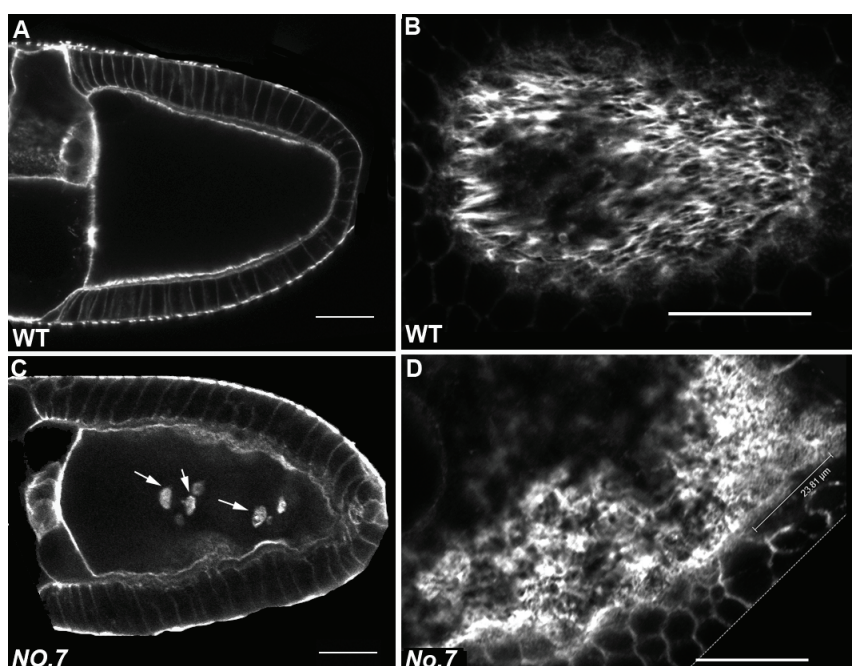


Fig. 19 Actin organisation in *Tao-1^{No.7}* mutant oocytes (A, C) Sagittal sections and (B, D) cortical sections of stage 10a oocytes stained for actin with genotypes indicated. (A, B) In wild type, the oocyte cortex is smooth (A); cortical actin is organised into bundles (B). (C, D) In *Tao-1^{No.7}* mutant, the oocyte cortex appears wavy and ectopic actin clumps (arrows) are observed in the oocyte (C); Cortical actin bundles are disrupted (D). Scale bar: 25 μ m

In summary, in *Tao-1^{No.7}* mutant oocytes cortical actin bundling is disrupted. MT minus-ends are not anchored at the cortex but redistribute into the entire ooplasm.

Organising from these dispersed minus-ends, MTs are spreading through the entire ooplasm. Such defects have not been described before. Therefore, the cytoskeletal organisation in *Tao-1^{No.7}* mutant oocytes might represent a novel phenotype for the MT and actin cytoskeleton organisation of the oocyte.

3.5. Screen for new *Tao-1* alleles

The P-element mobilisation experiment generated only one allele of *Tao-1*. This allele reduces but does not abolish *Tao-1* transcription. We therefore applied other strategies to generate more alleles of *Tao-1*, with the expectation to obtain an amorph allele.

3.5.1. *Tao-1^{ETA}* complements *Tao-1^{No.7}*

The EP element carries GAL binding sites (UAS) and a basal promoter. If the binding sites are orientated in the same direction as the transcription unit of the gene lying adjacent to the EP element insertion site, providing a source of Gal4 will induce the expression of the adjacent gene (Rorth, 1996). The orientation of *Tao-1* EP(X)1455 element is known to be in the same orientation as the *Tao-1* transcription unit (Shulman and Feany, 2003). When the flies carrying a ubiquitous Gal4 driver line *zygotic-tubulin:Gal4* were crossed to flies carrying the insertion of *Tao-1^{EP(X) 1455}*, the progeny carrying both the promoter and the EP element insertion was lethal. The lethality is most likely due to the overexpression of *Tao-1*. Based on this lethality, an EMS mutagenesis was performed to screen for alleles disrupting the function of *Tao-1*, by reversing the lethality caused by the overexpression of *Tao-1* (Verena Benecke's Diploma thesis).

The allele, *Tao-1^{ETA}* was identified in this screen. Sequencing analysis revealed a Cytosine to Thymine transition at amino acid position 63 of the predicted protein containing the Ser/Thr kinase domain (Fig. 11). The rest of the genomic sequence in *Tao-1* locus appeared no alteration. The C-A transition changed a glutamine codon (CAG) to a stop codon (TAG). This premature stop codon will truncate the translation to approximately 6% of the normal protein (Fig. 11). Furthermore, the truncated

protein only harbours 14% of the kinase domain. None of the predicted catalytic sites of the kinase domain (Hanks and Hunter, 1995) remains in the truncated protein. This strongly suggests that *Tao-1^{ETA}* is an allele that does not produce functional Tao-1 protein, with the lacking of the Ser/Thr kinase domain and the coiled-coil domains.

Tao-1^{ETA} homozygous flies were lethal. It was next asked whether the lethality was caused by the disrupted function of Tao-1 protein. This question was addressed by testing whether the ubiquitous expression of 4-kb *Tao-1* cDNA could rescue the lethality. Indeed, when this *Tao-1* cDNA was expressed by a ubiquitous driver, *zygotin-tubulin:Gal4*, the lethality was rescued, verifying that the lethality of *Tao-1^{ETA}* mutants was caused by the disrupted function of Tao-1 protein. When the same *Tao-1* cDNA construct was expressed in the germline of *Tao-1^{No.7}* mutant females, the cytoskeletal organisation defects of the oocyte were completely rescued. The ability of the *Tao-1* cDNA, which encodes the full length Tao-1 protein containing the kinase domain and the coiled-coil domains, to rescue both the *Tao-1^{ETA}* lethality and the *Tao-1^{No.7}* fertility suggest that *Tao-1^{No.7}* and *Tao-1^{ETA}* both suffer from the disruption of Tao-1 protein, but to different extent. *Tao-1^{ETA}* may represent a strong allele, as no functional Tao-1 protein could be produced in *Tao-1^{ETA}* mutants; *Tao-1^{No.7}* may represent a weak allele, as *Tao-1* transcripts were not completely abolished and some Tao-1 protein could be produced in *Tao-1^{No.7}* mutants. If this is the case, one would expect to detect the defects in MT organisation and Oskar protein localisation of a higher penetrance in *Tao-1^{ETA}* oocytes, than that in *Tao-1^{No.7}* oocytes. To test this possibility, the oogenesis in *Tao-1^{ETA}* mutants was analysed. As *Tao-1^{ETA}* homozygous flies were lethal, *Tao-1^{ETA}* germline clones were generated to examine the oogenesis. To our surprise, *Tao-1^{ETA}* germline clones did not show defects in the organisation of MTs and the localisation of Oskar protein (Fig. 20B), which have been observed in *Tao-1^{No.7}* oocytes. To test whether these two mutants complement each other, *Tao-1^{No.7}* flies were crossed to *Tao-1^{ETA}* flies. Transheterozygous flies of *Tao-1^{No.7}* and *Tao-1^{ETA}* were viable and did not manifest defects in the oocyte, with regard to MT organisation and Oskar protein localisation (Table 2). Thus, *Tao-1^{ETA}* complements the oogenesis defects observed in *Tao-1^{No.7}* mutants.

To summarise, neither in oocytes homozygous for *Tao-1^{ETA}*, nor in oocytes transheterozygous for *Tao-1^{No.7}* and *Tao-1^{ETA}*, the patterning defects described in *Tao-1^{No.7}* oocytes has been observed. In *Tao-1^{ETA}* mutants the functional Tao-1 protein is most likely not present. We therefore propose that Tao-1 protein is dispensable for the MT organisation and the polarity establishment of the oocyte during oogenesis. This suggests a possible role of *Tao-1* transcripts involved in the cytoskeleton organisation of the oocyte. The reduced level of *Tao-1* transcripts in *Tao-1^{No.7}* mutants may be the cause of the oogenesis phenotype. The provision of *Tao-1* transcripts by *Tao-1^{ETA}* in oocytes transheterozygous for *Tao-1^{No.7}* and *Tao-1^{ETA}* may therefore rescue the oogenesis defects observed in *Tao-1^{No.7}*.

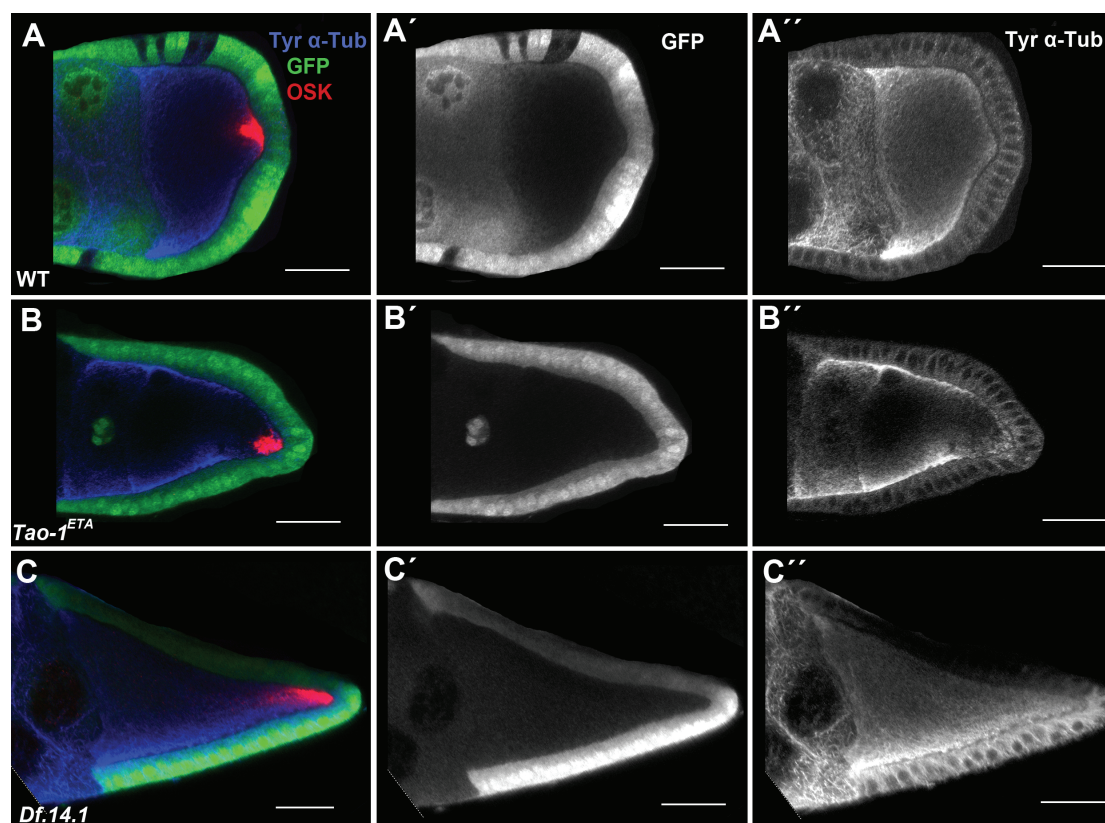


Fig. 20 The organisation of MT cytoskeleton and the localisation of Oskar protein in *Tao-1^{ETA}* and *Df.14.1* mutant oocytes Sagittal sections of stage 9/10a egg chambers triple stained for GFP (A'-C'), tyrosinated α -tubulin (A''-C'') and Oskar (red in A-C) with genotypes indicated. (A) Wild type control. (B, C) Germline clones of *Tao-1^{ETA}* (B) and *Df.14.1* (C), marked by the loss of GFP in the germline. They both manifest normal MT organisation and correct localisation of Oskar protein, like in the wild type. Scale bar: 25 μ m

3.5.2. Deficiency 14.1 complements *Tao-1*^{No.7}

To test whether the cytoskeletal organisation of the oocyte is regulated at the level of *Tao-1* transcripts, we generated an allele that completely deletes the *Tao-1* locus. For this purpose, we applied a strategy that allowed the deletion of defined genomic region. This method is based on the Flp-recombination target (FRT) sites of the piggyBac transposons that are inserted at various sites in the fly genome. When two FRT sites orientated in the same direction are present at different locations on homologous chromosomes, the recombination event between these two FRT sites induced by the presence of Flpase (FRT/FLP-recombination) will remove the genomic region between these two FRT sites (Thibault et al., 2004; Parks et al., 2004).

In the Exelixis collection of piggyBac insertion mutants, one insertion *e01713* was found to be inserted at the position about 300bp upstream from the *Tao-1* open reading frame (Fig. 21). Downstream of the *Tao-1* locus, the nearest P-element insertion suitable for FRT/FLP-recombination was *d02300*, which was inserted in the first intron of CG32532, the third gene downstream of *Tao-1*(Fig. 21). After the trans-recombination between *e01713* and *d02300*, a deficiency (*Df.14.1*) was acquired (see Materials and Methods). The genomic PCR and subsequent sequencing analysis revealed that this deficiency removed *Tao-1*, together with other two genes, *Dgrip84* and *carnation* completely. The first exon (5'UTR) of another gene, CG32532 of unknown function was also removed (Fig. 21). Thus, *Df.14.1* is an allele that does not produce any *Tao-1* transcripts.

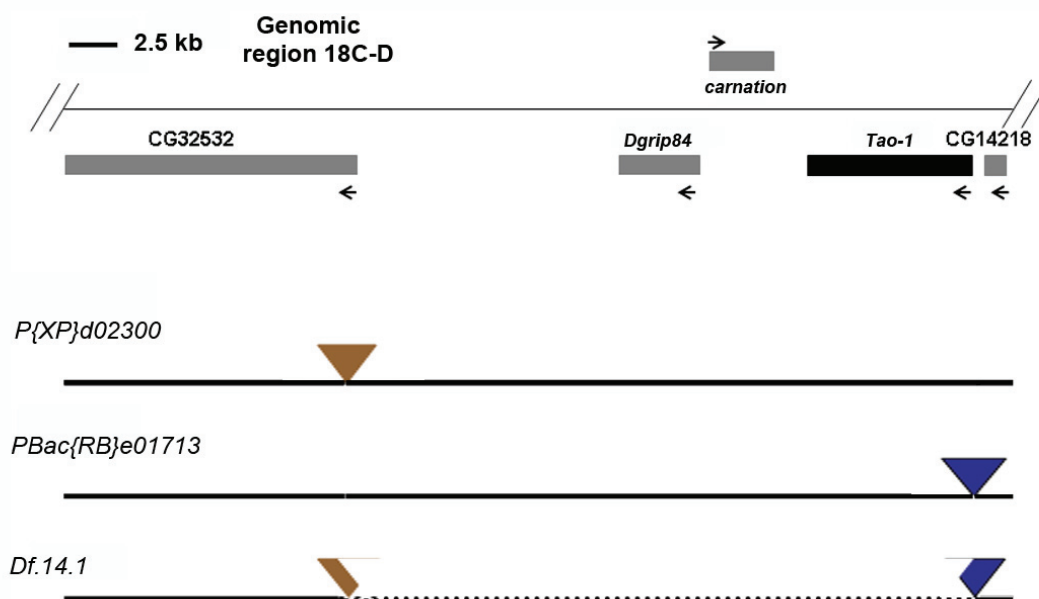


Fig. 21 Schematic drawing of genomic structures for Exelixis P-element insertions and deficiency 14.1 The top line shows a representation of the genomic region 18C to D. The neighboring genes of *Tao-1* are shown in grey boxes. Arrows indicate the direction of transcription. *PBac{RB}e01713* indicated by the brown triangle is inserted 300bp upstream of the *Tao-1* open reading frame. *P{XP}d02300* indicated by the blue triangle is inserted in the first intron of CG32532. After the trans-recombination between *e01713* and *d02300*, the deficiency *Df.14.1* is induced, which deletes *Tao-1*, *Dgrip84* and *carnation* completely, together with the first exon (5' UTR) of CG32532. The deleted region is indicated by the dash line.

If the cytoskeletal organisation of the oocyte is regulated at the level of *Tao-1* transcripts, one would expect to detect the defects in MT organisation and Oskar protein localisation of a higher penetrance in *Df.14.1* mutant oocytes, than that in *Tao-1^{No.7}* oocytes. As *Df.14.1* homozygous flies were also lethal, the oogenesis was analysed in germline clones of *Df.14.1*. Surprisingly, in *Df.14.1* mutant oocytes, MTs were correctly organised and Oskar protein was localised at the posterior pole (Fig. 20C). This result shows that in the absence of *Tao-1* transcripts, the oogenesis proceeds normally. Thus, *Tao-1* transcripts are not required for the cytoskeletal organisation of the oocyte. Additionally, this result also excludes the roles of other three affected genes involved in the oogenesis. To test whether *Df.14.1* and *Tao-1^{No.7}* complements each other, flies transheterozygous for *Tao-1^{No.7}* and *Df.14.1* were generated. These transheterozygous flies were viable and did not exhibit any defect in

cytoskeletal organisation and Oskar protein localisation of the oocytes (Table2). Thus, *Df.14.1* complements the oogenesis defects in *Tao-1^{No.7}* mutants.

	stage 10a oocytes with the localisation of Oskar protein at the posterior pole			
	18°C		29°C	
<i>Tao-1^{ETA}/Tao-1^{No.7}</i>	100%	n=29	100%	n=25
<i>Df.14.1/Tao-1^{No.7}</i>	100%	n=35	100%	n=35

Table 2 *Tao-1^{ETA}* and *Df.14.1* complements the localisation defect of Oskar protein in *Tao-1^{No.7}* mutants Flies transheterozygous for *Tao-1^{ETA}/Tao-1^{No.7}* and *Df.14.1/Tao-1^{No.7}* were raised in different temperatures as indicated. Egg chambers from these flies were double stained for tyrosinated α -tubulin and Oskar. Only stage 10a oocytes were analysed for the localisation of Oskar protein. “n” represents the number of analysed samples.

Genotype	Defects in the MT organisation and Oskar protein localisation
<i>Tao-1^{No.7}/Tao-1^{No.7}</i>	yes
<i>Tao-1^{No.7}/Tao-1^{No.7}; Tao-1 cDNA (4-kb)</i>	no
<i>Tao-1^{ETA}/Tao-1^{ETA}</i>	no
<i>Tao-1^{ETA}/Tao-1^{No.7}</i>	no
<i>Df.14.1/Df.14.1</i>	no
<i>Df.14.1/Tao-1^{No.7}</i>	no

Table 3 Summary of the oogenesis phenotypes in various mutants of *Tao-1* alleles

These data further complicated the characterisation of the genetic nature of *Tao-1^{No.7}*. The rescue of the cytoskeleton organisation defects observed in *Tao-1^{No.7}* oocytes by the expression of a *Tao-1* cDNA (4-kb) verified that *Tao-1^{No.7}* is an allele of *Tao-1*. However, neither mutants of *Tao-1^{ETA}* that do not produce functional Tao-1 protein, nor mutants of *Df.14.1* that delete the *Tao-1* locus completely, exhibit the defects in the cytoskeletal organisation of the oocyte that have been observed in *Tao-1^{No.7}* mutants (Table 3). Moreover, both *Tao-1^{ETA}* and *Df.14.1* mutants complement the oogenesis defects in *Tao-1^{No.7}* mutants. These evidences strongly suggest that the cytoskeleton organisation defects observed in *Tao-1^{No.7}* mutants can not be explained

as a loss of function of *Tao-1*. We therefore propose that *Tao-1^{No.7}* is a gain of function allele of *Tao-1*; while this gain of function effect is recessive, as two copies of *Tao-1^{No.7}* are required to induce the phenotype (Table 3).

4. DISCUSSION

4.1. Cytoskeletal organisation and reorganisation of the oocyte from stage 9/10a to stage10b

In this study, we show that at stage 9/10a the actin cytoskeleton at the oocyte cortex is assembled into long bundles, which are involved in the cortical localisation of γ -tubulin. γ -tubulin is part of the γ -tubulin ring complex (γ TuRC) that is localised to the MT minus-ends. It has been shown that the γ TuRC is necessary but not sufficient to restore the MT nucleation activity of salt-stripped *Drosophila* centrosomes. Besides the γ TuRC, additional factors seem to be required for the MT nucleation (Moritz et al., 1998). Thus, the presence of γ -tubulin alone does not allow us to conclude whether this protein is part of the MT nucleation sites. Here, we use γ -tubulin solely as the marker for the MT minus-ends, which are embedded within the cortical actin bundles of the oocyte before stage 10b.

The rearrangements of cytoskeletal organisation at stage 10b include the disassembly of the cortical actin bundles, the redistribution of the MT minus-ends from the cortex to subcortical regions and the formation of MT arrays parallel to the oocyte cortex. Concomitantly with these cytoskeletal changes, the transition from slow to fast ooplasmic streaming is triggered. How is the series of changes coordinated? The finding that interfering with actin bundle formation by drug treatment or GFPactin5C overexpression results in MT minus-ends redistribution, MT array formation and premature fast streaming indicates that actin bundling acts upstream of MT reorganisation.

The analysis of *Khc* mutants allows us to further dissect the sequential steps in the reorganisation of the MT cytoskeleton. In the absence of streaming caused by the loss of Kinesin function, the redistribution of MT minus-ends occurs normally; while the formation of MT arrays is abolished. Thus, minus-end redistribution is upstream of streaming, and array formation is downstream. We propose the following model for

the cytoskeletal reorganisation of the oocyte from stage 10a to stage 10b. At stage 10a, the actin bundles anchor MT minus-ends at the cortex. This cortical anchoring of MT minus-ends is essential to prevent fast ooplasmic streaming before stage 10b. At stage 10b, the cortical actin bundles disassemble, which results in the loss of MT minus-end anchoring at the cortex and the cortical release of MTs. This redistribution of MTs is the prerequisite of fast ooplasmic streaming.

This model raises the question how the localisation of MT minus-ends regulates the occurrence of fast ooplasmic streaming. It has been proposed that fast ooplasmic streaming involving MTs and Kinesin: Kinesin transports cargos to the MT plus-ends, exerting the force on the surrounding ooplasm. The concerted movement of multiple impellers along the neighbouring MTs that are oriented in the same general direction creates the fast streaming (Serbus et al., 2005). Our data suggest that the actin bundles tether the MT minus-ends to the cortex. This tethering makes the MTs resistant to the force exerted by the concerted movement of cargos, thereby limits the speed of ooplasm movement and prevents the MTs from being washed into parallel arrays. As the actin bundles disassemble, the tethering of minus-ends is lost and MTs can be released from the cortex. The free MTs are subject to the force exerted by the concerted movement of cargos, and thereby fast ooplasmic streaming can be initiated. At this step, a previously suggested self amplifying loop could be initiated, in which MT array formation and Kinesin movement enhances each other. In this loop the Kinesin driving streaming helps to sweep MTs into parallel arrays, which in turn allow more robust currents in the ooplasm (Serbus et al., 2005).

4.2. Cortical anchoring of MT minus-ends of the oocyte

Organised from the cortically localised minus-ends, MTs radiate to the interior of the oocyte at stage 9/10a. These non-centrosomal cortical MTs are analogous to MTs in some differentiated cells, such as in *Drosophila* wing epidermal cells, where apical-basal MT radiate from multiple nucleation sites associated with the apical plasma membrane (Mogensen et al., 1989). Although the plasma membrane

associated MT nucleating system is widely employed in polarised epithelial cells, it is not clear how they are anchored. Our finding that the cortical localisation of MT minus-ends is mediated by the actin bundles may gain insight into the general mechanisms how cortical MTs are anchored.

4.3. The cortical actin bundling of the oocyte, a novel actin based structure in the egg chamber

Previously, several specialised actin-based structures have been identified in the egg chamber. One of them is the ring canal. Ring canals interconnect 16 germline cells and transport the cytoplasmic components from the nurse cells to the oocyte. Another specialised actin structure is the actin bundle in the nurse cell cytoplasm. These actin bundles are required to anchor the nurse cell nucleus in the centre of the cell from stage 11 on during the process of “dumping”. The third specialised actin structure is the parallel actin bundling at the basal cortex of the epithelial cells surrounding the oocyte during mid-oogenesis. These actin bundles are required for the egg chamber elongation (Bateman et al., 2001; Frydman and Spradling, 2001). Here, we report the existence of a novel specialised actin-based structure, the actin bundles at the oocyte cortex. These actin bundles have not been analysed at an ultrastructural level, and it is not known how the actin filaments are crosslinked. In this study these actin filaments are referred to “actin bundles” because their organisation is reminiscent of bundles.

The actin bundles are predominantly oriented in an anterior-posterior direction. In addition, the density of the actin bundles at the posterior pole is very low. Thus, actin bundling reveals features of anterior-posterior polarity. Although the area of low actin bundle density at the posterior pole overlaps with the domain of Oskar localisation, our data reveal that the organisation of the posterior actin cytoskeleton does not require Oskar. This suggests that actin bundling is upstream of Oskar localisation. It has been suggested that Oskar localisation to the posterior pole is required for polarising the MT cytoskeleton in the oocyte (Zimyanin et al., 2007). Thus, actin bundling precedes the repolarisation of the oocyte MT cytoskeleton. This raises the

possibility that the establishment of the polarity of actin bundling may be one of the earliest events in polarising the oocyte during mid-oogenesis. One question to be considered is whether the actin organisation is in response to the polarising signaling sent back from the follicle cell at stage 6 to 7. To address this question, we can analyse actin bundling in *gurken* mutant oocytes. In *gurken* mutants, the oocyte fails to produce the TGF- α signaling to the underlying follicle cells at the posterior. As a consequence, those follicle cells can not adopt a posterior fate to send the signal back to the oocyte (Roth et al., 1995; Neumansilberberg and Schupbach, 1993) If the polarity of actin bundling is induced by the back signaling, we would expect actin bundling in *gurken* mutant oocytes to be organised in an un-polarised manner.

The recruitment of a Par-1 isoform, Par-1 N1, to the posterior cortex of the oocyte at stage 7 has been suggested to be the earliest marker for the posterior of the oocyte. The finding that treatment of egg chambers with the actin-destabilising drug latrunculinA abolishes the posterior enrichment of GFP Par-1 N1 indicates a role of actin in regulating the Par-1 N1 recruitment to the posterior (Doerflinger et al., 2006). This raises the question of whether the establishment of the actin bundling polarity is upstream or downstream of the Par-1 N1 recruitment to the posterior. To address this issue we first need to know how the actin cortex is organised during early oogenesis (stage 6-7). In other words, we need to know when the actin bundles are formed. However, at present we can detect the existence of actin bundling in the oocyte not earlier than stage 8. Before stage 8 the oocyte is very small and the lateral cortex is shaped in a steep curve, which prevents the high resolution analysis of the cytoskeletal organisation at the cortex.

Recently Dahlgaard (Dahlgaard et al., 2007) reported the existence of another actin based structure in the oocyte, which is also involved in regulating the onset of fast ooplasmic streaming. The authors show that an isotropic mesh of actin filaments is present in the oocyte cytoplasm at stage 9/10a. This actin mesh is required to prevent the fast streaming by suppressing the Kinesin motility. At stage 10b, the actin mesh disassembles and fast ooplasmic streaming is therefore induced. We therefore propose that the cortical actin bundling and the actin mesh in the ooplasm act together in

regulating the MT organisation of the oocyte.

4.4. The assembly of actin bundles at the oocyte cortex

How are the actin bundles at the oocyte cortex assembled? We show that *chic/profilin* mutants and latrunculinA treatment both interfere with actin bundle formation. LatrunculinA treatment inhibits the actin polymerisation by binding to and sequestering actin monomers. Profilin is involved in actin polymerisation by delivering actin monomers to the growing ends of actin filaments (Goode and Eck, 2007). Thus, latrunculinA treatment and *profilin* mutants appear to interfere with actin bundling by limiting the pool of monomers that can be added to growing actin filaments.

We also demonstrate that overexpression of GFPactin5C in the germline abolishes the formation of cortical actin bundles. The mechanism underlying this is not clear. Nevertheless, it seems unlikely that actin polymerisation is ubiquitously affected, given that GFPactin5C is incorporated into some other actin based structures without causing abnormalities (Roeper et al., 2005). We therefore speculate that the fusion of GFP protein to Actin5C monomer interferes with the binding of proteins crosslinking the actin filaments to form actin bundles.

4.5. The role of Capu and Spire in the cytoskeletal organisation of the oocyte

capu and *spire* mutants do not affect the formation of actin bundles at the oocyte cortex. Rosales-Nieves (Rosales-Nieves et al., 2006) have shown that Capu and Spire proteins are able to crosslink F-actin and MTs in vitro and that GFP-Spire and GFP-Capu fused proteins expressed in the germline localise to the oocyte cortex. Recently, Quilan (Quinlan et al., 2007) further examined the localisation of endogenous Spire by antibody staining. Endogenous Spire is, like the GFP fusion protein, localised to the oocyte cortex through stage 9. In addition, Quilan (Quinlan et

al., 2007) demonstrate that the actin-MT crosslinking activity of Capu is regulated by the formation of Spire-Capu complex. We therefore propose that Capu and Spire anchor the MT minus-ends in a scaffold provided by the cortical actin bundles (Fig. 22A). The lack of Capu and Spire activity in the mutants prevents cortical MT anchoring and allows the fast streaming in the presence of actin bundles.

Quilan (Quinlan et al., 2007) also demonstrate that the localisation of endogenous Spire disappears from the oocyte cortex at stage 10b when the fast streaming is initiated. This finding led to the speculation that the displacement or the destruction of Spire from the oocyte cortex triggers the initiation of the fast streaming (Quinlan et al., 2007). Due to the lack of antibodies recognising Capu, it is unclear whether endogenous Capu is, like Spire, localised to the oocyte cortex. However, when a GFP tagged version of Spire is overexpressed we and others observed high levels of GFP-Spire at the oocyte cortex before and after onset of fast ooplasmic streaming (Rosales-Nieves et al., 2006). The discrepancy between the detection of endogenous Spire and that of overexpressed GFP-Spire might well be explained by overloading the machinery for the protein displacement or destruction. Nevertheless, the observation that GFP-Spire still accumulates at the oocyte cortex when fast ooplasmic streaming is initiated argues against the idea that fast streaming is simply triggered by the displacement or the destruction of cortical Spire. It seems therefore unlikely that the initiation of fast streaming is regulated at the level of Capu and Spire localisation. Alternatively, it is possible that the activity of Capu and Spire to crosslink MTs with actin bundles is regulated. In such a model the crosslinking activities of Capu and Spire would be inhibited after stage 10a and thereby allow MT organisation.

How are the activities of Capu and Spire modulated? One mode of regulation for the Capu and Spire activities is suggested by their genetic and biochemical interaction with Rho1 (Wellington et al., 1999; Magie et al., 1999). This interaction led to a model in which Rho1 initiates fast streaming by regulating the crosslinking activities of Capu and Spire (Rosales-Nieves et al., 2006). We show that the prevention of fast streaming requires not only Capu and Spire but also the presence of actin bundles. The formation of these bundles occurs, however, independently of Capu and Spire.

Thus, the onset of fast streaming is not only controlled by regulating Capu and Spire activities, but also by disassembly of the actin bundles (Fig. 22B). Whether Rho1 works also as a regulator for the actin bundling remains to be tested.

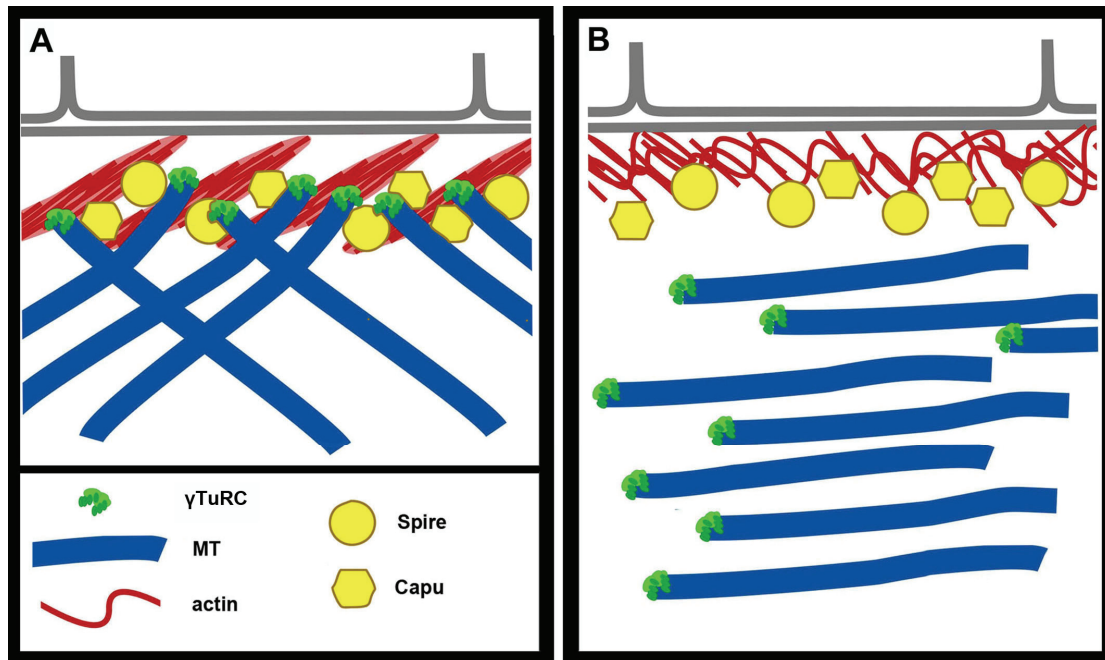


Fig. 22 Scheme of the oocyte cytoskeleton (A) At stage 9/10a, the cortical actin is organised into long thick bundles, that are aligned in parallel. By crosslinking MTs and actin Capu and Spire anchor the MT minus-ends at the cortex. (B) At stage 10b, the cortical actin rearranges, and bundles disappear. This reorganisation results in the release of the MT minus-ends from the cortex, triggering the fast cytoplasm streaming.

4.6. Alternative splicing of *Tao-1* transcripts during oogenesis

According to EST clones, four *Tao-1* transcripts are annotated: *Tao-1*-RD and -RE are of about 4 kb and encode the *Tao-1* isoforms containing a serine/threonine protein kinase domain at the N-terminus, coupled with some coiled-coil regions at the C-terminus. *Tao-1*-RA and -RB are approximately equivalent to the C-terminal part of *Tao-1*-RD and -RE, with the length of 2.3 kb. These short transcripts encode the *Tao-1* isoforms containing only the coiled-coil regions.

A primer pair was designed on the basis of the 4-kb transcripts annotated by the database. One primer was located at the 5' UTR and other one was located at the 3' UTR of the transcripts. Using this primer pair, RT-PCR of the total mRNAs of ovaries amplified the expected DNA fragment of about 4 kb. This verifies the expression of the 4-kb transcripts that have been annotated by EST clones. To our surprise, using this *Tao-1* cDNA isolated by RT-PCR as the probe, the Northern blot analysis of ovarian RNAs did not detect the presence of 4-kb transcripts of *Tao-1*. Instead, one 3-kb transcript and another 6-kb transcript were detected by the Northern blot analysis. Therefore, we conclude that the annotation of *Tao-1* according to EST clones does not completely predict the complexity of *Tao-1* transcripts expressed during oogenesis. The predominant *Tao-1* transcripts expressed during oogenesis are the 6-kb and 3-kb transcripts. Low expression levels of the 4-kb transcripts may explain why they were not detected by the Northern blot analysis. Given the lower sensitivity of Northern blot analysis, it was not clear whether the transcripts predicted as 2.3 kb are present during oogenesis. Even if these 2.3 kb transcripts are expressed, the expression level must be relatively low.

So far, the sequence information of these different *Tao-1* transcripts is not known. Nevertheless, these transcripts may represent different splicing forms of *Tao-1* gene. For example, the 3-kb transcripts may contain identical exons as the 4-kb transcripts, with the difference that one or two more exons are spliced out. Conversely, if fewer exons are spliced out, longer transcripts, like the one of 6 kb would be produced.

Another possible explanation is that there is an alternative transcriptional termination or initiation site that has not been annotated, so that the length of the produced transcripts differs from the annotation. For the future, a RT-PCR method aimed to isolate all expressed transcripts, together with the subsequent sequencing analysis should give us a thorough idea of *Tao-1* transcripts expressed during oogenesis.

4.7. The molecular and genetic nature of *Tao-1*^{No.7}

By mobilising the EP element, *Tao-1* EP(X) 1455, which is inserted in the 5' UTR of *Tao-1*, *Tao-1*^{No.7} mutants have been generated. Northern blot analysis reveals that the transcription level of 3-kb *Tao-1* transcripts is greatly reduced in mutant ovaries. Sequence analysis shows that in the *Tao-1*^{No.7} mutant, the original EP element is imprecisely excised and a 4-kb fragment of the EP element is left at the original insertion site; while the rest of the genomic sequence of the *Tao-1* locus is not affected. We suspect that this unexcised 4-kb P-element sequence alters the transcription level of *Tao-1*. Similar situations have been reported in other studies. For example, in the work of Lee and Chung (Lee et al., 2003), which identified new alleles of *blistery* by mobilising an EP element, *by*^{ex10} was recovered. In this mutant line, a 1.1-kb fragment of the original P-element remained at the 5' upstream of the *by* locus. RT-PCR analysis revealed that the expression level of *by* was greatly reduced. Another example comes from the work of Zhang (Zhang et al., 2003). P-element mobilisation was applied to generate alleles of *JIL-1*. In this study, *JIL-1*²⁸ generated a line in which a 3.6-kb fragment from the original EP element is left in the 5'UTR. In this mutant, the expression level of JIL-1 protein was reduced to 45% of the wild type level. Thus, after P-element mobilisation the fragment of P-element remaining at the 5' upstream of the gene adjacent to the insertion site can affect the transcription or translation level of the gene.

When a *Tao-1* cDNA was expressed in the germline of *Tao-1*^{No.7} females, the cytoskeletal organisation defects of the oocyte were completely rescued. This verifies that *Tao-1*^{No.7} is an allele of *Tao-1*. Given the fact that the transcription level of 3-kb

Tao-1 transcripts is greatly reduced in the *Tao-1^{No.7}* ovaries, one would suspect that the phenotypes observed in *Tao-1^{No.7}* oocytes are due to the reduced level of *Tao-1* transcription. However, complementation test of *Tao-1^{No.7}* and other alleles of *Tao-1* indicates that this is not the case.

An EMS induced allele of *Tao-1*, *Tao-1^{ETA}*, was generated in this study. Sequence analysis revealed that a premature stop codon was introduced in 5' region of the *Tao-1* gene. In *Tao-1^{ETA}* mutant flies, a truncated protein is expressed that lacks the functional Ser/Thr kinase domain and the coiled-coil domains. *Tao-1^{ETA}* flies are lethal and the lethality was rescued by ubiquitously expressing the 4-kb *Tao-1* cDNA. The expression of this cDNA in *Tao-1^{No.7}* female germline likewise rescued the cytoskeletal organisation defects of the oocyte. The ability of the *Tao-1* cDNA, which encodes a full length protein containing the kinase domain and the coiled-coil domains, to rescue both the *Tao-1^{ETA}* lethality and the *Tao-1^{No.7}* fertility suggest that these two alleles both suffer from the disrupted function of Tao-1 protein, but to different extent. *Tao-1^{ETA}* may represent a strong allele, as no functional Tao-1 protein can be produced in *Tao-1^{ETA}* mutants; *Tao-1^{No.7}* may represent a weak allele, as *Tao-1* transcripts are not completely abolished and some Tao-1 protein can be produced in *Tao-1^{No.7}* mutants. If this is the case, one would expect to detect defects in MT organisation and Oskar protein localisation of a higher penetrance in *Tao-1^{ETA}* oocytes, than that in *Tao-1^{No.7}* oocytes. Surprisingly, *Tao-1^{ETA}* germline clones did not show defects regarding the organisation of MTs and the localisation of Oskar protein. Moreover, *Tao-1^{ETA}* complements the oogenesis defects observed in *Tao-1^{No.7}* mutants. This indicates that the cytoskeletal organisation defect of *Tao-1^{No.7}* oocytes is not the result of reduced Tao-1 function.

We further analysed the Tao-1 function with a deletion called *Df.14.1*. *Df.14.1* is a deletion that removes the *Tao-1* locus completely. In *Df.14.1* mutant flies, *Tao-1* transcripts are most likely not produced at all. If the cytoskeletal organisation defects observed in *Tao-1^{No.7}* oocytes result from the reduced levels of *Tao-1* transcripts, one would expect to detect the defects in MT organisation and Oskar protein localisation of a higher penetrance in *Df.14.1* mutant oocytes, than that in *Tao-1^{No.7}* oocytes.

However, both in the germline clones of *Df.14.1* and in oocytes trans-heterozygous for *Tao-1^{No.7}* and *Df.14.1*, the MT cytoskeleton is properly organised and Oskar protein is correctly localised to the posterior. These results further argue against the suggestion that the phenotype observed in *Tao-1^{No.7}* oocytes is the result of the reduced level of *Tao-1* transcription.

Therefore, although the transcription level of *Tao-1* transcripts is reduced in *Tao-1^{No.7}* mutants, the cytoskeletal organisation defects observed in *Tao-1^{No.7}* mutants can not be explained as the result of a reduced function of *Tao-1*. The genetic complementation test of *Tao-1^{No.7}*, *Tao-1^{ETA}*, and *Df.14.1* suggests that *Tao-1^{No.7}* is most likely a gain of function allele of *Tao-1*. This gain of function effect is recessive, as two copies of *Tao-1^{No.7}* (*Tao-1^{No.7}/Tao-1^{No.7}*) are required to induce the phenotype. Neither one copy of *Tao-1^{No.7}* (*Tao-1^{ETA}/Tao-1^{No.7}*; *Df.14.1/Tao-1^{No.7}*) nor addition of *Tao-1* cDNA in *Tao-1^{No.7}/Tao-1^{No.7}* induces the phenotype. A good example for recessive gain of function allele has been reported for *torso: tor^{RL3}* (Klingler M, 1988). How the gain of function is achieved in *Tao-1^{No.7}* mutants remains to be elucidated. One possibility is that a novel (ultimately toxic) protein is produced in *Tao-1^{No.7}*. This idea can be tested by molecular and genetic analysis. Molecular analysis should aim to isolate transcripts expressed in *Tao-1^{No.7}* mutants by RT-PCR, and to obtain the sequence information by sequencing analysis. For genetic analysis, one possible way is to mutagenise *Tao-1^{No.7}* allele, such as by EMS, and look for the revertants that do not exhibit the cytoskeletal organisation defects of the oocyte. The revertants are expected to bear mutations at the essential regulatory domains of the toxic protein, and thereby disrupt the function of this toxic protein. Subsequent analysis of the revertants, including the sequence analysis and the genetic interaction with other *Tao-1* alleles should help us to understand the nature of *Tao-1^{No.7}*.

4.8. The unique patterning defects of *Tao-1^{No.7}* mutants

Tao-1^{No.7} mutants cause patterning defects during oogenesis, resulting in eggs and embryos that show alterations along the dorsal-ventral and anterior-posterior axis. We

demonstrate that *oskar*, *gurken* and *bicoid* mRNAs are all ectopically localised within the ooplasm, instead of accumulating at the posterior pole, dorsal-anterior corner and anterior corners, respectively, of stage 9/10a oocytes. Those mislocalised mRNAs are not translated efficiently, resulting in greatly reduced level of Gurken and Oskar protein in the oocyte. The decrease of Gurken protein explains the ventralisation of the egg shell; while the decrease of Oskar protein prevents the pole plasm formation and causes the posterior group defect of the embryo produced by *Tao-1^{No.7}* mutants. We further show that the defect of mRNA localisation starts specifically at mid-oogenesis.

Over the past years, a number of genes have been identified to be required for proper localisation of RNAs in the *Drosophila* oocyte. However, to our knowledge, none of those reported phenotypes resembles the defects of the RNA localisation observed in *Tao-1^{No.7}* mutants. The unique feature of the mRNA localisation defects observed in *Tao-1^{No.7}* oocytes is the diffuse distribution of *oskar*, *gurken* and *bicoid* mRNAs occurred at the same time. These three mRNAs are spreading through the entire ooplasm like dispersed particles, indicating that the polarity of the oocyte is thoroughly disrupted. In contrast, in most of the mutants that affect mRNA localisation in the oocyte, mRNAs accumulated at ectopic locations. For example, in *gurken*, *Pka* and *mael* mutants, *bicoid* mRNA is detected at the posterior pole, while *oskar* mRNA is detected at the centre of the oocyte. The oocytes from these mutants are polarised, but the polarity is not established in the correct way. In other mutants, mRNAs may exhibit a diffuse distribution pattern. However, in these mutants, the localisation defects are not observed for *oskar*, *gurken* and *bicoid* mRNAs simultaneously, but primarily restricted to certain type of mRNA. For example, in *spire* and *capu* mutants *oskar* mRNA is spreading through the entire ooplasm; while *bicoid* mRNA is correctly localised at the anterior corners of the oocytes (Emmons et al., 1995; Manseau et al., 1996; Theurkauf, 1994). In *spn-F* and *ik2* mutants, *gurken* mRNA is diffusely present at the ooplasm; while the localisation of *oskar* mRNA at the posterior of the oocyte is not affected (Abdu et al., 2006; Shapiro and Anderson, 2006). These data suggest that the polarity of the oocytes in these mutants is only

partially disrupted. The fact that in *Tao-1^{No.7}* mutants the polarity of the oocyte is completely disrupted makes *Tao-1^{No.7}* unique among patterning mutants.

4.9. The novel cytoskeletal organisation phenotype of *Tao-1^{No.7}* mutant oocytes

What is the mechanism by which *oskar*, *gurken* and *bicoid* mRNA localisation is disrupted, and why are these mRNAs dispersed through the entire ooplasm? The localisation of mRNAs to the correct position within the oocyte depends on the transport driven by motors along MTs. The localisation of Tao-1 protein, which is restricted to the oocyte cortex, places Tao-1 protein at the ideal location to regulate actin and MT organisation. In *Tao-1^{No.7}* mutant oocytes, cortical actin bundling is disrupted, MT minus-ends are not anchored at the cortex but relocate to the entire ooplasm, and a high density of interlacing MTs within the ooplasm was observed, with minus-ends and plus-ends randomly distributed. It seems impossible that the motor dependent transport of transcripts along the MTs to the plus-ends or minus-ends can be directed to certain subcellular locations, as the whole ooplasm is filled with randomly distributed MTs.

In *Tao-1^{No.7}* oocytes, actin bundling is affected, which results in the relocation of MT minus-ends from the cortex into the entire ooplasm leading to a completely disrupted MT cytoskeleton. One question to be considered is that whether the altered MT organisation resulting from the actin bundling defect is enough to explain the simultaneous mislocalisation of *oskar*, *gurken* and *bicoid* mRNAs. If so, one would expect that *oskar*, *gurken* and *bicoid* mRNAs are also simultaneously mislocalised in *chic* mutants or in actin inhibitory drug treated egg chambers, in which the cortical actin bundling is disrupted and the MT organisation is subsequently altered. However, both in the oocytes of *chic* mutants and in the oocytes treated with drugs, only *oskar* mRNA is mislocalised; while *bicoid* mRNAs is correctly localised at the anterior corners (Emmons et al., 1995; Manseau et al., 1996). The localisation of *gurken* mRNAs has not been unambiguously defined in *chic* and the drug treated oocytes.

Therefore, we mainly focus on the behaviour of *oskar* and *bicoid* mRNAs in the following discussion.

In *Tao-1^{No.7}* oocytes *oskar* and *bicoid* mRNA are both mislocalised; while in *chic* mutant oocytes or in drug treated oocytes, only *oskar* mRNA is affected. How to explain this discrepancy? It has been proposed that there are three populations of MT existed in the oocyte during mid-oogenesis: MTs extending from the anterior cortex, which are involved in localising *bicoid* mRNA to the anterior poles; MTs extending from the oocyte nucleus around the anterior cortex, which are involved in localising *gurken* mRNA to the dorsal anterior corner; MTs extending from the lateral cortex, which are required for localising *oskar* mRNA to the posterior pole (St Johnston D., 2005). This organisation offers the possibility that the MTs that are regulated by cortical actin bundles are only responsible for localising *oskar* mRNA to the posterior pole; while the other subset of MTs responsible for localising *bicoid* mRNA is not dependent on the actin bundling. For this reason, in the oocytes of *chic* and the oocytes treated with drugs, only *oskar*, but not *bicoid* mRNA is mislocalised. Thus, the altered organisation of the MT cytoskeleton in *Tao-1^{No.7}* oocytes resulting from the actin bundling defect is not sufficient to explain the simultaneous mislocalisation of *oskar*, *gurken* and *bicoid* mRNAs. Therefore, one should consider other mechanisms that globally affect the motor dependent transport of transcripts along the MTs in *Tao-1^{No.7}* oocytes. One possibility is that *Tao-1^{No.7}* directly affects the MT organisation. This speculation is supported by the finding that the MTs present in *Tao-1^{No.7}* oocytes appear thicker than that in the wild type.

How *Tao-1^{No.7}* is directly regulating MTs remains elusive. Over the past year, despite that fact that numerous genes affecting the MT organisation in the oocyte during mid-oogenesis have been characterised (Steinhauer and Kalderon, 2006), none of them has been demonstrated to directly interact with MTs or to be MT organising factors. Understanding the mechanism underlying the defects of *Tao-1^{No.7}* in regulating the organisation of MTs during oogenesis may provide general insight into the mechanism regulating the organisation of MT network.

5. SUMMARY

In this study, a careful examination was conducted to analyse the actin and microtubule (MT) cytoskeleton organisation during *Drosophila* oogenesis. We found that at stage 9/10a the actin cytoskeleton at the oocyte cortex is assembled into long bundles, which are essential for anchoring the MT minus-ends at the cortex. The formation of actin bundles requires the function of Profilin. Capu and Spire act downstream of the bundle formation, most likely by anchoring MT minus-ends at the cortex by crosslinking F-actin and MTs. At stage 10b, the actin bundles disassemble and the MT minus-ends are relocated from the actin cortex to subcortical regions. Subsequently, fast ooplasmic streaming is initiated and MTs form parallel arrays at subcortical regions.

To identify the regulators of the organisation of the oocyte cytoskeleton, a mutation in a serine/threonine kinase *Tao-1*, *Tao-1^{No.7}* was generated. The analysis of *Tao-1^{No.7}* mutants revealed a novel phenotype for the cytoskeleton organisation of the oocyte. In *Tao-1^{No.7}* mutant oocytes the cortical actin bundling is disrupted. Unlike in other mutants which affect actin bundling, in *Tao-1^{No.7}* oocytes MTs are not forming parallel arrays at subcortical regions; but show high MT density within the entire ooplasm. Thus, the MT network is completely disrupted in *Tao-1^{No.7}* oocytes. As a result, the transcripts for the axis determinants are not transported to correct subcellular locations, and as a consequence the embryonic axis is not properly established.

The oogenesis phenotypes observed in *Tao-1^{No.7}* mutants was rescued by the expression of a *Tao-1* cDNA, verifying that *Tao-1^{No.7}* is an allele of *Tao-1*. Nevertheless, a deletion removing the *Tao-1* locus completely does not exhibit the defects in the cytoskeletal organisation of the oocyte. Therefore, *Tao-1^{No.7}* is most likely a gain of function allele of *Tao-1*, which shows a phenotype only in a homozygous situation (recessive gain of function).

6. ZUSAMMENFASSUNG

Bei dieser Arbeit wurden die Zusammenhänge der Zytoskelett-Organisation von Aktin und mikrotubuli (MT) während der Embryogenese von *Drosophila* sorgfältig untersucht. Wir konnten zeigen, dass sich während des Stadiums 9/10a das Aktin-Zytoskelett am Kortex der Oocyte in langen Bündeln ansammelt. Diese Bündel sind nötig, um die Minus-Enden der MT am Kortex zu verankern.

Die Ausbildung der Aktinbündel ist auf die Funktion von Profilin angewiesen. Capu und Spire wirken downstream von der Bündelentwicklung, höchstwahrscheinlich durch Quervernetzung von F-Aktin mit den MT, wodurch deren Minus-Enden an dem Kortex verankert werden können. Im Stadium 10b gehen die Aktinbündel auseinander. Die Minus-Enden der MT verlagern sich vom Aktin-Kortex in subkortikale Regionen. Anschließend wird die schnelle Ooplasma-Strömung eingeleitet, und die MT ordnen sich parallel in den subkortikalen Regionen an.

Um Regulatoren der Zytoskelett-Organisation in der Eizelle zu identifizieren, wurde eine Mutation in der Serin/Threonin-Kinase Tao-1 erzeugt (*Tao-1^{No.7}*). Die Analyse der *Tao-1^{No.7}*-Mutanten zeigte einen bislang unbekanntes Phänotyp der Zytoskelett-Organisation in der Eizelle. In den *Tao-1^{No.7}*-Oocyten sind die kortikalen Aktinbündel unterbrochen. Anders als in zuvor beschriebenen, die Aktin-Bündel betreffenden, Mutanten, ordnen sich MT in *Tao-1^{No.7}*-Eizellen nicht parallel in den subkortikalen Regionen an; stattdessen zeigen diese Mutanten eine hohe Dichte der Mikrotubuli im gesamten Ooplasma. Dadurch ist das Mikrotubulinetzwerk in *Tao-1^{No.7}*-Oocyten vollständig gestört. Eine Folge hiervon ist, dass die für die Achsendetermination benötigten Transkripte nicht an die richtige subzelluläre Position transportiert werden. Folglich wird die embryonale Achse nicht richtig aufgebaut.

Die Oogenese-Phänotypen, die in *Tao-1^{No.7}*-Mutanten beobachtet wurden, konnten durch Expression von *Tao-1* cDNA gerettet werden, was bestätigt, dass *Tao-1^{No.7}* ein Allel von *Tao-1* ist. Dennoch führt eine Deletion des gesamten *Tao-1*-Bereiches zu

keinen Defekten der Zytoskelett-Organisation in der Oocyte. Daher ist *Tao-1^{No.7}* höchstwahrscheinlich ein Gain-of-function-Allel von *Tao-1*, das diesen Phänotyp ausschließlich im homozygoten Zustand zeigt (rezessive Gain-of-Function-Mutation.).

7. REFERENCES

- Abdu,U., Bar,D., and Schupbach,T. (2006). spn-F encodes a novel protein that affects oocyte patterning and bristle morphology in *Drosophila*. *Development* 133, 1477-1484.
- Ashburner,M. (1989). *Drosophila - A laboratory handbook*. Cold Spring Harbor Laboratory Press).
- Bartolini,F. and Gundersen,G.G. (2006). Generation of noncentrosomal microtubule arrays. *Journal of Cell Science* 119, 4155-4163.
- Bashirullah,A., Cooperstock,R.L., and Lipshitz,H.D. (1998). RNA localization in development. *Annual Review of Biochemistry* 67, 335-394.
- Bateman,J., Reddy,R.S., Saito,H., and Van Vactor,D. (2001). The receptor tyrosine phosphatase Dlar and integrins organize actin filaments in the *Drosophila* follicular epithelium. *Current Biology* 11, 1317-1327.
- Baum,B., Li,W., and Perrimon,N. (2000). A cyclase-associated protein regulates actin and cell polarity during *Drosophila* oogenesis and in yeast. *Current Biology* 10, 964-973.
- Benton,R., Palacios,I.M., and St Johnston,D. (2002). *Drosophila* 14-3-3/PAR-5 is an essential mediator of PAR-1 function in axis formation. *Developmental Cell* 3, 659-671.
- Berleth,T., Burri,M., Thoma,G., Bopp,D., Richstein,S., Frigerio,G., Noll,M., and Nussleinvohard,C. (1988). The Role of Localization of Bicoid Rna in Organizing the Anterior Pattern of the *Drosophila* Embryo. *Embo Journal* 7, 1749-1756.
- Bilder,D., Li,M., and Perrimon,N. (2000). Cooperative regulation of cell polarity and growth by *Drosophila* tumor suppressors. *Science* 289, 113-116.
- Brand,A.H. and Perrimon,N. (1993). Targeted Gene-Expression As A Means of Altering Cell Fates and Generating Dominant Phenotypes. *Development* 118, 401-415.

- Breitwieser,W., Markussen,F.H., Horstmann,H., and Ephrussi,A. (1996). Oskar protein interaction with Vasa represents an essential step in polar granule assembly. *Genes & Development* 10, 2179-2188.
- Brendza,R.P., Serbus,L.R., Duffy,J.B., and Saxton,W.M. (2000). A function for kinesin I in the posterior transport of oskar mRNA and Stauf protein. *Science* 289, 2120-2122.
- Cha,B.J., Koppetsch,B.S., and Theurkauf,W.E. (2001). In vivo analysis of *Drosophila* bicoid mRNA localization reveals a novel microtubule-dependent axis specification pathway. *Cell* 106, 35-46.
- Cha,B.J., Serbus,L.R., Koppetsch,B.S., and Theurkauf,W.E. (2002). Kinesin I-dependent cortical exclusion restricts pole plasm to the oocyte posterior. *Nature Cell Biology* 4, 592-598.
- Chou,T.B., Noll,E., and Perrimon,N. (1993). Autosomal P[ovoD1] dominant female-sterile insertions in *Drosophila* and their use in generating germ-line chimeras. *Development* 119, 1359-1369.
- Chou,T.B. and Perrimon,N. (1992). Use of a yeast site-specific recombinase to produce female germline chimeras in *Drosophila*. *Genetics* 131, 643-653.
- Clark,I., Giniger,E., Ruoholabaker,H., Jan,L.Y., and Jan,Y.N. (1994). Transient Posterior Localization of A Kinesin Fusion Protein Reflects Anteroposterior Polarity of the *Drosophila* Oocyte. *Current Biology* 4, 289-300.
- Clark,I.E., Jan,L.Y., and Jan,Y.N. (1997). Reciprocal localization of Nod and kinesin fusion proteins indicates microtubule polarity in the *Drosophila* oocyte, epithelium, neuron and muscle. *Development* 124, 461-470.
- Cooley,L., Verheyen,E., and Ayers,K. (1992). Chickadee Encodes A Profilin Required for Intercellular Cytoplasm Transport During *Drosophila* Oogenesis. *Cell* 69, 173-184.
- Cooper,J.A. (1987). Effects of Cytochalasin and Phalloidin on Actin. *Journal of Cell Biology* 105, 1473-1478.
- Cox,D.N., Lu,B.W., Sun,T.Q., Williams,L.T., and Jan,Y.N. (2001). *Drosophila* par-1

is required for oocyte differentiation and microtubule organization. *Current Biology* 11, 75-87.

Dahlgaard,K., Raposo,A.A.S.F., Niccoli,T., and St Johnston,D. (2007). Capu and spire assemble a cytoplasmic actin mesh that maintains microtubule organization in the *Drosophila* oocyte. *Developmental Cell* 13, 539-553.

Dan,I., Watanabe,N.M., and Kusumi,A. (2001). The Ste20 group kinases as regulators of MAP kinase cascades. *Trends Cell Biol.* 11, 220-230.

Desai,A. and Mitchison,T.J. (1997). Microtubule polymerization dynamics. *Annual Review of Cell and Developmental Biology* 13, 83-117.

Doerflinger,H., Benton,R., Shulman,J.M., and St Johnston,D. (2003). The role of PAR-1 in regulating the polarised microtubule cytoskeleton in the *Drosophila* follicular epithelium. *Development* 130, 3965-3975.

Doerflinger,H., Benton,R., Torres,I.L., Zwart,M.F., and St Johnston,D. (2006). *Drosophila* anterior-posterior polarity requires actin-dependent PAR-1 recruitment to the oocyte posterior. *Current Biology* 16, 1090-1095.

Drewes,G., Trinczek,B., Illenberger,S., Biernat,J., Schmittulms,G., Meyer,H.E., Mandelkow,E.M., and Mandelkow,E. (1995). Microtubule-Associated Protein Microtubule Affinity-Regulating Kinase (P110(Mark)) - A Novel Protein-Kinase That Regulates Tau-Microtubule Interactions and Dynamic Instability by Phosphorylation at the Alzheimer-Specific Site Serine-262. *Journal of Biological Chemistry* 270, 7679-7688.

Duncan,J.E. and Warrior,R. (2002). The cytoplasmic dynein and kinesin motors have interdependent roles in patterning the *Drosophila* oocyte. *Current Biology* 12, 1982-1991.

Emmons,S., Phan,H., Calley,J., Chen,W.L., James,B., and Manseau,L. (1995). Cappuccino, A *Drosophila* Maternal Effect Gene Required for Polarity of the Egg and Embryo, Is Related to the Vertebrate Limb Deformity Locus. *Genes & Development* 9, 2482-2494.

Ephrussi,A., Dickinson,L.K., and Lehmann,R. (1991). Oskar Organizes the Germ Plasm and Directs Localization of the Posterior Determinant Nanos. *Cell* 66, 37-50.

Ephrussi,A. and Lehmann,R. (1992). Induction of Germ-Cell Formation by Oskar. *Nature* 358, 387-392.

Evangelista,M., Blundell,K., Longtine,M.S., Chow,C.J., Adames,N., Pringle,J.R., Peter,M., and Boone,C. (1997). Bni1p, a yeast formin linking Cdc42p and the actin cytoskeleton during polarized morphogenesis. *Science* 276, 118-122.

Forrest,K.M. and Gavis,E.R. (2003). Live imaging of endogenous RNA reveals a diffusion and entrapment mechanism for nanos mRNA localization in *Drosophila*. *Current Biology* 13, 1159-1168.

Freeman,N.L., Chen,Z.X., Horenstein,J., Weber,A., and Field,J. (1995). An Actin Monomer Binding-Activity Localizes to the Carboxyl-Terminal Half of the *Saccharomyces-Cerevisiae* Cyclase-Associated Protein. *Journal of Biological Chemistry* 270, 5680-5685.

Frydman,H.M. and Spradling,A.C. (2001). The receptor-like tyrosine phosphatase Lar is required for epithelial planar polarity and for axis determination within *Drosophila* ovarian follicles. *Development* 128, 3209-3220.

Gieselmann,R. and Mann,K. (1992). Asp-56, A New Actin Sequestering Protein from Pig Platelets with Homology to Cap, An Adenylate Cyclase-Associated Protein from Yeast. *Febs Letters* 298, 149-153.

Glotzer,J.B., Saffrich,R., Glotzer,M., and Ephrussi,A. (1997). Cytoplasmic flows localize injected oskar RNA in *Drosophila* oocytes. *Current Biology* 7, 326-337.

Goode,B.L. and Eck,M.J. (2007). Mechanism and function of formins in the control of actin assembly. *Annual Review of Biochemistry* 76, 593-627.

Gottwald,U., Brokamp,R., Karakesisoglou,I., Schleicher,M., and Noegel,A.A. (1996). Identification of a cyclase-associated protein (CAP) homologue in *Dictyostelium discoideum* and characterization of its interaction with actin. *Molecular Biology of the Cell* 7, 261-272.

Gutzeit,H.O. and Arendt,D. (1994). Blocked Endocytotic Uptake by the Oocyte Causes Accumulation of Vitellogenins in the Hemolymph of the Female-Sterile Mutants Quit(Px61) and Stand Still(Ps34) of *Drosophila*. *Cell and Tissue Research* 275, 291-298.

- Gutzeit,H.O. and Koppa,R. (1982). Time-Lapse Film Analysis of Cytoplasmic Streaming During Late Oogenesis of *Drosophila*. *Journal of Embryology and Experimental Morphology* 67, 101-111.
- Hall,A. (1998). Rho GTPases and the actin cytoskeleton. *Science* 279, 509-514.
- Horne-Badovinac,S. and Bilder,D. (2005). Mass transit: epithelial morphogenesis in the *Drosophila* egg chamber. *Dev. Dyn.* 232, 559-574.
- Huang,Z.M., Pokrywka,N.J., Yoder,J.H., and Stephenson,E.C. (2000). Analysis of a swallow homologue from *Drosophila pseudoobscura*. *Development Genes and Evolution* 210, 157-161.
- Huynh,J.R., Shulman,J.M., Benton,R., and St Johnston,D. (2001). PAR-1 is required for the maintenance of oocyte fate in *Drosophila*. *Development* 128, 1201-1209.
- Idriss,H.T. (2000). Man to trypanosome: The tubulin tyrosination/detyrosination cycle revisited. *Cell Motility and the Cytoskeleton* 45, 173-184.
- Izumi,Y., Hirose,T., Tamai,Y., Hirai,S., Nagashima,Y., Fujimoto,T., Tabuse,Y., Kempfues,K.J., and Ohno,S. (1998). An atypical PKC directly associates and colocalizes at the epithelial tight junction with ASIP, a mammalian homologue of *Caenorhabditis elegans* polarity protein PAR-3. *Journal of Cell Biology* 143, 95-106.
- Jacinto,A. and Baum,B. (2003). Actin in development. *Mechanisms of Development* 120, 1337-1349.
- Jankovics,F., Sinka,R., Lukacsovich,T., and Erdelyi,M. (2002). MOESIN crosslinks actin and cell membrane in *Drosophila* oocytes and is required for OSKAR anchoring. *Current Biology* 12, 2060-2065.
- Januschke,J., Gervais,L., Dass,S., Kaltschmidt,J.A., Lopez-Schier,H., St Johnston,D., Brand,A.H., Roth,S., and Guichet,A. (2002). Polar transport in the *Drosophila* oocyte requires Dynein and Kinesin I cooperation. *Current Biology* 12, 1971-1981.
- Januschke,J., Gervais,L., Gillet,L., Keryer,G., Bornens,M., and Guichet,A. (2006). The centrosome-nucleus complex and microtubule organization in the *Drosophila* oocyte. *Development* 133, 129-139.

- Joberty,G., Petersen,C., Gao,L., and Macara,I.G. (2000). The cell-polarity protein Par6 links Par3 and atypical protein kinase C to Cdc42. *Nature Cell Biology* 2, 531-539.
- Kamal,A. and Goldstein,L.S.B. (2002). Principles of cargo attachment to cytoplasmic motor proteins. *Current Opinion in Cell Biology* 14, 63-68.
- Kemphues,K.J., Priess,J.R., Morton,D.G., and Cheng,N.S. (1988). Identification of genes required for cytoplasmic localization in early *C. elegans* embryos. *Cell* 52, 311-320.
- Kimha,J., Kerr,K., and Macdonald,P.M. (1995). Translational Regulation of Oskar Messenger-Rna by Bruno, An Ovarian Rna-Binding Protein, Is Essential. *Cell* 81, 403-412.
- Kimha,J., Smith,J.L., and Macdonald,P.M. (1991). Oskar Messenger-Rna Is Localized to the Posterior Pole of the *Drosophila* Oocyte. *Cell* 66, 23-34.
- Kuchinke,U., Grawe,F., and Knust,E. (1998). Control of spindle orientation in *Drosophila* by the Par-3-related PDZ-domain protein Bazooka. *Current Biology* 8, 1357-1365.
- Lecuyer,E., Yoshida,H., Parthasarathy,N., Alm,C., Babak,T., Cerovina,T., Hughes,T.R., Tomancak,P., and Krause,H.M. (2007). Global analysis of mRNA localization reveals a prominent role in organizing cellular architecture and function. *Cell* 131, 174-187.
- Lee,S.B., Cho,K.S., Kim,E., and Chung,J. (2003). Blistery encodes *Drosophila* tensin protein and interacts with integrin and the JNK signaling pathway during wing development. *Development* 130, 4001-4010.
- Lehmann,R. and Nusslein-Volhard,C. (1986). Abdominal segmentation, pole cell formation, and embryonic polarity require the localized activity of oskar, a maternal gene in *Drosophila*. *Cell* 47, 141-152.
- Lin,D., Edwards,A.S., Fawcett,J.P., Mbamalu,G., Scott,J.D., and Pawson,T. (2000). A mammalian PAR-3-PAR-6 complex implicated in Cdc42/Rac1 and aPKC signalling and cell polarity. *Nature Cell Biology* 2, 540-547.

Machesky,L.M. and Insall,R.H. (1998). Scar1 and the related Wiskott-Aldrich syndrome protein, WASP, regulate the actin cytoskeleton through the Arp2/3 complex. *Current Biology* 8, 1347-1356.

Magie,C.R., Meyer,M.R., Gorsuch,M.S., and Parkhurst,S.M. (1999). Mutations in the Rho1 small GTPase disrupt morphogenesis and segmentation during early *Drosophila* development. *Development* 126, 5353-5364.

Manseau,L., Calley,J., and Phan,H. (1996). Profilin is required for posterior patterning of the *Drosophila* oocyte. *Development* 122, 2109-2116.

Markussen,F.H., Michon,A.M., Breitwieser,W., and Ephrussi,A. (1995). Translational Control of Oskar Generates Short Osk, the Isoform That Induces Pole Plasm Assembly. *Development* 121, 3723-3732.

Martin,S.G. and St,J.D. (2003). A role for *Drosophila* LKB1 in anterior-posterior axis formation and epithelial polarity. *Nature* 421, 379-384.

McCartney,B.M. and Fehon,R.G. (1996). Distinct cellular and subcellular patterns of expression imply distinct functions for the *Drosophila* homologues of moesin and the neurofibromatosis 2 tumor suppressor, merlin. *Journal of Cell Biology* 133, 843-852.

Meng,J. and Stephenson,E.C. (2002). Oocyte and embryonic cytoskeletal defects caused by mutations in the *Drosophila* swallow gene. *Development Genes and Evolution* 212, 239-247.

Miki,H. and Takenawa,T. (1998). Direct binding of the verprolin-homology domain in N-WASP to actin is essential for cytoskeletal reorganization. *Biochemical and Biophysical Research Communications* 243, 73-78.

Mogensen,M.M., Tucker,J.B., and Stebbings,H. (1989). Microtubule Polarities Indicate That Nucleation and Capture of Microtubules Occurs at Cell-Surfaces in *Drosophila*. *Journal of Cell Biology* 108, 1445-1452.

Moritz,M., Zheng,Y.X., Alberts,B.M., and Oegema,K. (1998). Recruitment of the gamma-tubulin ring complex to *Drosophila* salt-stripped centrosome scaffolds. *Journal of Cell Biology* 142, 775-786.

Morton,D.G., Shakes,D.C., Nugent,S., Dichoso,D., Wang,W.F., Golden,A., and

Kemphues,K.J. (2002). The *Caenorhabditis elegans* par-5 gene encodes a 14-3-3 protein required for cellular asymmetry in the early embryo. *Developmental Biology* 241, 47-58.

Mueller-Klieser,W. (2000). Tumor biology and experimental therapeutics. *Critical Reviews in Oncology Hematology* 36, 123-139.

Neumansilberberg,F.S. and Schupbach,T. (1993). The *Drosophila* Dorsoventral Patterning Gene Gurken Produces A Dorsally Localized Rna and Encodes A Tgf-Alpha-Like Protein. *Cell* 75, 165-174.

Palacios,I.M. and St Johnston,D. (2002). Kinesin light chain-independent function of the Kinesin heavy chain in cytoplasmic streaming and posterior localisation in the *Drosophila* oocyte. *Development* 129, 5473-5485.

Parks,A.L., Cook,K.R., Belvin,M., Dompe,N.A., Fawcett,R., Huppert,K., Tan,L.R., Winter,C.G., Bogart,K.P., Deal,J.E., al-Herr,M.E., Grant,D., Marcinko,M., Miyazaki,W.Y., Robertson,S., Shaw,K.J., Tabios,M., Vysotskaia,V., Zhao,L., Andrade,R.S., Edgar,K.A., Howie,E., Killpack,K., Milash,B., Norton,A., Thao,D., Whittaker,K., Winner,M.A., Friedman,L., Margolis,J., Singer,M.A., Kopczynski,C., Curtis,D., Kaufman,T.C., Plowman,G.D., Duyk,G., and Francis-Lang,H.L. (2004). Systematic generation of high-resolution deletion coverage of the *Drosophila melanogaster* genome. *Nature Genetics* 36, 288-292.

Petronczki,M. and Knoblich,J.A. (2001). DmPAR-6 directs epithelial polarity and asymmetric cell division of neuroblasts in *Drosophila*. *Nature Cell Biology* 3, 43-49.

Pokrywka,N.J. and Stephenson,E.C. (1995). Microtubules Are A General Component of Messenger-Rna Localization Systems in *Drosophila* Oocytes. *Developmental Biology* 167, 363-370.

Pokrywka,N.J. and Stephenson,E.C. (1991). Microtubules Mediate the Localization of Bicoid Rna During *Drosophila* Oogenesis. *Development* 113, 55-66.

Polesello,C., Delon,I., Valenti,P., Ferrer,P., and Payre,F. (2002). Dmoesin controls actin-based cell shape and polarity during *Drosophila melanogaster* oogenesis. *Nature Cell Biology* 4, 782-789.

Quinlan,M.E., Heuser,J.E., Kerkhoff,E., and Mullins,R.D. (2005). *Drosophila* Spire is an actin nucleation factor. *Nature* 433, 382-388.

- Quinlan,M.E., Hilgert,S., Bedrossian,A., Mullins,R.D., and Kerkhoff,E. (2007). Regulatory interactions between two actin nucleators, Spire and Cappuccino. *Journal of Cell Biology* 179, 117-128.
- Riechmann,V. and Ephrussi,A. (2001). Axis formation during *Drosophila* oogenesis. *Current Opinion in Genetics & Development* 11, 374-383.
- Riechmann,V. and Ephrussi,A. (2004). Par-1 regulates bicoid mRNA localisation by phosphorylating Exuperantia. *Development* 131, 5897-5907.
- Riechmann,V., Gutierrez,G.J., Filardo,P., Nebreda,A.R., and Ephrussi,A. (2002). Par-1 regulates stability of the posterior determinant Oskar by phosphorylation. *Nat. Cell Biol.* 4, 337-342.
- Riparbelli,M.G. and Callaini,G. (1995). Cytoskeleton of the *Drosophila* egg chamber: new observations on microfilament distribution during oocyte growth. *Cell Motil. Cytoskeleton* 31, 298-306.
- Robertson,H.M., Preston,C.R., Phillis,R.W., Johnsonschlitz,D.M., Benz,W.K., and Engels,W.R. (1988). A Stable Genomic Source of P-Element Transposase in *Drosophila-Melanogaster*. *Genetics* 118, 461-470.
- Roeper,K., Mao,Y.L., and Brown,N.H. (2005). Contribution of sequence variation in *Drosophila* actins to their incorporation into actin-based structures in vivo. *Journal of Cell Science* 118, 3937-3948.
- Rongo,C., Gavis,E.R., and Lehmann,R. (1995). Localization of Oskar Rna Regulates Oskar Translation End Requires Oskar Protein. *Development* 121, 2737-2746.
- Rorth,P. (1996). A modular misexpression screen in *Drosophila* detecting tissue-specific phenotypes. *Proceedings of the National Academy of Sciences of the United States of America* 93, 12418-12422.
- Rorth,P. (1998). Ga14 in the *Drosophila* female germline. *Mechanisms of Development* 78, 113-118.
- Rosales-Nieves,A.E., Johndrow,J.E., Keller,L.C., Magie,C.R., Pinto-Santini,D.M., and Parkhurst,S.M. (2006). Coordination of microtubule and microfilament dynamics by *Drosophila* Rho1, Spire and Cappuccino. *Nature Cell Biology* 8, 367-U47.

Roth,S., Neumansilberberg,F.S., Barcelo,G., and Schupbach,T. (1995). Cornichon and the Egf Receptor Signaling Process Are Necessary for Both Anterior-Posterior and Dorsal-Ventral Pattern-Formation in *Drosophila*. *Cell* 81, 967-978.

Rubin,G.M. and Spradling,A.C. (1982). Genetic transformation of *Drosophila* with transposable element vectors. *Science* 218, 348-353.

Schnorrer,F., Bohmann,K., and Nusslein-Volhard,C. (2000). The molecular motor dynein is involved in targeting Swallow and bicoid RNA to the anterior pole of *Drosophila* oocytes. *Nature Cell Biology* 2, 185-190.

Schnorrer,F., Luschnig,S., Koch,I., and Nusslein-Volhard,C. (2002). gamma-Tubulin37C and gamma-tubulin ring complex protein 75 are essential for bicoid RNA localization during *Drosophila* oogenesis. *Developmental Cell* 3, 685-696.

Schultz,J., Milpetz,F., Bork,P., and Ponting,C.P. (1998). SMART, a simple modular architecture research tool: Identification of signaling domains. *Proceedings of the National Academy of Sciences of the United States of America* 95, 5857-5864.

Schupbach,T. (1987). Germ Line and Soma Cooperate During Oogenesis to Establish the Dorsoventral Pattern of Eggshell and Embryo in *Drosophila-Melanogaster*. *Cell* 49, 699-707.

Serbus,L.R., Cha,B.J., Theurkauf,W.E., and Saxton,W.M. (2005). Dynein and the actin cytoskeleton control kinesin-driven cytoplasmic streaming in *Drosophila* oocytes. *Development* 132, 3743-3752.

Shapiro,R.S. and Anderson,K.V. (2006). *Drosophila* Ik2, a member of the I kappa B kinase family, is required for mRNA localization during oogenesis. *Development* 133, 1467-1475.

Shulman,J.M., Benton,R., and St Johnston,D. (2000). The *Drosophila* homolog of *C-elegans* PAR-1 organizes the oocyte cytoskeleton and directs oskar mRNA localization to the posterior pole. *Cell* 101, 377-388.

Shulman,J.M. and Feany,M.B. (2003). Genetic modifiers of tauopathy in *Drosophila*. *Genetics* 165, 1233-1242.

Spradling,A.C. and Rubin,G.M. (1982). Transposition of cloned P elements into Drosophila germ line chromosomes. *Science* 218, 341-347.

Spradling,A.C., Stern,D., Beaton,A., Rhem,E.J., Lavery,T., Mozden,N., Misra,S., and Rubin,G.M. (1999). The Berkeley Drosophila Genome Project gene disruption project: Single P-element insertions mutating 25% of vital Drosophila genes. *Genetics* 153, 135-177.

St Johnston D. (2005). Moving messages: the intracellular localization of mRNAs. *Nat. Rev. Mol. Cell Biol.* 6, 363-375.

St Johnston,D. and Nussleinvolhard,C. (1992). The Origin of Pattern and Polarity in the Drosophila Embryo. *Cell* 68, 201-219.

Steinhauer,J. and Kalderon,D. (2006). Microtubule polarity and axis formation in the Drosophila oocyte. *Developmental Dynamics* 235, 1455-1468.

Suzuki,A., Yamanaka,T., Hirose,T., Manabe,N., Mizuno,K., Shimizu,M., Akimoto,K., Izumi,Y., Ohnishi,T., and Ohno,S. (2001). Atypical protein kinase C is involved in the evolutionarily conserved PAR protein complex and plays a critical role in establishing epithelia-specific junctional structures. *Journal of Cell Biology* 152, 1183-1196.

Tautz,D. and Pfeifle,C. (1989). A non-radioactive in situ hybridization method for the localization of specific RNAs in Drosophila embryos reveals translational control of the segmentation gene hunchback. *Chromosoma* 98, 81-85.

Tavosanis,G. and Gonzalez,C. (2003). gamma-Tubulin function during female germ-cell development and oogenesis in Drosophila. *Proc. Natl. Acad. Sci. U. S. A* 100, 10263-10268.

Theurkauf,W.E. (1994). Premature Microtubule-Dependent Cytoplasmic Streaming in Cappuccino and Spire Mutant Oocytes. *Science* 265, 2093-2096.

Theurkauf,W.E., Smiley,S., Wong,M.L., and Alberts,B.M. (1992). Reorganization of the Cytoskeleton During Drosophila Oogenesis - Implications for Axis Specification and Intercellular Transport. *Development* 115, 923-936.

Thibault,S.T., Singer,M.A., Miyazaki,W.Y., Milash,B., Dompe,N.A., Singh,C.M.,

- Buchholz,R., Demsky,M., Fawcett,R., Francis-Lang,H.L., Ryner,L., Cheung,L.M., Chong,A., Erickson,C., Fisher,W.W., Greer,K., Hartouni,S.R., Howie,E., Jakkula,L., Joo,D., Killpack,K., Laufer,A., Mazzotta,J., Smith,R.D., Stevens,L.M., Stuber,C., Tan,L.R., Ventura,R., Woo,A., Zakrajsek,I., Zhao,L., Chen,F., Swimmer,C., Kopczynski,C., Duyk,G., Winberg,M.L., and Margolis,J. (2004). A complementary transposon tool kit for *Drosophila melanogaster* using P and piggyBac. *Nature Genetics* 36, 283-287.
- Timm,T., Li,X.Y., Biernat,J., Jiao,J., Mandelkow,E., Vandekerckhove,J., and Mandelkow,E.M. (2003). MARKK, a Ste20-like kinase, activates the polarity-inducing kinase MARK/PAR-1. *Embo Journal* 22, 5090-5101.
- Tomancak,P., Piano,F., Riechmann,V., Gunsalus,K.C., Kemphues,K.J., and Ephrussi,A. (2000). A *Drosophila melanogaster* homologue of *Caenorhabditis elegans* par-1 acts at an early step in embryonic-axis formation. *Nature Cell Biology* 2, 458-460.
- Tsukita,S., Yonemura,S., and Tsukita,S. (1997). ERM (ezrin/radixin/moesin) family: From cytoskeleton to signal transduction. *Current Opinion in Cell Biology* 9, 70-75.
- Van,D.M., Williamson,A.L., and Lehmann,R. (1998). Regulation of zygotic gene expression in *Drosophila* primordial germ cells. *Curr. Biol.* 8, 243-246.
- Verheyen,E.M. and Cooley,L. (1994). Profilin Mutations Disrupt Multiple Actin-Dependent Processes During *Drosophila* Development. *Development* 120, 717-728.
- Verkhusha,V.V., Tsukita,S., and Oda,H. (1999). Actin dynamics in lamellipodia of migrating border cells in the *Drosophila* ovary revealed by a GFP-actin fusion protein. *FEBS Lett.* 445, 395-401.
- Wallar,B.J. and Alberts,A.S. (2003). The formins: active scaffolds that remodel the cytoskeleton. *Trends in Cell Biology* 13, 435-446.
- Watts,J.L., EtemadMoghadam,B., Guo,S., Boyd,L., Draper,B.W., Mello,C.C., Priess,J.R., and Kemphues,K.J. (1996). par-6, A gene involved in the establishment of asymmetry in early *C-elegans* embryos, mediates the asymmetric localization of PAR-3. *Development* 122, 3133-3140.
- Wehland,J., Willingham,M.C., and Sandoval,I.V. (1983). A Rat

Monoclonal-Antibody Reacting Specifically with the Tyrosylated Form of Alpha-Tubulin .1. Biochemical-Characterization, Effects on Microtubule Polymerization Invitro, and Microtubule Polymerization and Organization Invivo. *Journal of Cell Biology* 97, 1467-1475.

Wellington,A., Emmons,S., James,B., Calley,J., Grover,M., Tolia,P., and Manseau,L. (1999). Spire contains actin binding domains and is related to ascidian posterior end mark-5. *Development* 126, 5267-5274.

Wiese,C. and Zheng,Y.X. (2006). Microtubule nucleation: gamma-tubulin and beyond. *Journal of Cell Science* 119, 4143-4153.

Wodarz,A. (2000). Tumor suppressors: Linking cell polarity and growth control. *Current Biology* 10, R624-R626.

Xu,T. and Rubin,G.M. (1993). Analysis of genetic mosaics in developing and adult *Drosophila* tissues. *Development* 117, 1223-1237.

Zhang,W.G., Jin,Y., Ji,Y., Girton,J., Johansen,J., and Johansen,K.M. (2003). Genetic and phenotypic analysis of alleles of the *Drosophila* chromosomal JIL-1 kinase reveals a functional requirement at multiple developmental stages. *Genetics* 165, 1341-1354.

Zimyanin,V., Lowe,N., and St Johnston,D. (2007). An oskar-dependent positive feedback loop maintains the polarity of the *Drosophila* oocyte. *Current Biology* 17, 353-359.

8. ABBREVIATIONS

BL	Bloomington stock centre
EMS	Ethyl methanesulfonate
GTPase	Guanine triphosphatase
kDa	Kilo Dalton
bp	Base pairs
kb	Kilo base
PCR	Polymerase Chain Reaction
RT-PCR	Reverse transcription PCR
TGF- α	Transforming growth factor α
PBS	Phosphate buffer saline
BSA	Bovine Serum Albumen
PBT	PBS+Tween
SSC	Saline-sodium citrate buffer
DEPC	Diethylpyrocarbonate
TEMED	N,N,N',N'-Tetramethylethylenediamine

9. ACKNOWLEDGEMENT

One of the hardest things to do is to properly recognise everyone that impacts your graduate career. Without a doubt, the most supportive person in the last four years has been Veit Riechmann, my research advisor. It is indeed an immense pleasure for me to acknowledge Veit Riechmann for his patience and support with my work at the University of Cologne. I thank Siegfried Roth for his guidance. I had a lot of interesting discussions with him and received many useful suggestions.

Thanks to all the lab members, past and present for a wonderful atmosphere, especially to Claudia Wunderlich and Martin Technau. Thanks to Stefen Kölzer for his technical help. Thanks to Britta Grewe for her comments on my thesis.

I thank Professors of my graduate programme, especially Maria Leptin, Angelika Anna Noegel for their guidance and help. I am thankful to Eberhard Rudloff, Kristina Rafinski, Claudia Kreiten, Sebastian Granderath and Brigitte Wilcken-Bergmann for the administrative help.

My parents and family have been one of the biggest factors in my life. Their constant push for me to excel academically led to my choice of biology as a career. Special thanks to Yu for being with me always.

Financial help from Graduate School (IGSGFG) and SFB572 is gratefully acknowledged.

Ying Wang

10. ERKLÄRUNG

Ich versichere, daß ich die von mir vorgelegte Dissertation selbständig angefertigt, die benutzten Quellen und Hilfsmittel vollständig angegeben und die Stellen der Arbeit – einschließlich Tabellen, Karten und Abbildungen –, die anderen Werken im Wortlaut oder dem Sinn nach entnommen sind, in jedem Einzelfall als Entlehnung kenntlich gemacht habe, adß diese Dissertation noch keiner anderen Fakultät oder Universität zur Prüfung vorgelegen hat; daß sie – abgesehen von unten angegebenen Teilpublikationen – noch nicht veröffentlicht worden ist sowie, daß ich eine solche Veröffentlichung vor Abschluß des Promotionsverfahrens nicht vornehmen werde.

Die Bestimmungen dieser Promotionsordnung sind mir bekannt. Die von mir vorgelegte Dissertation ist von Professor Dr. S. Roth betreut worden.

Ich versichere, daß ich alle Angaben wahrheitsgemäß nach bestem Wissen und Gewissen gemacht habe und verpflichte mich, jedmögliche, die obigen Angaben betreffenden Veränderungen, dem Dekanat unverzüglich mizuteilen.

Unterschrift:

Köln, den 18.12.2007

11. LEBENS LAUF

Personal Data

Name	Ying Wang
Geschlecht	Weiblich
Geburtsdatum	23.11.1977
Geburtsort	Guangxi, V. R. China
Familienstand	ledig, keine Kinder
Angehörigkeit	V. R. China

Hochschulbildung

09/1996 - 07/2000	Shandong Universität, Jinan, V. R. China Abschluss: Bakkalaureus der Wissenschaften mit der Note „sehr gut“
11/2001 - 12/2002	Doktorarbeit an der „University of Cincinnati“, Cincinnati, USA
09/2003 -	Doktorarbeit an der Universität zu Köln Thema: Organisation of the cytoskeleton of the <i>Drosophila</i> oocyte.

Schulbildung

09/1984 - 07/1996	Grundschule und Gymnasium in Liuzhou, V. R. China Abschluss: Abitur Note: „sehr gut“
-------------------	--------------------------------------------------------------------------------------------

Praktische Tätigkeiten und und Berufserfahrung

09/2000 - 04/2001	Forschungsassistent an der Tsinghua Universität, Beijing, V.R. China
05/2001 - 10/2001	Praktikum bei der aquatischen Zuchtbauernhof zu Liuzhou, Liuzhou, V.R. China

Veröffentlichungen

- Y. Wang** and V. Riechmann The role of the actomyosin cytoskeleton in coordination of tissue growth during *Drosophila* oogenesis, *Current Biology*, 17, 1349-1355, 2007.
- Y. Wang** and V. Riechmann Microtubule anchoring by cortical actin bundles prevents streaming of the oocyte cytoplasm, *Mechanisms of Development*, in Press, 2007.
- N. Gotoh, M. Ito, S. Yamamoto, I. Yoshino, N. Song, **Y. Wang**, M. Shibuya and R. A. Lang Tyrosine phosphorylation sites on FRS2 α responsible for Shp2 recruitment are critical for induction of lens and retina. *Proc Natl Acad Sci*, 101(49):17144-17149, 2004.
- A. K. Molyneaux, **Y. Wang**, K. Schaible and C. Wylie Transcriptional profiling identifies genes differentially expressed during and after migration in murine primordial germ cells, *Gene Expression Patterns*, 4(2):167-181, 2004.
- M. Li, C. Zhao, **Y. Wang**, Z. Zhao and A. Meng Zebrafish *sox9b* is an early neural crest marker, *Dev Genes Evol*, 212(4):203-206, 2002.
- L. Liang, M. Li, **Y. Wang**, C. Zhao, Z. Zhao and A. Meng The zygotic expression of zebrafish *trebf* during embryogenesis is restricted to the embryonic shield and its derivatives, *Dev Genes Evol*, 211 (8-9): 445-448, 2001.